İSTANBUL TECHNICAL UNIVERSITY ★ INSTITUTE OF SCIENCE AND TECHNOLOGY

ELECTROCHEMICAL COMPOSITE FORMATION OF THIOPHENE AND N-METHYL PYROLLE ONTO CARBON FIBER MICROELECTRODES AND THEIR CHARACTERIZATIONS

M.Sc. Thesis by

Hülya GEYİK

(515031019)

Date of submission : 19 December 2005

Date of defence examination: 1 February 2006

Supervisor (Chairman) : Prof. Dr. A.Sezai SARAÇ (İ.T.Ü)

Members of the Examining Committee : Prof. Dr. Ayşen ÖNEN (İ.T.Ü.)

Prof. Dr. Ferhat YARDIM (İ.T.Ü.)

FEBRUARY 2006

İSTANBUL TEKNİK ÜNİVERSİTESİ ★ FEN BİLİMLERİ ENSTİTÜSÜ

TİYOFEN VE N-METİLPİROLÜN KARBONFİBER MİKROELEKTROT ÜZERİNE ELEKTROKİMYASAL KOMPOZİT OLUŞTURULMASI VE KARAKTERİZASYONU

YÜKSEK LİSANS TEZİ

Hülya GEYİK

(515031019)

Tezin Enstitüye Verildiği Tarih : 19 Aralık 2005

Tezin Savunulduğu Tarih : 1 Şubat 2006

Tez Danışmanı : Prof.Dr. A.Sezai SARAÇ (İ.T.Ü.)

Diğer Jüri Üyeleri : Prof.Dr. Ayşen ÖNEN (İ.T.Ü.)

Prof. Dr. Ferhat YARDIM (İ.T.Ü.)

ŞUBAT 2006

ACKNOWLEDGEMENT

This master study has been carried out in ELECTROPOL Laboratory (Electropolymerization Research Group), located at Faculty of Science and Letters in İstanbul Technical University.

I would like to thank my advisor, Professor Dr. A. Sezai SARAC, for his guidance, inspiration and encouragement throughout this work, and for the opportunity to work in his research group.

Special thanks go to Fevzi Çakmak CEBECİ for his good suggestions, invaluable help, and support.

I would like to acknowledge Elif Alturk PARLAK sharing her knowledge and experiences with me generously throughout this research.

I would like to acknowledge POLMAG Research Group, located at Faculty of Science and Letters in Istanbul Technical University for their great generous help for performing Thermal Analysis.

I would like to acknowledge Marina Serantoni for her great generous help for performing Atomic Force Microscope Analysis at Limerick Institute of Technology, Ireland.

Many thanks go to my colleagues in this great research group for their assistance and friendship. I would like to especially acknowledge and all members of Sarac Research Group for their helps.

Finally, I would like to offer the most gratitude to my parents for their patience, understanding, moral support and encouragement during all stages in the preparation of this thesis.

December 2005 Hülya GEYİK

TABLE OF CONTENTS

ACKNOWLEDGEMENTS ii
TABLE OF CONTENTS iii
LIST OF ABBREVIATIONS v
LIST OF TABLES vi
LIST OF FIGURES vii
LIST OF SCHEMES x
SUMMARY xi
ÖZET xiv

1. INTRODUCTION 1

2. THEORETICAL PART 2
2.1. Conducting Polymers 2
2.1.1. Theory of band gap and electrical conductivity 2
2.1.1.1. The extended π-system 3
2.1.1.2. Doping and electrical conductivity 6
2.1.1.3. Charge transport 10
2.1.2. Stability and processability 11
2.1.3. Polypyrroles 14
2.1.4. Polythiophenes 15
2.1.5. Application areas of conducting polymers 16
2.2. Electropolymerization Techniques 17
2.3. Factors Effecting Electropolymerization 18
2.3.1. Effect of electrolyte 18
2.3.2. Effect of monomer concentration 19
2.4. Characterization Techniques 21
2.4.1. Electrochemical impedance spectroscopy (EIS) 21
2.4.2. Measurement of conductivity: Four point probe 23
2.4.3. Thermal analysis 25
2.4.3.1 Differential scanning calorimetry (DSC) 25
2.4.3.2 Thermogravimetrik analysis (TGA) 26
2.4.4. Attenuated total reflectance (ATR)-FTIR 27
2.5. Carbon Fiber Microelectrodes 30
2.6. Electrochemical Composite Systems 32

3. EXPERIMENTAL WORK
3.1. Materials 38
3.2. Characterizations 38
3.3. Preparation of Carbon Fibre Microelectrodes (CFME) 39
3.4. Electropolymerization and the Characterization of the Polymers On CFME 39
3.4.1. Electrochemical polymerization procedure of CFME/PTh base electrode. 39

3.4.2. Electrografting of NMPy on CFME/Pth base electrode as an electrochemical composite 40

4. RESULTS AND DISCUSSION
4.1. Thiophene Polymer Characterization 42
4.2. Characterization of Electrochemical Composite Formation of N-Methylpyrrole on CFME/PTh base electrode 44
4.2.1. Cyclovoltammetric investigations 44
4.2.1.1. Effect of NMPy concentration 44
4.2.1.2. Effect of NMPy's cycle number on CFME/PTh base electrode 48
4.2.1.3. Effect of electrolyte 50
4.2.1.4. Stability of electrochemical composites in different electrolytes 52
4.3. ATR-FTIR Characterization of Electrocoated Polymer Surfaces 53
4.3.1. Effect of NMPy's concentration on CFME/PTh 53
4.3.2. Effect of NMPy's cycle number on CFME/PTh 55
4.3.3. Effect of electrolyte 56
4.4. Morphological Analysis 56
4.5. Thermal Analysis 60
4.6. Electrical Conductivity 63
4.7. Electrochemical Impedance Spectroscopy (EIS) 64

5. CONCLUSIONS 71

REFERENCES 73

APPENDICES 79

BIOGRAPHY 84

LIST OF ABBREVIATIONS

Py	**:**	Pyrrole
PPy	**:**	Polypyrrole
NMPy	**:**	N-Methylpyrrole
Th	**:**	Thiophene
PTh	**:**	Polythiophene
MMA	**:**	Methylmethacrylate
PMMA	**:**	Polymethylmethacrylate
ACN	**:**	Acetonitrile
TEATFB	**:**	Tetraethylammoniumtetrafluoroborate
SEM	**:**	Scanning Electron Microscope
CV	**:**	Cyclic Voltammetry
CF	**:**	Carbon Fibre
CFME	**:**	Carbon Fibre Micro Electrode
ITO	**:**	Indium Tin Oxide
ECD	**:**	Electrochromic Device
FTIR	**:**	Fourier Transform Infrared
CP	**:**	Conducting Polymer
DSC	**:**	Differential Scaning Calorimetry
TGA	**:**	Thermogravimetrical Analysis
PPV	**:**	Poly(p-phenylene vinylene)
PPS	**:**	Poly(phenylenesulfide)
EPR	**:**	Electron Paramagnetic Resonance
PEDOT	**:**	Polyethylenedioxythiophene

LIST OF TABLES

		Sayfa No
Table 2.1.	Stability and Processing Attributes of Some Conducting Polymers.	14
Table 2.2.	Axial tensile properties of carbon fibers [53]	31
Table 4.1.	Corresponding potential and current ratio values of Th on CF and PE obtained from CV	44
Table 4.2.	Redox parameters in effect of NMPy's concentration for electrogrowth and monomer free conditions.	46
Table 4.3.	Electrogrowth redox parameters in effect of electrolyte	52
Table 4.4.	Assignment of the bands in the ATR-FTIR spectra of NMPy.	56
Table 4.5.	Summary of the results obtained from TGA and DSC	61
Table 4.6.	Electrical conductivities of the polymers measured with four point probe solid conductivity	64

LIST OF FIGURES

			Sayfa No
Figure 2.1	**:**	The π-system model.	3
Figure 2.2	**:**	Molecular orbital (MO) diagram	4
Figure 2.3	**:**	**a)** Ideal conducting polymer impedance response **b)** Finite transmission line in series with an uncompensated solution resistance	22
Figure 2.4	**:**	**a)** Two point measurements, **b)** four point measurements, and **c)** four points in a line	23
Figure 2.5	**:**	Schematic representation of total internal reflection with: **a)** Single reflection; **b)** Multiple reflection IRE (internal reflection element) n_1=Refractive index of the internal reflection element; n_2=Refractive index of the sample with $n_2 < n_1$; θ = Angle of incidence; d_p=Depth of penetration	28
Figure 4.1	**:**	Electrogrowth of thiophene in 0.2M $NaClO_4$ in ACN with 50 mV/s for 4 cycles on CFME. Inset: Scan Rate dependence of 0.5M Th coated CFME in monomer free electrolyte between 50-300 mV/s	42
Figure 4.2	**:**	Electrogrowth of PTh in 0.2M $NaClO_4$ in ACN at 50 mV/s on Platinum Button electrode and CFME	43
Figure 4.3	**:**	Electrogrowth of PTh 0.1M and 0.5M Th concentration and in 0.2M $NaClO_4$ in ACN at 50 mV/s on CFME	44
Figure 4.4	**:**	Multisweep experiment for the electropolymerization of NMPy ([NMPy]= 0.008M) on CFME/PTh base electrode in 0.2M $NaClO_4$ in ACN	45
Figure 4.5	**:**	Multisweep experiment for the electropolymerization of NMPy ([NMPy]= 0.08M) on CFME/PTh base electrode in 0.2M $NaClO_4$ in ACN	46
Figure 4.6	**:**	Multisweep experiment for the electropolymerization of NMPy ([NMPy]= 0.5M) on CFME/PTh base electrode in 0.2M $NaClO_4$ in ACN	46
Figure 4.7	**:**	Cyclic Voltammogram of 0.08M PNMPy on CFME/Th base electrode in monomer free solution of 0.2M $NaClO_4$ in ACN at a scan rate of a)50 b)100 c)150 d)200 e)250 f)300 mV/s	47
Figure 4.8	**:**	Comparison of composites current values in monomer free electrolyte	48
Figure 4.9	**:**	Multisweep experiment for oxidation 0.08M NMPy on CFME/PTh base electrode for 2 cycles in 0.2M $NaClO_4$ in ACN in 50mV/sec.Inset: Scan rate dependence of 0.08M NMPy on CFME/PTh base electrode in 0.2M $NaClO_4$ in ACN from 50-300 mV/sec	49
Figure 4.10	**:**	Multisweep experiment for oxidation 0.08M NMPy on CFME/PTh base electrode for 8 cycles in 0.2M $NaClO_4$ in ACN in 50mV/sec.	49

Figure 4.11 :	Electrogrowth of 0.08M NMPy on CFME/PTh base electrode in 0.1M TEATFB in ACN with a scan rate of 50mVs^{-1}. Inset : Monomer free solution results in 0.1M TEATFB	50
Figure 4.12 :	Electrogrowth of 0.08M NMPy on CFME/PTh base electrode in 0.1M $LiClO_4$ in ACN with a scan rate of 50mVs^{-1}. Inset: Monomer free solution results in 0.1M $LiClO_4$ scan rate between 50-300mVs^{-1}	51
Figure 4.13 :	Electrogrowth of 0.08M NMPy on CFME/PTh base electrode in 0.1M $NaClO_4$ in ACN with a scan rate of 50 mVs^{-1}	51
Figure 4.14 :	Effect of electrolyte on current vs. scan rate.	52
Figure 4.15 :	Current relations between stability effect of 0.08M NMPy on CFME/PTh base electrode in different electrolytes.	52
Figure 4.16 :	Effect of different electrolytes on the stability for 50 cycles in monomer free solutions with a sweep rate of 100mVs^{-1}	53
Figure 4.17 :	Initial concentration effect of increasing NMPy concentration in the ATR-FTIR anaylsis. Thiophene concentration was held constant at 0.5M Th and NMPy concentration varies as a) [NMPy]=0.008M b) thiophene homopolymer c) [NMPy]=0.08M d) [NMPy]=0.5M	54
Figure 4.18 :	IR analysis of cycle effect.Thiophene cycle number was held constant at 4 cycle,NMPy cycle number was changed for 0.5M Th // 0.08M NMPy composite. a) 8 cycle of NMPy b) 4 cycle of NMPy c) 2 cycle of NMPy	55
Figure 4.19 :	FTIR-ATR analyses of different electrolytes in ACN for 0.08M NMPy on CFME/PTh. a) 0.1M $LiClO_4$ b) 0.1M $NaClO_4$ c) 0.1M TEATFB d) 0.2M $NaClO_4$.	56
Figure 4.20 :	**a)** SEM image of NMPY on CFME/PTh 0.04M NMPy on CFME/PTh with a thickness of 0.6μm **b)** SEM image of NMPY on CFME/PTh 0.08M NMPy on CFME/PTh with a thickness of 0.7μm	57
Figure 4.21 :	**a)** SEM images of NMPY on CFME/PTh 0.08M NMPy on CFME/PTh with 2 cycles. **b)** SEM images of NMPY on CFME/PTh 0.08M NMPy on CFME/PTh with 8 cycles	58
Figure 4.22 :	AFM images electrografting NMPy on CFME/PTh **a)** 0.008M NMPy **b)** 0.8M NMPy **c)** 0.5M NMPy	59
Figure 4.23 :	DSC thermogram of PTh was prepared in 0.5M Th and 0.1M $NaClO_4$ on CFME	61
Figure 4.24 :	TGA of **a)** 0.1M TEATFB **b)** 0.1M $NaClO_4$ **c)** bare CF	62
Figure 4.25 :	TGA of **a)** 0.5M Th on CFME Homopolymers **b)** 0.008M NMPy on CFME/PTh base electrode Composite.	62
Figure 4.26 :	Nyquist plots of 0.02, 0.04 and 0.08M NMPy on CFME/PTh base electrode and 0.5M Th homopolymer on CFME in in 0.2M $NaClO_4$ in ACN at 50 mV/s.	64
Figure 4.27 :	Bodephase graphics of 0.008M, 0.02M, 0.04M, 0.08M and 0.5M NMPy on CFME/PTh base electrode in 0.2M $NaClO_4$ in ACN at 50mV /s.	65
Figure 4.28 :	Bode magnitude of Z vs frequency plot of the composites obtained with different NMPy concentrations on CFME/PTh in 0.2M $NaClO_4$/ACN.	65

Figure 4.29 :	Bodephase graphics of 0.5M Th homopolymers, 0.08M NMPy on CFME/PTh base electrode and copolymer of 0.08M NMPy and 0.5M Th in 0.2M $NaClO_4$ in ACN at 50mV/s.	66
Figure 4.30 :	Nyquist plot of 0.08M NMPy on CFME/PTh base electrode repeated by 4 and 2 cycles of Th in 0.2M $NaClO_4$ in ACN at 50 mV/s.	67
Figure 4.31 :	Bodephase graphics of 0.08M NMPy on CFME/PTh base electrode for 2 and 4 cycles of 0.5M Th in 0.2M $NaClO_4$ in ACN at 50 mV/s.	67
Figure 4.32 :	Nyquist plots of 0.08M NMPy with 2 , 4 and 8 cycles on CFME/Pth base electrode in 0.2M $NaClO_4$ in ACN at 50 mV/s.	68
Figure 4.33 :	Bodephase graphics of 0.08M NMPy on CFME/PTh base electrode for 2, 4 and 8 cycles in 0.2M $NaClO_4$ in ACN at 50 mV/s.	68
Figure 4.35 :	Nyquist plot data of 0.08M NMPy on CFME/PTh base electrode in different electrolytes	69
Figure 4.36 :	Bode phase graphics of 0.08M NMPy on CFME/PTh base electrode with different electrolytes as 0.1M TEATFB, 0.1M $LiClO_4$, 0.1M $NaClO_4$ and 0.2M $NaClO_4$ in 0.2M $NaClO_4$ in ACN at 50 mV/s.	69
Figure A. 1 :	Multisweep experiment for the electropolymerization of NMPy ([NMPy]= 0.02M) on CFME/PTh base electrode in 0.2M $NaClO_4$ in ACN. 0.04M NMPy.	79
Figure A. 2 :	TGA of a) bare CF b)K40: 0.08M NMPy in 0.1M TEATFB in ACN c)K41: 0.08M NMPy in 0.1M $LiClO_4$ in ACN d)K42 SMP4 0.08M NMPy in 0.1M $NaClO_4$ in ACN e) SMP1: 0.5M Th on CFME in 0.2M $NaClO_4$ in ACN f) SMP2: 0.008M NMPy on CFME/PTh base electrode in 0.2M $NaClO_4$ in ACN.	79
Figure A. 3 :	SEM images of 0.04M NMPy on CFME/PTh base electrode	80
Figure A. 4 :	SEM image of 0.02M NMPy on CFME/PTh base electrode	80
Figure A. 5 :	SEM image of 8 cycles of 0.08M NMPy on CFME/PTh base electrode	81
Figure A. 6 :	SEM image of 2 cycles of 0.08M NMPy on CFME/PTh base electrode	81
Figure A. 7 :	SEM image of copolymer. [Th]= 0.5M and [NMPy]= 0.08M	82
Figure A. 8 :	SEM image of 0.5M Thiophene on CFME in 0.2M $NaClO_4$ in ACN.	82
Figure A. 9 :	IR analysis of copolymer of P(Th-co-NMPy) and composite of 0.08M NMPy on CFME/PTh base electrode.	83

LIST OF SCHEMES

		Sayfa No
Scheme 2.1:	Some conducting polymers.	4
Scheme 2.2:	Classification of materials, and schematic of valence and conduction bands and band gap	6
Scheme 2.3:	P-doping of polyacetylene	7
Scheme 2.4:	The energy region of the band gap	8
Scheme 2.5:	Bipolaron unit on polythiophene	9
Scheme 2.6:	Oxidative doping of pyrrole. (A: dopant)	11
Scheme 3.1:	Schematic representation of electrochemical composite preparation on CFME.	41
Scheme 3.2:	Electrochemical polymerization conditions.	41
Scheme 5.1:	Electrochemical composite reaction mechanism of NMPy on CFME/Th base electrode.	73

ELECTROCHEMICAL COMPOSITE FORMATION OF THIOPHENE AND N-METHYL PYRROLE ON CFME AND THEIR CHARACTERIZATIONS

SUMMARY

Until about 30 years ago all carbon based polymers were rigidly regarded as insulators. The idea that plastics could be made to conduct electricity would have been considered to be absurd. Indeed, plastics have been extensively used by the electronics industry because of this very property. They were utilized as inactive packaging and insulating material. This very narrow perspective is rapidly changing as a new class of polymer known as intrinsically conductive polymer or electroactive polymers are being discovered.

In the early days, the 1970s, scientists were laying out the initial discoveries and then building up the framework of the polymer science field. The big thing in the early 1980s was the theoretical work on solitons etc., and then the synthesis of a range of new materials that really began to lead to the promise that they would have soluble, processable polymers that would still have the optical properties of metals and semiconductors. At that time, two main conjugated polymers had appeared in labs, polyacetylene and polypyrrole. These polymers were shown to switch between two states, one neutral insulating, and the other oxidized and electrically conducting. Polyacetylene showed, however, to be highly unstable toward air and humidity, and polypyrrole was only stable in its oxidized conducting state. Garnier and his research group developed their environmentally stable in their both neutral and conducting state and proposed in literature firstly polythiophenes were synthesized electrochemically.

Conducting polymers are conducting because the electrons are delocalized in the conjugated structure. This in turn brings insolubility and infusibility to the polymers, resulting in a poor processability. A number of general techniques have been developed in order to improve the processability of conducting polymers. These techniques include block copolymerization, increase of chain flexibility via

incorporation of flexible centers in the main chain, side chain substitution, use of processable precursor polymers, and the formation of polymer blends and composites. Similarly conducting polymer composites become increasingly important for technical applications.

The aim of this study was to combine unique properties of carbon fibers and remarkable advantages of conducting polymers in order to obtain novel composite materials which have better thermal, mechanical, conductivity and processing properties. Electrochemical composite formation of thiophene (Th) and N-methylpyrrole (NMPy) onto carbon fiber microelectrodes were investigated in different monomer concentrations and cycle numbers of NMPy. Also effects of different electrolytes were investigated. All of the composites were characterized by ATR-FTIR, Cyclic Voltammetry (CV) and Electrochemical Impedance Spectroscopy (EIS). Some of electrochemical composites were also characterized in morphology by Scanning Electron Microscopy (SEM) and Atomic Force Microscopy (AFM). The results were discussed in detail. The resulting electrical, mechanical and thermal properties of such materials are illustrated by a variety of experimental examples.

Firstly, thiophene was electrodeposited on carbon fiber microelectrode. The electrochemical behaviors were investigated by cyclic voltammetry. The roles of using carbon fibre microelectrodes rather than platinium button electrode as working electrode were discussed.

In order to determine the most efficient concentration of thiophene during electrochemical composite formation with NMPy was also investigated by cyclic voltammetry. 0.5M Thiophene concentration was chosen as a standard monomer concentration for the base electrode which will be entitled as CFME/PTh base electrode during this study.

The second step is the electrografting of NMPy on CFME/PTh base electrode in different concentrations and cycle numbers. Increasing concentration and cycle number of NMPy also increases the inclusion of NMPy in the structure. From the cyclic voltammetry results and ATR-FTIR analysis, 0.08M NMPy was chosen as an optimum condition for the investigations in effect of electrolyte. SEM and AFM images were also supported the CV and ATR-FTIR results in inclusion of NMPy in composite electrode structure.

Thermal analyses were also performed and TGA results indicate that composite material on CF increases the thermal stability of CF.

In order to perform solid state conductivity measurements, polymerization reactions were performed electrochemically at a constant current in ACN solution containing $NaClO_4$ and the monomers. Polymer films were deposited with galvanostatically onto platinum plate electrodes. The conductivity measurements were shown very high values as 423.7S cm^{-1} for 0.5M Thiophene homopolymer and 126.1S cm^{-1} for 0.08M NMPy on platinum electrode.

EIS was employed to monitor the electrochemical behavior of the composite electrodes. Effect of NMPy's different concentration and cycle numbers on CFME/PTh base electrode was investigated. Rather than homopolymer, composites showed a better capacitive behavior. All EIS results confirmed that 0.08M NMPy on CFME/PTh base electrode was the optimum composite coating concentration during effect of electrolyte investigations.

TİYOFEN VE N-METİLPİROL'ÜN KARBON FİBER MİKROELEKTROTLAR ÜZERİNE ELEKTROKİMYASAL YOLLA KOMPOZİT OLUŞTURULMASI VE BUNLARIN KARAKTERİZASYONU

ÖZET

Bundan 30 yıl öncesine kadar bütün karbon bazlı polimerler yalıtkan olarak adlandırılıyorlardı. Plasitiğin elektriği iletmesi fikri tamamen olanaksız gibi görünüyordu. Hakikaten, plastik bu özelliğinden dolayı elektronik endüstrisinde, aktif olmayan paketleme sistemlerinde ve yalıtkanlık işlevlerinde yaygın olarak kullanılmaktaydı. Bu dar görüşler iletken polimer veya elektroaktif polimer olarak adlandirilan yeni bir polimer sınıfının keşfedilmesi ile hızla değişmeye başlamıştır.

1970'li yılların başında bilimadamları, polimer biliminin temellerini atacak buluşların planlarını tasarlıyor ve çatısını oluşturmaya çalışıyorlardı. 1980'lerin başindaki en önemli olay solitonlar üzerine yapılan teorik çalışmalardı.Daha sonra ise metaller ve yarı-iletkenlerle aynı optik özelliklere sahip işlenebilir polimerlerin yeni malzemeler olarak sentezlenebilmesi ön plana çıkmaya başlamıştı. O dönemde iki yeni konjugasyonlu polimer olan polipirol ve poliasetilen laboratuarlarda yerini almıştı. Bu polimerler nötr iken yalıtkan, oksitlenince ise iletken özellik gösterebilmekteydiler. Poliasetilen, havaya ve neme karşı son derece kararsız ve polipirol ise sadece oksitlenmiş iletken halde iken kararlı durumdaydılar. Garnier ve çalışma grubu bu polimerlerin hem nötr hem de oksitlenmiş haldeyken kararlı davranış göstermesini sağlayacak durumları keşfetmişlerdir ve politiyofeni ilk olarak literatürde elektrokimyasal yolla polimerleştirebilmişlerdir.

İletken polimerlerin iletken olmasının sebebi konjuge yapısındaki elektronların hareketli olmasıdır.Bu diğer bir taraftan polimere, işlenebilirlik özelliğinin azalması ile sonuçlanan çözünmeme ve erimeme özellikleri getirmektedir. İletken polimerlerin işlenebilirliğini arttırmak amaçlı pekcok genel teknik geliştirilmiştir. Bu teknikler, blok kopolimerizasyonu, yan zincir eklenmesi, işlenebilir öncü polimerlerin kullanılması ve polimer karışımları ve kompozitlerinin oluşturulması işlemlerini içermektedir. Benzer olarak iletken polimer kompozitler oluşturmak da teknik uygulamalar açısından gittikçe önem kazanmaktadır.

Bu çalışmadaki amaç, karbon fiberlerin üstün özellikleri ile iletken polimerlerin öne çıkan özelliklerini birleştirerek çok daha iyi termal, mekanik, iletkenlik ve işlenebilirlik

özelliklerine sahip bir kompozit malzeme oluşturmaktır. Tiyofen ve N-metilpirolün (NMPy) karbon fiber elektrot üzerine elektrokimyasal kompozit oluşturmak yolu ile farklı NMPy konsantrasyonlarının ve döngü sayılarının sonuçları inclenmiştir. Ayrıca farklı elektrolitlerin etkileri de incelenmiştir. Bütün kompozit kaplamalr ATR-FTIR, Döngülü Voltametri ve Elektrokimyasal İmpedans Spektroskopisi yolu ile incelenmiştir. Bununla beraber bazı kompozit kaplamalar morfolojik olarak Taramalı Elektron Mikroskobu ve Atomik Kuvvet Mikroskobu ile karakterize edilmiştir. Sonuçlar detaylı olarak tartışılmıştır. Malzemelerin elektriksel, mekanik, ve termal özellikleri pekçok sayıda deneysel örnek ile tanımlanmıştır.

Öncelikle, tiyofen karbon fiber elektrot üzerine elektrokimyasal yolla biriktirilmiştir. Döngülü voltametri ile elektrokimyasal özellikler incelenmiştir. Platin elektrotun çalışma elektrotu olarak kullanılmasından ise karbon fiberin kullanılması tartışılmıştır.

NMPy ile elektrokimyasal kompozit oluşturma işlemi sırasında en etkili olabilecek tiyofen konsantrasyonunun belirlenmesi de döngülü voltametri ile yapılmıştır. 0.5M tiyofen CFME/PTh olarak adlandırılan baz elektrot için bu çalışma boyunca standart olarak belirlenmiştir.

İkinci adım ise NMPy'ün CFME/PTh baz elektrot üzerine farklı konsantrasyonlar ve döngü sayılarında elektrografting yapılmasıdır. Konsantrasyonun ve döngü sayısının arttırılması NMPy'ün de yapıya girişinde artış gözlenmiştir. Döngülü voltametri ve ATR-FTIR analiz sonuçlarından 0.08M NMPy elektrolit etkisini incelerken optimum koşul olarak seçilmiştir.

Taramalı Elektron ve Atomik Kuvvet Mikroskoplarının sonuçları da Döngülü Voltametri ve ATR-FTIR sonuçları ile belirlenen NMPy 'ün kompozitin yapısına girişindeki artışı desteklemektedirler.

Termal analizler yapılmış ve TGA sonuçları karbon fiber üzerindeki kompozit malzemenin karbon fiberin termal dayanımını arttırdığını kanıtlamıştır.

Katı iletkenlik ölçümlerini yapabilmek için polimerizasyon reaksiyonaları sabit potansiyel altında sodyumperklorat ve monomerleri içeren asetonitril çözeltisi içerisinde otuz dakika süreyle elektrokimyasal olarak gerçekleştirilmiştir. Polimer filmler sabit potansiyel altında platin levha elektrot üzerinde biriktirilmiştir. İletkelik değerleri 0.5M tiyofen homopoilermi için 423.7S cm^{-1} ve 0.08M NMPy ile hazırlanmış elektrokimyasal kompozit için 126.1S cm^{-1} olarak hesaplanmıştır.

Elektrokimyasal İmpedans Spektroskopisi (EIS) kompozit elektrotların elektrokimyasal özelliklerini görüntülemek amaçlı uygulanmaktadır. NMPy'ün değişik konsantrasyonlarının ve döngü sayılarının CFME/PTh baz elektrot üzerinde etkileri incelenmiştir. Homopolimerle kıyaslanınca kompozit elektrotların çok daha yüksek kapasitif davranış gösterdiği sonucuna ulaşılmıştır. Elektrolit değişiminin EIS sonuçlarına etkisi incelenirken 0.08M NMPy kompoziti optimum koşul olmasından dolayı seçilmiştir.

1. INTRODUCTION

Conducting polymer composites become increasingly important for technical applications. In this work, the resulting electrical, mechanical and thermal properties of such materials are illustrated by a variety of experimental examples. The major problems associated with the use of conducting electroactive polymers include their very fragile structure and insolubility, which give rise to processing difficulties. Thus attempts to overcome these have centered on incorporating a polymer with another polymer type which can be thought to tolerate the problems.

There are three general techniques to the preparation of conducting polymer composites. One technique involves mechanically blending a conducting polymer with an insulating material; another method involves the electrochemical or chemical oxidative polymerization of the conducting polymer onto or within another polymer matrix that has been deposited onto some substrate; while the third technique involves the creation of a composite by co-deposition of the conducting polymer and the insulating polymer.

In this study it is pursued the second approach for producing electrically conducting composites. A short review is given of the theoretical background for the understanding of the electrical transport in such materials. The arrangement and the formation of polymer composite on carbon fiber microelectrodes and the resulting conductivity can be explained either by several parameters i.e. monomer concentration, electrolyte effect, cycle effect. It can also be related to different types of charge carrier transport processes depending on the internal composite structure. It is shown that the polymer matrix has a strong influence on the electrical conductivity due to its elastic properties and the response to external thermal and mechanical stimulation. Strong changes in the electrical conductivity of conducting polymer composites can be realized either by thermal stimuli, leading to a positive and negative temperature coefficient in resistivity, or by applying mechanical stress.

2. THEORETICAL PART

2.1. Conducting Polymers

Electrical conductivity in a conjugated polymer (polyacetylene) in 1977 were reported by Shirakawa, Heeger and MacDiarmird [1], the field of conducting polymer has attracted the interest of thousands of academic and industrial researchers for more than three decades. The possibility of combining in these new materials the properties of organic polymers and the electronic properties of semiconductors has been the driving force for various applications [2-4]. Conducting polymers can be prepared via chemical or electrochemical polymerization [5]. Films of electronically conducting polymers are generally obtained onto a support electrode surface by anodic oxidation (electropolymerization) of the corresponding monomer in the presence of an electrolyte solution. Different electrochemical techniques can be used including potentiostatic (constant potential), galvanostatic (constant current) and potentiodynamic (potential scanning *i.e.* cyclic voltammetry) methods [6]. Electrical conductivity is achieved in the film of conducting polymer by oxidation (p-doping) or reduction (n-doping), followed respectively by the insertion of anionic or cationic species [6], Due to the double bond alternation in the conjugated polymer backbone, the charged species formed upon doping are able to move along the carbon chain (delocalization) allowing electron transport and thus giving an electronically conductive material [7].

2.1.1. Theory of band gap and electrical conductivity

The polyacetylene (PA) produced by Shirakawa [1] in the late 1970s exhibited a 12 order of magnitude increase in electrical conductivity when exposed to oxidizing agents. Since that discovery, vast arrays of other conducting polymers (CP) have been synthesized. The most common of these, in addition to PA, are shown below in Scheme 2.1.

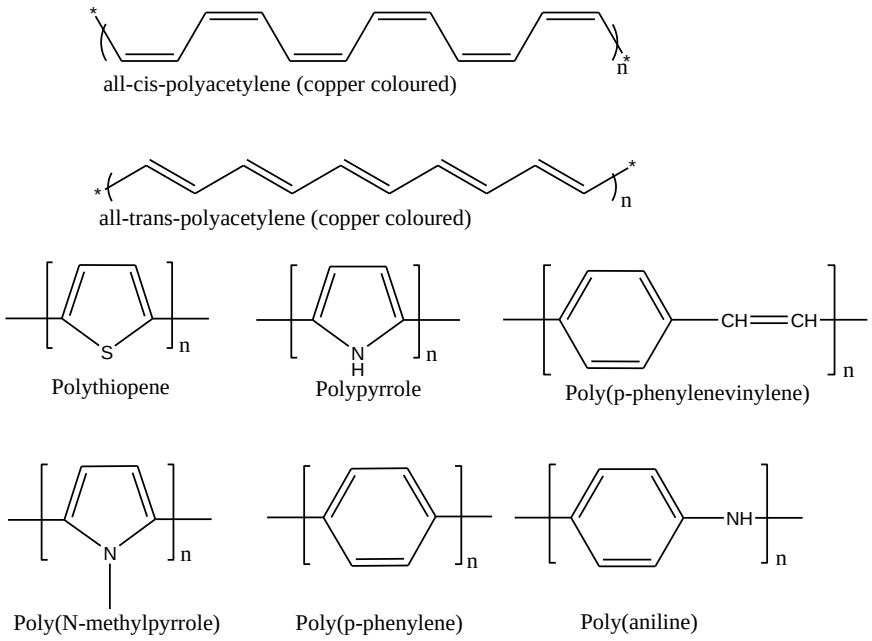

Scheme 2.1: Some conducting polymers.

2.1.1.1 The extended π-system

Since that discovery of conducting polymers, vast arrays of other (Conducting Polymers) CPs have been synthesized. Apart from polyaniline, all of these systems share one common structural feature, namely a rigid nature brought about by the sp^2 carbon-based backbone. The utilization of the conjugated construction affords polymer chains possessing extended π-systems, and it is this feature alone that separates CPs from their other polymeric counterparts.

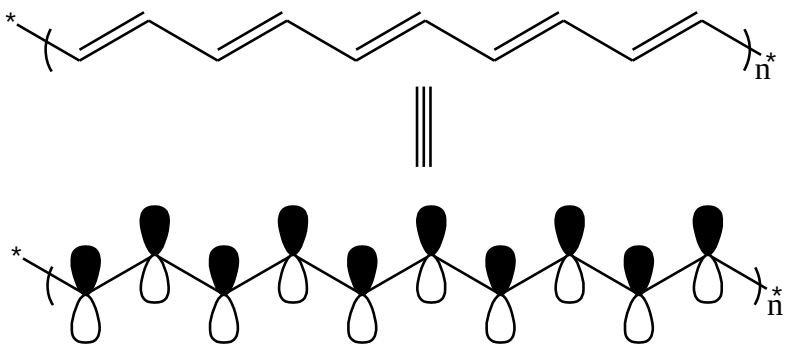

Figure 2.1: The π-system model.

Using this generic, lowest energy (fully bonding) molecular orbital (MO) representation as shown by the π-system model, the picture of primary concern that is generated by these networks consists of a number of π and π* levels (Figure 2.1).

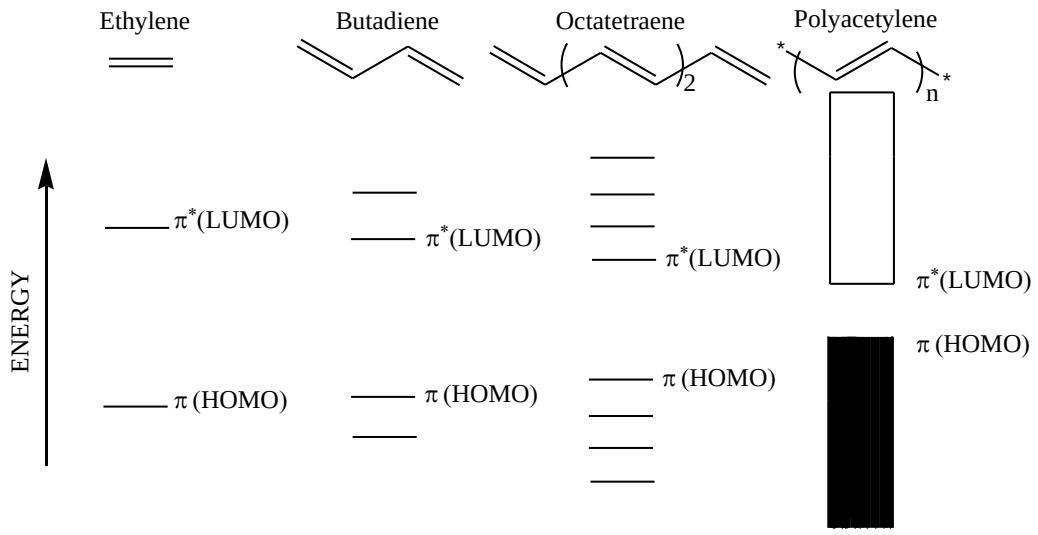

Figure 2.2: Molecular orbital (MO) diagram.

The electrical properties of any material are a result of the material's electronic structure. The presumption that CP's form bands through extensive molecular orbital overlap leads to the assumption that their electronic properties can be explained by band theory. With such an approach, the bands and their electronic population are the chief determinants of whether or not a material is conductive. Here, materials are classified as one of three types shown in Scheme 2.2, being metals, semiconductors, or insulators. Metals are materials that possess partially filled bands, and this characteristic is the key factor leading to the conductive nature of this class of materials. Semiconductors, on the other hand, have filled (valence bands) and unfilled (conduction bands) bands that are separated by a range of forbidden energies (known as the "***band gap***"). The conduction band can be populated, at the expense of the valence band, by exciting electrons (thermally and/or photochemically) across this band gap. Insulators possess a band structure similar to semiconductors except here the band gap is much larger and inaccessible under the environmental conditions employed.

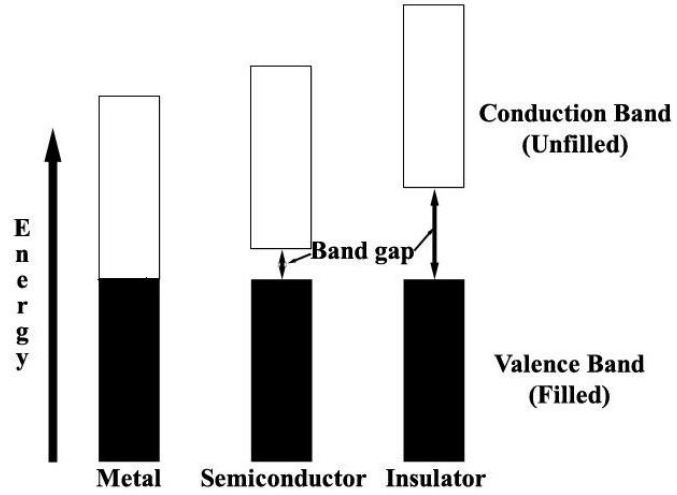

Scheme 2.2: Classification of materials, and schematic of valence and conduction bands and band gap.

At first glance one might necessarily expect that the p electrons of polyacetylene would produce a half-filled band and result in the polymer being metallic in nature. However, the one-dimensional nature of the polyacetylene chain leaves it susceptible to an instability that forces the polymer to retain its strict, alternating series of long and short bonds. This instability, analogous to a "Peierl's distortion", is very common among molecular solids and is the result of the coupling of electrons with phonons (lattice vibrations) [8]. Given the relatively soft nature of the lattice in such low dimensional solids, the total energy of the system can be decreased through a doubling of the unit cell, concomitantly opening a gap in the conduction band at the Brillouin zone boundary. In fact, structural studies of polyacetylene have shown the polymer to possess a localized backbone consisting of alternating long and short bonds [9]. This is in stark contrast to aromatic molecules, such as benzene, where the bonds are completely delocalized.

It is the Peierl's instability that is believed to be responsible for the fact that most CPs in their neutral state are insulators or, at best, weak semiconductors. Hence, there is enough of an energy separation between the conduction and valence bands that thermal energy alone is insufficient to excite electrons across the band gap. To explain the conductive properties of these polymers, several concepts from band theory and solid state physics have been adopted. For electrical conductivity to occur, an electron must have a vacant place (a hole) to move to and occupy. When bands are completely filled or empty, conduction can not occur. Metals are highly conductive because they possess unfilled bands. Semiconductors possess an energy

gap small enough that thermal excitation of electrons from the valence to the conduction bands is sufficient for conductivity; however, the band gap in insulators is too large for thermal excitation of an electron across the band gap.

2.1.1.2 Doping and electrical conductivity

In the late 1970s Heeger and MacDiarmid found that polyacctylene [$(CH)_n$] pro duced by Shirikawa's method exhibited a 12 order of magnitude increase in electrical conductivity when exposed to oxidizing agents. So how does this 12 order of magnitude increase in electrical conductivity for polyacetylene occur? The diffuse nature of the extended π-system readily allows electron removal from, or injection, into the polymer. The term "***doping***" has been borrowed from semiconductor physics with "***p-doping***" and "***n-doping***" being used to describe polymer oxidation and reduction, respectively. Doping in regards to semiconductors is quite different as it is a very distinct process carried out at low levels (<l%) as compared to CP doping (usually 20-40%). However, the manner by which doping transforms a neutral CP into a conductor remained a mystery for many years.

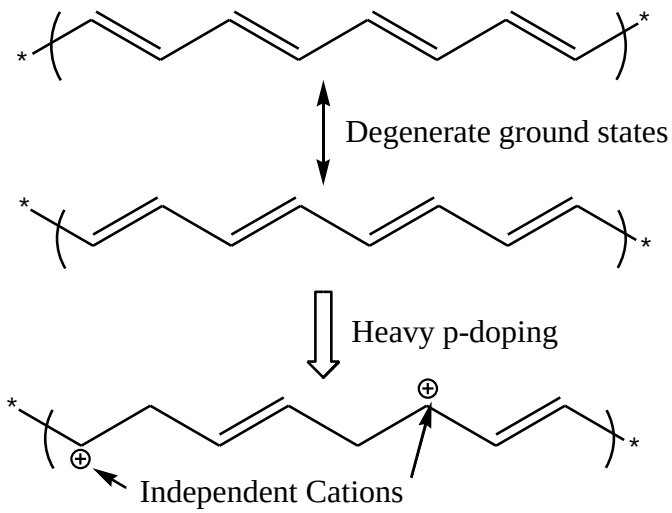

Scheme 2.3: P-doping of polyacetylene

Electron Paramagnetic Resonance (EPR) studies have shown that both the neutral and heavily doped CPs possess no net spin, interpreted as no unpaired electrons, while moderately doped materials were discovered to be paramagnetic in nature. Conductivity experiments showed that it was the "spin-less", heavily-doped form that is the most conductive for a given CP. Such behavior marks an abrupt departure from simple band theory, which centers around spin-containing charge carriers.

Polyacteylene turns out to be a special case when considering its neutral and doped forms. Comparison of the two neutral forms, shown in Scheme 2.3, reveals them to be structurally identical, and thus, their ground states are degenerate in energy. Two successive oxidations on one chain could yield radical cations that, upon radical coupling, become non-associated charges termed positive "***soliton***s".

In contrast to polyacetylene, the other CPs shown in Scheme 2.1 have non-degenerate ground states (i.e. they do not possess two equivalent resonance forms), and thus, do not show evidence of soliton formation. In this instance, the oxidation of the CP is believed to result in the destabilization (rising of the energy) of the orbital from which the electron is removed. This orbital's energy is increased and can be found in the energy region of the band gap as shown in Scheme 2.4. Initially, if only one electron per level is removed a radical cation is formed and is known as a "***polaron***" (Scheme 2.4b). Further oxidation removes this unpaired electron yielding a dicationic species termed a "bipolaron" (Scheme 2.4c). High dopant concentrations create a bipolaron-"rich" materials and eventually lead to band formation of bipolaron levels. Such a theoretical treatment, thereby, explains the appearance, and subsequent disappearance, of the EPR signal of a CP with increased doping as the neutral polymer transitions to the polaronic form and subsequently to the spinless bipolaronic state.

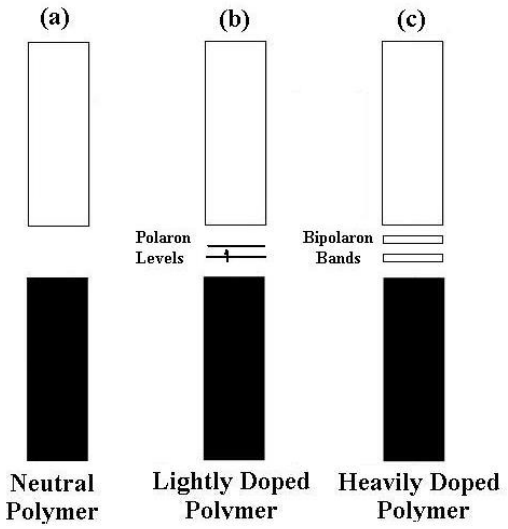

Scheme 2.4: The energy region of the band gap.

Contrary to polyacetylene's independent charges, the bipolaron unit remains intact and the entire entity propagates along the polymer chain. Scheme 2.5 shows this

behavior using polythiophene as an example. In the case of unsubstituted polythiophene, the bipolaronic unit is believed to be spread over six to eight rings. This "bipolaron length" is by no means an absolute number as different polymer backbone and substituent types yield various lengths.

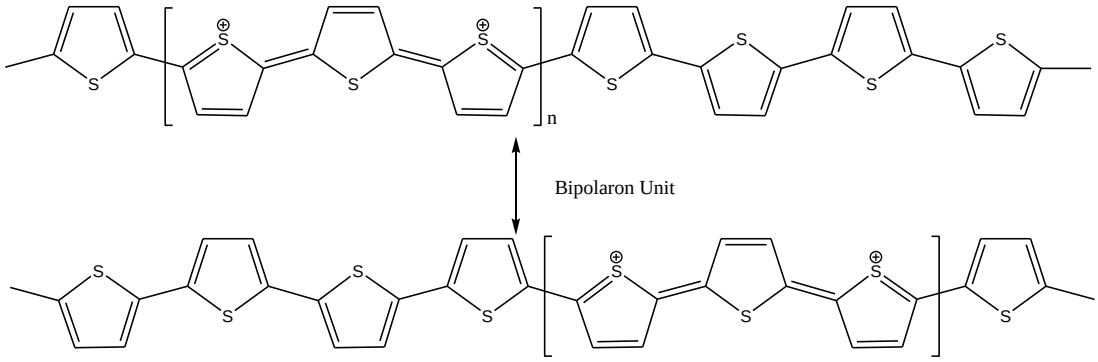

Scheme 2.5: Bipolaron unit on polythiophene.

While this general model for charge carrier generation has developed over the years, it is not without conjecture. As one alternate possibility, the presence of diamagnetic π-dimers, resulting from the combination of cation radicals, has been proposed [10,11]. Much of the basis for these theories comes from investigations into the structural and electronic properties of small conjugated molecules.

One early explanation of conducting polymers used band theory as a method of conduction. This said that a half filled valence band would be formed from a continuous delocalized π-system. This would be an ideal condition for conduction of electricity. However, it turns out that the polymer can more efficiently lower its energy by bond alteration (alternating short and long bonds), which, introduces a band width of 1.5 eV making it a high energy gap semiconductor. The polymer is transformed into a conductor by doping it with either an electron donator or an electron acceptor. This is reminiscent of doping of silicon based semiconductors where silicon is doped with either arsenic or boron. However, while the doping of silicon produces a donor energy level close to the conduction band or a acceptor level close to the valence band, this is not the case with conducting polymers. The evidence for this is that the resulting polymers do not have a high enough concentration of free spins, as determined by electron spin spectroscopy. Initially the free spins concentration increases with concentration of dopant. At larger concentrations, however, the concentration of free spins levels of at a maximum. To

understand this it is necessary to examine the way in which charge is stored along the polymer chain and its effect.

The polymer may store charge in two ways. In an oxidation process it could either lose an electron from one of the bands or it could localize the charge over a small section of the chain. Localizing the charge causes a local distortion due a change in geometry, which costs the polymer some energy. However, the generation of this local geometry decreases the ionization energy of the polymer chain and increases its electron affinity making it more able to accommodate the newly formed charges. This method increases the energy of the polymer less than it would if the charge was delocalized and, hence, takes place in preference of charge delocalization. This is consistent with an increase in disorder detected after doping by Raman spectroscopy. A similar scenario occurs for a reductive process.

Typical oxidizing dopants used include iodine, arsenic pentachloride, iron(III) and chloride. A typical reductive dopant is sodium naphthalide. The main criteria is its ability to oxidize or reduce the polymer without lowering its stability or whether or not they are capable of initiating side reactions that inhibit the polymers ability to conduct electricity. An example of the latter is the doping of a conjugated polymer with bromine. Bromine it too powerful an oxidant and adds across the double bonds to form sp^3 carbons.

The oxidative doping of polypyrrole proceeds in the following way (Scheme 2.6). An electron is removed from the π-system of the backbone producing free radical and a spinless positive charge. The radical and cation are coupled to each other via local resonance of the charge and the radical. In this case, a sequence of quinoid-like rings is used. The distortion produced by this is of higher energy than the remaining portion of the chain. The creation and separation of these defects costs a considerable amount of energy. This limits the number of quinoid-like rings that can link these two bound species together. In the case of polypyrrole it is believed that the lattice distortion extends over four pyrrole rings. This combination of a charge site and a radical is called a polaron. This could be either a radical cation or radical anion. This creates a new localized electronic state in the gap, with the lower energy states being occupied by a single unpaired electron. The polaron state of polypryyole is symmetrically located about 0.5 eV from the band edges.

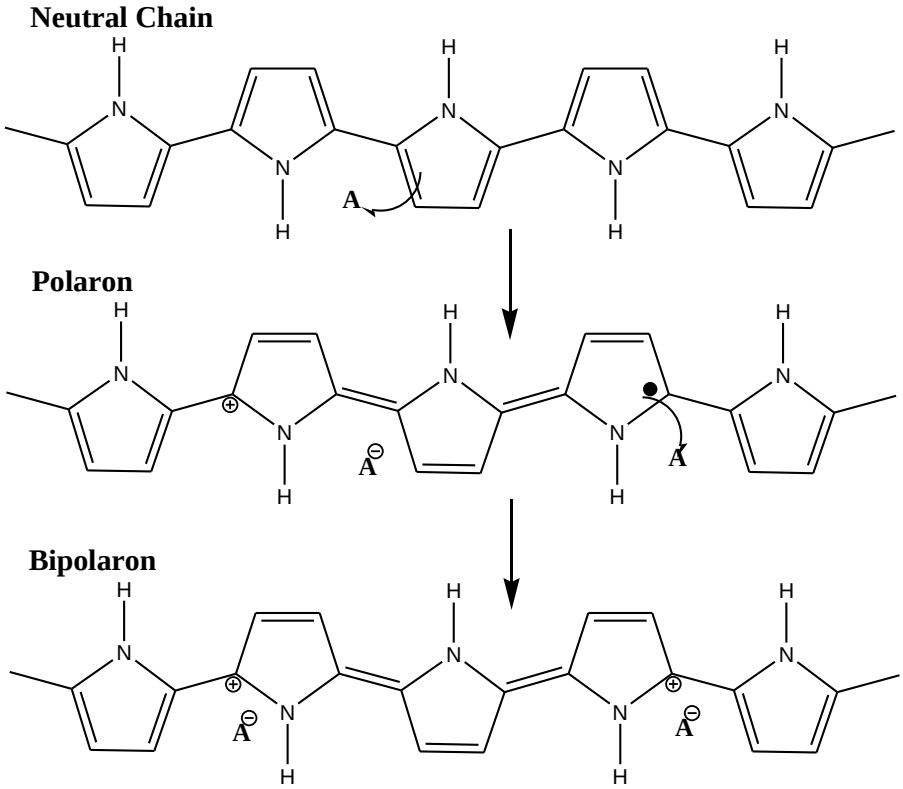

Scheme 2.6: Oxidative doping of pyrrole. (A: dopant)

Upon further oxidation the free radical of the polaron is removed, creating a new spinless defect called a bipolaron. This is of lower energy than the creation of two distinct polarons. At higher doping levels it becomes possible that two polarons combine to form a bipolaron. Thus at higher doping levels the polarons are replaced with bipolarons. The bipolarons are located symmetrically with a band gap of 0.75 eV for polypryyole. This eventually, with continued doping, forms into a continuous bipolaron bands. Their band gap also increases as newly formed bipolarons are made at the expense of the band edges. For a very heavily dope polymer it is conceivable that the upper and the lower bipolaron bands will merge with the conduction and the valence bands respectively to produce partially filled bands and metallic like conductivity.

2.1.1.3. Charge transport

Although solitons and bipolarons are known to be the main source of charge carriers, the precise mechanism is not yet fully understood. The problem lies in attempting to trace the path of the charge carriers through the polymer. All of these polymers are highly disordered, containing a mixture of crystalline and amorphous regions. It is

necessary to consider the transport along and between the polymer chains and also the complex boundaries established by the multiple numbers of phases. This has been studied by examining the effect of doping, of temperature, of magnetism and the frequency of the current used. These test show that a variety of conduction mechanisms are used. The main mechanism used is by movement of charge carriers between localized sites or between solitons, polaron or bipolaron states. Alternatively, where inhomogeneous doping produces metallic island dispersed in an insulating matrix, conduction is by movement of charge carriers between highly conducting domains. Charge transfer between these conducting domains also occurs by thermally activated hopping or tunneling. This is consistent with conductivity being proportional to temperature

2.1.2. Stability and processability

There are two distinct types of stability. Extrinsic stability is related to vulnerability to external environmental agent such as oxygen, water, peroxides. This is determined by the polymers susceptibility of charged sites to attack by nucleophiles, electrophiles and free radicals. If a conducting polymer is Extrinsic unstable then it must be protected by a stable coating.

Many conducting polymers, however, degrade over time even in dry, oxygen free environment. This intrinsic instability is thermodynamic in origin. It is likely to be cause by irreversible chemical reaction between charged sites of polymer and either the dopant counter ion or the π-system of an adjacent neutral chain, which produces an sp^3 carbon, breaking the conjugation. Intrinsic instability can also come from a thermally driven mechanism which causes the polymer to lose its dopant. This happens when the charge sites become unstable due to conformational changes in the polymer backbone. This has been observed in alkyl substituted polythiophenes.

Conjugated polymers may be made by a variety of techniques, including cationic, anionic, radical chain growth, co-ordination polymerization, step growth polymerization or electrochemical polymerization. Electrochemical polymerization occurs by suitable monomers which are electrochemically oxidized to create an active monomeric and dimeric species which react to form a conjugated polymer backbone. The main problem with electrically conductive plastics stems from the very property that gives it its conductivity, namely the conjugated backbone. This

causes many such polymers to be intractable, insoluble films or powders that cannot melt. There are two main strategies to overcoming these problems. There are to either modify the polymer so that it may be more easily processed, or to manufacture the polymer in its desired shape and form. There are, at this time, four main methods used to achieve these aims.

The first method is to manufacture a malleable polymer that can be easily converted into a conjugated polymer. This is done when the initial polymer is in the desired form and then, after conversion, is treated so that it becomes a conductor. The treatment used is most often thermal treatment. The precursor polymer used is often made to produce highly aligned polymer chain which is retained upon conversion. These are used for highly orientated thin films and fibers. Such films and fibers are highly anisotropic, with maximum conductivity along the stretch direction.

The second method is the synthesis of copolymers or derivatives of a parent conjugated polymer with more desirable properties. This method is the more traditional one for making improvements to a polymer. What is done is to try to modify the structure of the polymer to increase its processibility without compromising its conductivity or its optical properties. All attempts to do this on polyacetylene have failed as they always significantly reduced its conductivity. However, such attempts on polythiophenes and polypyrroles proved more fruitful. The hydrogen on carbon 3 on the thiophene or the pyrrole ring was replaced with an alkyl group with at least four carbon atoms in it. The resulting polymer, when doped, has a comparable conductivity to its parent polymer whilst be able to melt and it is soluble. A water soluble version of these polymers has been produced by placing carboxylic acid group or sulphonic acid group on the alkyl chains. If sulphonic acid groups are used along with built-in ionizable groups then such system can maintain charge neutrality in its oxidized state and so they effectively dope themselves. Such polymers are referred to as "self-doped" polymers. One of the most highly conductive derivatives of polythiophene is made by replacing the hydrogen on carbon three with a $-CH_2-O-CH_2CH_2-O-CH_2CH_2-O-CH_3$. This is soluble and reaches a conductivity of about 1000 S cm^{-1} upon doping.

The third method is to grow the polymer into its desired shape and form. An insulating polymer impregnated with a catalyst system is fabricated into its desired

form. This is then exposed to the monomer, usually a gas or a vapour. The monomer then polymerizes on the surface of the insulating plastic producing a thin film or a fibre. This is then doped in the usual manner. A variation of this technique is electrochemical polymerization with the conducting polymer being deposited on an electrode either the polymerization stage or before the electrochemical polymerization. This cast may be used for further processing of the conducting polymer. For instance, by stretching aligned bends of polyacetylene/polybutadiene the conductivity increase 10 fold, due to the higher state of order produced by this deformation.

The final method is the use of Langmuir-Blodgett trough to manipulate the surface active molecules into a highly ordered thin films whose structure and thickness which are controllable at the molecular layer. Amphiphilic molecules with hydrophilic and hydrophobic groups produces monolayers at the air-water surface interface of a Langmuir-Blodgett trough. This is then transferred to a substrate creating a multilayer structure comprised of molecular stacks which are normal about 2.5 nm thick. This is a development from the creation of insulating films by the same technique. The main advantage of this technique is its unique ability to allow control over the molecular architecture of the conducting films produced. It can be used to create complex multilayer structures of functionally different molecular layers as determined by the chemist. By producing alternating layers of conductor and insulator it is possible to produce highly anisotropic film which is conducting within the plane of the film, but insulating across it

Table 2.1. Stability and Processing Attributes of Some Conducting Polymers.

POLYMER	Conductivity (Ω^{-1} cm^{-1})	Stability (doped state)	Processing Possibilities
Polyacetylene	10^3 - 10^5	poor	limited
Polyphenylene	1000	poor	limited
PPS	100	poor	excellent
PPV	1000	poor	limited
Polypyrroles	100	good	good
Polythiophenes	100	good	excellent
Polyaniline	10	good	good

2.1.3. Polypyrroles

Among the conducting polyheterocycles, the most intensively studied polymers are polypyrrole, polythiophene, and their derivatives as well as polyphenylene and polyphenylene chalcogenides. Polypyrrole was shown to be a conducting polymer in 1968. Dall'Olio et al [12] prepared it by oxidation of pyrrole in sulfuric acid as a black powder with room temperature conductivity of 8 S cm^{-1}. This work was then extended by workers at IBM who showed that films of this polymer can be obtained by electrochemical polymerization. These films could be cycled electrochemically between a conducting (doped) state and an insulating state, with conductivities varying from [13] 100 to 10^{-10} S cm^{-l}. Unlike the morphology of the Shirakawa's polyacetylene, which is fibrillar, polypyrrole films are dense. Thus, physically impermeable films of polypyrrole could be prepared.

A fairly long period elapsed before this organic π-system attracted general interest and was found to be electrically conductive. Conductive polypyrrole films are obtained directly by anodic polymerization of pyrrole in aqueous or organic electrolytes (acetonitrile) [13]. They are black and, under suitable reaction conditions, can be detached from the anode in the form of self-supporting films (minimum thickness ca. 30 μm). Some of the conducting salt used in the electrolyte solution is incorporated in the film as a counterion. In contrast to polyacetylene, polypyrrole has a high mechanical and chemical stability and can be produced continuously as flexible film (thickness 80 μm; trade name: Lutamer, BASF) by electrochemical techniques. The quality of the polymers is greatly influenced by many factors, e.g., impurities, electrode material, pressure, concentrations, temperature, and comonomers. The most decisive, however, are the current density and the electrolyte, particularly the conducting anion X^- [14] because it is incorporated into the polymer as a counterion. The properties of the counterion (e.g., its size, geometry, charge) influence the properties of the polymer. The amount of counterion (anion) incorporated depends on the reaction conditions. In general, one anion is incorporated for every three pyrrole units. Exceptions are pyrrole or thiophenesulfonic acids where the counterion is coupled directly to the monomer (self doping) [15]. Some typical conducting anions are fluoroborate, perchlorate, aromatic sulfonic acids, penicillin, n-dodecyl sulfate [14], phthalocyanine sulfonic

acid, poly(styrene sulfonic acid), camphor sulfonic acid, styrene sulfonic acid, and heparin.

By changing reaction conditions, polymers with different surface morphologies, (e.g., an open porous structure) can be obtained.

The anion X^- can also be released, e.g., by applying a negative potential. Release can be specifically controlled, offering interesting possibilities for active counterions of medical interest (e.g., heparin and monobactam) that are incorporated into polypyrrole. Variation of the monomers and their substituents yields polymers with conductivities between 10^2 and 10^{-4} S/cm. Alkyl substituents also increase the solubility of the polymers with the result that electrically conducting polymers can be applied as coatings from solutions. This also applies to polymers derived from bridged pyrroles. An interesting variant is the chemical oxidation of heterocycles (e.g., thiophene or pyrrole [16] dissolved in an organic solvent (e.g., ethanol) on the surface of various materials. Conductive coatings (thickness 0.01 μm) can be produced on films of poly(phenylene sulfone), block copolymers of butadiene and styrene (Ultrason, Styrolux), poly(vinyl chloride), or other polymer films to give transparent, antistatic films with conductivities of about 0.001 S/cm. Ceramics and glass can also be coated in this way. Porous material (e.g., wood, fabrics, and open celled foams) or fibers (e.g., polyamide, glass, or carbon fibers) can also be modified and rendered antistatic by this method. Conductive powders (e.g., polypyrrole) with particle sizes of about 0.1 μm and conductivities of up to 10 S/cm can also be produced by chemical oxidation and can be incorporated as fillers in thermoplastics. These materials can be used for chip carriers.

2.1.4. Polythiophene

Polythiophene and its derivatives are stable both in their doped and in their undoped states. The most important aspect of this heterocycle is the ease of 3-substitution, which can be used to prepare new polymers with exciting properties. By substituting long flexible chains in the 3-position, one can decrease the interchain interaction and achieve high solubility (and processibility) with some sacrifice in conductivity. Several organic solvent soluble and even water-soluble 3-substituted polythiophenes with high conductivities have been prepared. For example, poly(3-hexylthiophene) has a room temperature conductivity of 30 S cm^{-1}. Poly(3-methylthiophene) has

much higher conductivity (a = 500 S cm^{-1}). It has been reported {Bryce, 1987 #8} that certain substituted polythiophenes with conductivities above l000 S cm^{-1} can be prepared. The parent polythiophene has a room temperature conductivity of 50-100 S cm^{-1}. Molecular design concepts resulted in the modification of polythiophene; by benzannelation, a new polymer, poly(isothianaphthene), was synthesized with the smallest band gap among all conjugated conducting polymers. This polymer has a band gap of 1 eV compared with the parent polythiophene, which has a band gap of 2 eV.

2.1.5. Application areas of conducting polymers

The commercialisation exemplified by the following list of materials illustrates the effects of Heeger's, McDiarmid's and Shirakawa's work on the later development of conductive polymers. The principal interest in the use of polymers is in low-cost manufacturing using solution-processing of film-forming polymers. Light displays and integrated circuits, for example, could theoretically be manufactured using simple inkjet printer techniques. [5,17-19] Doped polyaniline is used as a conductor and for electromagnetic shielding of electronic circuits. Polyaniline is also manufactured as a corrosion inhibitor.

Poly(ethylenedioxythiophene) (PEDOT) doped with polystyrenesulfonic acid is manufactured as an antistatic coating material to prevent electrical discharge exposure on photographic emulsions and also serves as a hole injecting electrode material in polymer light-emitting devices.

Poly(phenylene vinylidene) derivatives have been major candidates for the active layer in pilot production of electroluminescent displays (mobile telephone displays).

Polythiophenes have been studied extensively for use in light-emitting diodes, among other applications, due to the chemical variability offered by substitution at the 3- and 4- positions. The regularity of the side-chain incorporation strongly affects the electronic band gap of the conjugated main chain and is critical to device performance. [20]

Poly(pyrrole) has been tested as microwave-absorbing "stealth" (radar-invisible) screen coatings and also as the active thin layer of various sensing devices. The conductivity of polypyrrole film suggests applications such as flexible conductive paths in printed circuits, heating films, and film keyboards. Polypyrrole films

showgood electromagnetic shielding effects of about 40 dB over a wide range of frequencies (0 – 1500 MHz).

Other possible applications of conductive polymers include supercapacitors and electrolytic-type capacitors. Some conductive polymers such as polyaniline show a whole range of colors as a result of their many protonation and oxidation forms. Their electrochromic properties can be used to produce, e.g. “smart windows” that absorb sunlight in summer. An advantage over liquid crystals is that polymers can be fabricated in large sheets and unlimited visual angles. They do not generally respond as fast as in electron-gun displays, because the dopant needs time to migrate into or out from the polymer - but still fast enough for many applications.

2.2. Electropolymerization Techniques

In an electrochemical polymerization, the monomer, dissolved in an appropriate solvent containing the desired anionic doping salt, is oxidized at the surface of an electrode by application of an anodic potential (oxidation). The choice of the solvent and electrolyte is of particular importance in electrochemistry since both solvent and electrolyte should be stable at the oxidation potential of the monomer and provide an ionically conductive medium. Organic solvents like acetonitrile or propylene carbonate have very large potential windows [21], and a high dielectric constant which allows a good dissociation of the electrolyte and thus a good ionic conductivity. As a result of the initial oxidation, the radical cation of the monomer is formed and reacts with other monomers present in solution to form oligomeric products and then the polymer. The extended conjugation in the polymer results in a lowering of the oxidation potential compared to the monomer. Therefore, the synthesis and doping of the polymer are generally done simultaneously. The anion is incorporated into the polymer to ensure the electrical neutrality of the film and, at the end of the reaction, a polymeric film of controllable thickness is formed at the anode. The anode can be made of a variety of materials including platinum, carbon fiber, gold, glassy carbon, and tin or indium-tin oxide (ITO) coated glass [22]. The electropolymerization is generally achieved by potentiostatic (constant-potential) or galvanostatic (constant-current) methods. These techniques are easier to describe quantitatively and have been therefore commonly utilized to investigate the nucleation mechanism and the macroscopic growth.

Potentiodynamic techniques such as cyclic voltammetry corresponds to a repetitive triangular potential waveform applied at the surface of the electrode. The latter method has been mainly used to obtain qualitative information about the redox processes involved in the early stages of the polymerization reaction, and to examine the electrochemical behavior of the polymer film after electrodeposition [22].

Cyclic voltammetry (CV) is very often used to characterize conducting polymer films. This is the method of choice for studying the reversibility of electron transfer because the oxidation and reduction can be monitored in the form of a current-potential diagram [23]. Intermediate species of very short lifetimes can be observed with microelectrodes using high scanning speeds [24]. These intermediate species (radical cations) are extremely important for the understanding of the polymerization mechanism. Another electrochemical technique, coulometry, and measures the amount of electricity involved in the oxidation process. The knowledge of the initial charge used to polymerize the monomer, and the charge involved in the doping process allows the estimation of the doping level in the conducting polymer

Chronoamperometry, *i.e.* measuring the current as a function of time, is a method of choice to study the kinetic of polymerization and especially the first steps [22]. When a potential step large enough to cause an electrochemical reaction is applied to an electrode, the current changes with time. The study of this current response as a function of time is called *chronoamperometry* (CA). CA is a useful tool for determining diffusion coefficients and for investigating kinetics and mechanisms. Unlike CV, CA can yield this information in a single experiment.

2.3. Factors Effecting Electropolymerization

2.3.1. Effect of electrolyte

One important parameter affecting the physical characteristics and morphology of PPy is the nature and the concentration of the dopant that represents about 30% of the weight of the polymer film. The choice of an electrolyte is made by considering its solubility and its nucleophilicity. Moreover, the anion oxidation potential should be higher than the monomer. The dopant can be organic or inorganic and can be of I varying sizes (from chloride to polystyrenesulfonate). The size of the anion controls

the microstructure and the porosity of the polymer. Indeed, this determines the ability of the polymer to undergo an easier diffusion of the dopants during the redox process [25]. The nature of the anion has an impact on the quality of the film produced which depends on the hydrophobic character of the anion, and the interactions between the polymer and the dopant. For instance, Kassim el al. [26] have shown that in aqueous solution, the utilization of a large aromatic sulfate anion (surfactant in nature) gives stable conducting polymers with better mechanical properties than when a perchlorate anion is used. Because of their hydrophobic interaction with water, one of the roles played by these organic anions is to orient the polymer chain parallel to the electrode surface. This chain orientation increases the order in the polymer structure [27]. Kuwabata el al. [28] have shown by studying a series of carboxylate anions that the basicity of the anion plays a role in polymer growth. The higher the basicity of the anion yields the lower the conductivity of the polymer. This phenomenon is due to an increase in the interactions between the positive charges of the polymer and the anions. Inversely, anion acidity leads to an increase in the conductivity of PPy [27]. On another hand, anion nucleophilicity interferes with the reaction by increasing the formation of soluble products. The electrolyte concentration is also important although the effect is not entirely understood. The polymers of the highest conductivity are produced when elevated concentrations of electrolyte are used. For instance, the conductivity and tensile strength of the as-prepared nitrate doped PPy films increased by ca. 50-70% when the electrolyte concentration changed from 0.2 to 1 M. Above 1 M, no improvement was observed in the quality of the PPy films. Note that the influence of the cation associated with the anion is not negligible. In fact, the size of the cation (for example tetraalkylammonium) can equally have an influence on the polymer conductivity. It has been found that the larger cation, the higher conductivity of the polymer [29].

2.3.2. Effect of monomer concentration

In a classical electropolymerization, monomers are continually oxidized while the electroactive polymer film forms at the electrode surface. Since the oxidation of the monomer occurs at a higher potential than that of the redox processes of the polymer, side reactions including crosslinking and/or over-oxidation of the polymer could take place. One disadvantage of pyrrole is the presence of available sites for coupling in the beta positions. Waltman el al. has shown by using theoretical calculations that the

ability to distinguish between the α and β positions decreases as the conjugation increases for pyrrole oligomers [30]. π-coupling leads to a conjugation break along the polymer backbone which results in an increase of the observed band gap and a decrease in conductivity. Cross et al [31] have shown that the α-disubstituted monomers yield only soluble products while the α-monosubstituted monomers can give a low molecular weight polymer where β-bonding is certainly present. However, substitution in β-position avoids the β couplings and causes an increase in crystallinity of the polymer. However, the steric effect of beta substitution cannot be ignored. For instance, 3,4-dimethylpyrrole produces polymers with lower conductivities and lower mean conjugation length relative to pyrrole [32]. However, the substituents in position 3- or 4- of the pyrrole ring can also affect the electron density of the heterocycle. Merz et al. have studied the effect of substitution in the 3.4-dimethoxypyrrole and showed that the electron donating effect of the methoxy groups results in a 350 mV decrease of the monomer oxidation potential. Thus, polymerization occurs exclusively through the alpha-positions and is likely to proceed without crosslinking and over-oxidation of the deposited polymer because of the lower potential required for the electropolymerization [33]. In order to substitute both the 3, 4 positions while avoiding steric interactions between repeat units of the polymer, Reynolds el al. have studied the electropolymerization of 3,4-alkylenedioxypyrrole monomers [34,35]. The resulting polymers exhibit a lower band gap (2.0 to 2.2 eV) and a lower half-wave oxidation potential (ca. -0.3 V vs. SCE) compared to polypyrrole. This low half-wave oxidation potential is of particular interest for biological applications since these new polymers, which are water compatible, are not reduced by strong biological reductants such as 1,4-dithiothreitol. Poly(3,4-alkylenedioxypyrrole)s have also demonstrated interesting properties as electrochromic materials switching rapidly from a red or orange neutral state to a light blue-gray doped state [35]. Substitution by halogen atoms in the 3,4 positions was found to result in a higher doping level compared to pyrrole [36]. This phenomenon is due to the greater charge delocalizatlon in the polyhalopyrroles because of the mesomeric effect of the halogen atoms.

N-substituted pyrroles are known to exhibit a conductivity three orders of magnitude lower than that of PPy as demonstrated by Diaz and coworkers for poly(N-methylpyrrole) [32]. These results were further confirmed by monitoring the conductivity of poly(3,4-dimethoxy-/V-methylpyrrole) which was found to be three

orders of magnitude lower than poly(3,4-dimethoxypyrrole) [33]. The larger the substituent on the nitrogen atom, the greater the steric interaction between repeating units and subsequently the weaker the conductivity. This drop in conductivity is due to fact that the pyrrole units are not totally coplanar in the polymer, as demonstrated by the X-ray studies performed by Street on the alpha-alpha-substituted tetramer of N-methylpyrrole [4]. The influence of N-substitution on the electropolymerization characteristics was examined by Waltman el al, [37]. The polymer yield and the rate of oxidation were found to decrease as the size of the alkyl group increases. Bonding large substituents to the nitrogen atom or to the beta-carbon stabilizes the cation radical without stopping the polymerization. If this intermediate is too stable it can diffuse into the solution and form soluble products. As a result, the yield and the molecular weight of the polymer will be low. It should also be noted that some specific N-substituent inhibit the polymerization because of their basicity, as observed for N-pyrrolidic pyrrole [31].

2.4. Characterization Techniques

2.4.1 Electrochemical impedance spectroscopy (EIS)

Impedance spectroscopy is a more advanced but very powerful method which allows the investigation of the electron transport and the electronic resistance (electron transfer), the ionic conductivity, and enables the measurement of film porosity in the polymer. Note that the interpretation of impedance spectroscopy results is based on equivalent circuits which are compatible with a variety of different physical and theoretical models [38].

This powerful technique was first applied to a conducting polymer (polypyrrole) by Bard and coworkers [39] and has proven to be very versatile [40,41]. One feature of impedance as it relates to the polymers of interest here is that it permits the measurement of the electronic resistance of the film. A comprehensive derivation of the theory as applicable to conducting polymers is given by Albery and Mount [38], and a few of the salient features will be summarized here.

The characteristic complex plane (Nyquist) impedance plot of the response of a conducting polymer is presented as an idealized diagram in Figure 2.3.a. Two distinct regions are evident: A low frequency vertical region and a high frequency 45 region whose origin stems from a diffusion process (electronic or ionic) within the

film. The dual rail finite transmission line, Figure 2.3.b has been proposed [42] as an equivalent circuit to model the physical behavior of the polymer. The components of this hypothetical electrical circuit correspond to real physical phenomena. A row of capacitors bridging the pair of resistance rails accounts for the Faradaic capacitance (C_F) of the system, while the resistance rails are assigned to the electronic resistance (R_e) and the ionic resistance (R_i) of the coating. An additional resistor has been included to describe uncompensated solution resistance (R_s), an experimental artifact. A useful advantage of impedance spectroscopy is that R_e and R_i are separable, which for example permits its use in the investigation of the influence of the counterion in the rate of electron hopping [41].

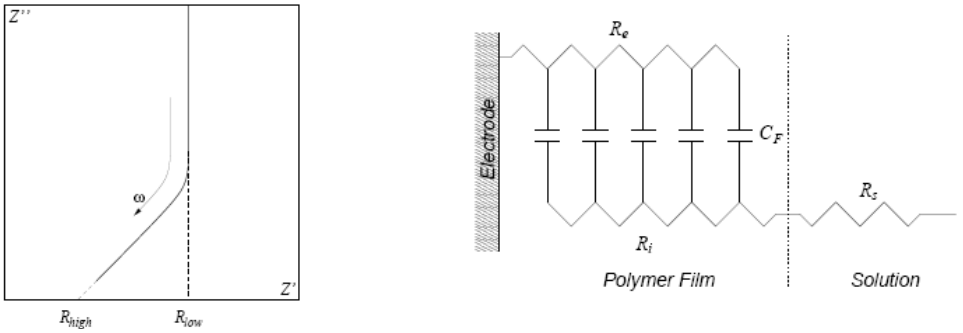

Figure 2.3: a) Ideal conducting polymer impedance response **b)** Finite transmission line in series with an uncompensated solution resistance

At the high frequency limit, the impedance of C_F becomes negligible and the transmission line behaves like two resistances in parallel:

$$\frac{1}{Z} = \frac{1}{R_i} + \frac{1}{R_e} \tag{2.1}$$

The extrapolation of the 45º region to the real axis in the Nyquist plot gives as the intercept:

$$R_{high} = R_s + \frac{1}{1/R_i + 1/R} \tag{2.2}$$

The low frequency response of the transmission line is described by equation 2.3.

$$Z = \frac{R_\Sigma}{3} - \frac{i}{\omega C_F} \tag{2.3}$$

where $R_\Sigma = R_i + R_e$. The real impedance is theoretically constant at all frequencies but in practice this portion of t he plot is not quite vertical. The real axis intercept of the low frequency data gives

$$R_{low} = R_s + R_\Sigma / 3 \tag{2.4}$$

When $R_i << R_e$, R_e is approximated by the difference between the real impedance intercepts of these two regions:

$$R_e = 3(R_{low} - R_{high}) \tag{2.5}$$

The effective electron diffusion coefficient can be extracted from the impedance data through equation (2.6) [43]:

$$D_e = d^2 / R_e C_{low} \tag{2.6}$$

where d is the film thickness, and C_{low} is the low frequency capacitance, which can be obtained as the inverse slope of a plot of imaginary impedance Z" against reciprocal frequency (in rad s^{-1}) for the low frequency data.

2.4.2. Measurement of conductivity: Four point probe

The electrical resistance R of an object is defined as the ratio between the voltage V that causes the current *I* to flow through the object, and the current I itself: So, the direct way to measuring resistance, is to measure these two magnitudes: Voltage and current.

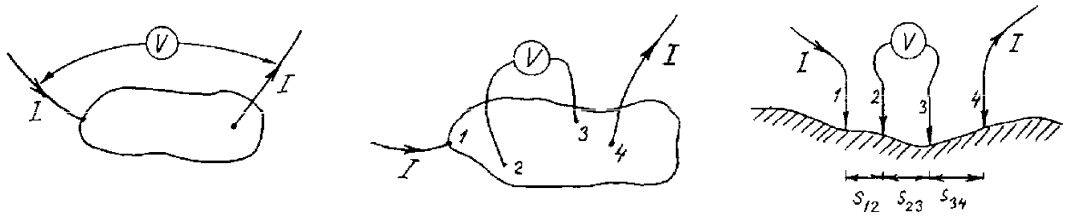

Figure 2.4: a) Two point measurements, **b)** four point measurements, and **c)** four points in a line

When the resistivity (ρ) of a sample (only homogeneous samples are considered) is wanted, the geometrical dimensions of the sample must also be known. The resistivity is given by:

$$\rho = G\frac{V}{I} \tag{2.7}$$

where: I is the current passed through the sample,

V is a measured voltage,

G is a correction factor dependent on sample shape and dimensions, and the arrangement of electrical contacts.

When performing direct current or low frequency resistance measurements, one has to make electrical contacts to the sample. By making two contacts, two-point resistivity measurements can be performed (Figure 2.4 a).

As the resistance of the contacts becomes comparable to sample resistance, it becomes necessary to separate the contacts conducting the current from the contacts between which the voltage is measured, in order not to measure contact resistance together with sample resistance. This is the rule when measuring resistivity of semiconducting materials, and also when measuring very small resistances of good conductors.

The separation of current and voltage contacts is fulfilled in the four-point method indicated in figure 2.4 b, and the resistivity is given by:

$$\rho = G\frac{V_{2-3}}{I_{1-4}} \qquad 2.8$$

Where: V_{2-3} is the voltage between contacts 2 and 3,

I_{1-4} is the current through contacts 1 and 4.

From the reciprocal theorem of electromagnetic theory we conclude that if instead we pass the current I through contacts 2 and 3, we shall get between the contacts 1 and 4 the same voltage V as before between 2 and 3.

Thus equation (2) can be extended;

$$\rho = G\frac{V_{2-3}}{I_{1-4}} = G\frac{V_{1-4}}{I_{2-3}} \qquad (2.9)$$

In words: We can deliberately exchange the current contact pair and the voltage contact pair, using the same correction factor G.

In semiconductor resistivity measurements the most common arrangement of the four points is in a line. This arrangement will be dealt with exclusively in the following. Normally, the outer contacts conduct the current and voltage is measured between the inner points as shown in figure 2.4.c.

In practice, the contacts are produced by four probes with parallel movements as indicated. The resistivity is same as in equation 2.7 where the correction factor G is a function of sample geometry, the position of the probes on the sample, and the spacing between probes. Normally, equal probe spacing $s_{12}=s_{23}=s_{34}=s$ is aimed at.

The very important task of calculating the correction factor G for various shapes and dimensions has been performed during the last decade for most practical applications. The results of highest interest for our application are compiled on the following pages. Where no other statement is made, it is assumed that the four points are in a line and are equidistant. As above, only homogeneous samples are considered.

2.4.3. Thermal analysis

Calorimetry with polymers is normally done using differential scanning calorimetry or DSC. In brief, DSC scans temperature and measures heat capacity of a specimen. The experiments are typically done at atmospheric pressure and thus DSC measures the constant-pressure heat capacity. Another thermal analysis technique that typically involves temperature scanning is thermogravimetric analysis or TGA. In TGA experiments, the temperature is scanned while measuring the weight of a specimen. Thermal degradation reactions typically cause the weight to decrease and thus decreases in weight are a sign of thermal instabilities.

2.4.3.1. Differential scanning calorimetry (DSC)

DSC measures a specimen's heat capacity at constant pressure — C_P . Heat capacity units are cal/K or J/K. It measures the amount of heat input (q) required to raise the temperature of the specimen by one degree Celsius while at constant pressure. Heat capacity is usually normalized by dividing the specimen heat capacity by the number of grams to get the heat required to raise one gram of specimen by one degree Celsius. If desired, heat capacity can be normalized by the number of moles.

DSC finds many uses in calorimetry and in polymer science. We list a few of the properties that can be measured by DSC. Many of these were discussed above. Others can be found discussed in the literature or in text books:

1. Temperature for thermal transitions: Tg, Tc, and Tm
2. Heat and entropy of transition: ΔH and ΔS (from q/T)
3. Heat capacity: CP
4. Percent crystallinity: (assuming Hf is known)
5. Heat absorbed or evolved during cure reactions or decomposition reactions
6. Sub-glass or solid state transitions

7. Crystallization kinetics (heat evolved during isothermal crystallization)

2.4.3.2 Thermogravimetric analysis (TGA)

Thermogravimetric analysis or TGA involves heating a sample to some temperature and then monitoring its weight as a function of time. It is commonly used to monitor polymer degradation reactions. TGA only requires a sensitive method for monitoring weight and a method for setting the temperature of the sample. Ideally the sample chamber should have a controllable environment to allow you to monitor degradation under various conditions (e.g., in the presence of oxygen or under dry nitrogen).The most accurate TGA experiments are to set the temperature to some constant value and follow weight as a function of time. The results will give quantitative information about the rate of degradation at that temperature. Repeating this experiment for several temperatures will give information about the temperature range under which this polymer can be used. Usually, people (i.e., industry) are not patient enough to do all those required experiments. Therefore, most TGAs are set up to scan temperature. Monitoring weight while scanning temperature will give useful results, but it must be realized that if the degradation is slow, the polymer will appear to survive to higher temperatures than it would actually survive under long term exposure. In other words, the results will also be very sensitive to rate. The sensitivity is large because degradation rates may be slow when compared to typical scanning rates such as 10-20 C/min. Coupling the by-products of a TGA experiment or the degradation products from the polymer to other instruments such as mass spectrometer, infrared spectrometry, gas chromatography, etc., can be useful in studying the mechanisms of polymer degradation. The coupled instruments can be used to identify the structure of the degradation products. Combining structural information with kinetics information can give a complete picture of the degradation process.

In order to improve the surface properties of carbon fiber without affecting the mechanical properties of the reinforcing fibers, various monomers (pyrrole (Py), carbazole (Cz) and thiophene (Th)) were used to electrograft conjugated copolymers. The electrocoated carbon fibers were characterized with respect to their surface morphology and surface composition, using scanning electron microscopy (SEM) and FTIR-reflectance spectroscopy, respectively. The pH-dependent zeta (zeta)-

potential measurements were perfomed and the performed zeta -potential measurements reflect that the surface state is strongly dependent not only on the composition of the grafted polymers (different homopolymers, copolymers and a single terpolymer). Such a detailed investigation of well known electrografted copolymers opens the possibility to use such 'superior' materials in the field of carbon fiber reinforced polymeric composite materials. The main advantages of such homogeneous and dense electrocoatings are their thermal stability and the fact that one can design the surface composition and morphology.[44]

Electrografting onto untreated high modulus (HM) and high strength (HS) carbon fibers as well as on electrochemically oxidized HM carbon fibers was carried out under preparative constant current electrolysis conditions by electrocopolymerizing carbazole-acrylamide. The electrografted copolymer exhibited good thermal stability, which was determined by thermogravimetric analysis (TGA) and differential scanning calorimetry (DSC) [45]

2.4.4. Attenuated total reflectance (ATR)-FTIR

Attenuated total reflectance (ATR) spectroscopy, also known as internal reflection spectroscopy or multiple internal reflectance (MIR), is a versatile, nondestructive technique for obtaining the infrared spectrum of the surface of a material or the spectrum of materials either too thick or too strongly absorbing to be analyzed by standard transmission spectroscopy. ATR spectroscopy has been developed since 1959, when it was reported that optical absorption spectra could conveniently be obtained by measuring the interaction of the evanescent wave with the external less dense medium [46]. In this technique, the sample is placed in contact with the internal reflection element (IRE), the light is totally reflected, generally several times, and the sample interacts with the evanescent wave (Figure 2.5) resulting in the absorption of radiation by the sample at each point of reflection. The internal reflection element is made from a material with a high refractive index; zinc selenide (ZnSe), thallium iodide – thallium bromide (KRS-5), and germanium (Ge) are the most commonly used. To obtain total internal reflection the angle of the incident radiation θ must exceed the critical angle θ_c. The critical angle is defined as:

$$\theta_c = \sin^{-1} \frac{n_2}{n_1} \qquad (2.10)$$

where n_1 is the refractive index of the internal reflection element and n_2 is the refractive index of the sample.

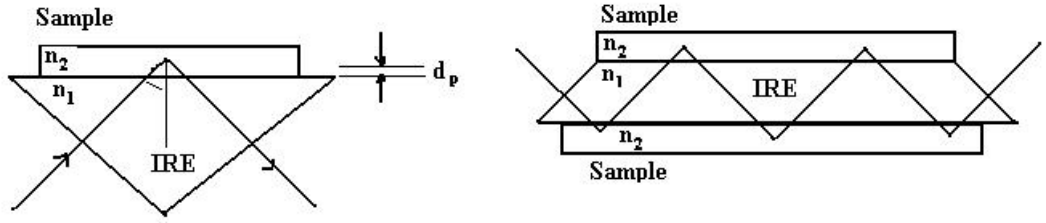

Figure 2.5: Schematic representation of total internal reflection with: **a)** Single reflection; **b)** Multiple reflection IRE (internal reflection element) n_1=Refractive index of the internal reflection element; n_2=Refractive index of the sample with $n_2 < n_1$; θ = Angle of incidence; d_p=Depth of penetration

What makes ATR a powerful technique is the fact that the intensity of the evanescent wave decays exponentially with the distance from the surface of the internal reflection element. As the effective penetration depth is usually a fraction of a wavelength, total internal reflectance is generally insensitive to sample thickness and so permits thick or strongly absorbing samples to be analyzed. The depth of penetration d_p, defined as the distance required for the electrical field amplitude to fall to e^{-1} of its value at the interface, is given by:

$$d_p = \frac{\lambda_1}{2\pi(\sin^2\theta - n_{21}^2)^{1/2}} \qquad (2.11)$$

where $\lambda_1 = \lambda/n_1$ is the wavelength in the denser medium, and $n_{21} = n_2 / n_1$ is the ratio of the refractive index of the less dense medium divided by that of the denser. Although ATR and transmission spectra of the same sample closely resemble each other, differences are observed because of the dependency of the penetration depth on wavelength: longer wavelength radiation penetrates further into the sample, so that in an ATR spectrum bands at longer wavelengths are more intense than those at shorter ones. The depth of penetration also depends on the angle of incidence; hence, an angle of 45°, which allows a large penetration depth, is generally used to analyze organic substances, rather than an angle of 60°, which results in a substantially weaker spectrum due to the decreased depth of penetration. The degree of physical contact between sample and internal reflection element determines the sensitivity of an ATR spectrum. To achieve this, a horizontal ATR accessory such as FastIR, in which the top plate is the sampling surface, is used; reproducible contact is ensured

by a special sample clamp or powder press. Good quality spectra are thus obtained for many materials that present problems of analysis with routine transmission methods, e.g., powders, pastes, adhesives, coatings, rubbers, fibers, thick films, textiles, papers, greases, foams, and viscous liquids. Liquid samples are also well suited to ATR analysis. Most liquids require a very short path length; aqueous samples, for instance, are measured at path lengths of no more than ca. 15 μm, which makes the design of transmission cells difficult because flow of liquids is hindered; they also exhibit interference fringes because of the small spacing between the high refractive index infrared windows. These problems are eliminated by using liquid ATR cells, a variant of solid ATR, in which the internal reflection element is surrounded by a vessel into which the liquid is poured.

Surface characterizations of thin film coating of random poly(N-vinylcarbazole-co-vinylbenzenesulfonic acid), [47,48] copolymer on carbon fiber was performed by Sarac et al. [47] Coatings of polymer thin films obtained, with different current densities, were characterized by scanning electron microscopy (SEM), atomic force microscopy (AFM), X-ray photoelectron spectroscopy (XPS), and Fourier transform infra red attenuated transform reflectometry (Fr-IR-ATR).

Copolymer films of pyrrole and 3,4-ethylenedioxythiophene (EDOT) were synthesized electrochemically on the carbon fiber microelectrodes (CFME). Deposition conditions on the carbon fiber and influence of the monomer concentrations to the copolymerization as well as the electrochemistry of the resulting polymers and copolymers were studied using cyclic voltammetry, in-situ spectroelectrochemistry, FTIR-ATR and scanning electron microscopy. [49]

Thin film electro-coated poly(N-vinylcarbazole-co-vinylbenzene sulfonic acid) [47,50,51] p(NVCzVBSA) [50], poly(carbazole-co-methylthiophene)[50], (p(CzMeTh)[50]) and polycarbazole (p(Cz)[52]) carbon fibre microelectrodes (CFMEs) were characterised by scanning electron microscopy (SEM) and FTIR-ATR spectroscopy. These modified carbon fibre electrodes were found to be effective systems for the determination of para-aminophenol (p-AP). Thin film coated p(NVCzVBSA)[50] was the most suitable modified electrode for the detection of p-AP.[50]

2.5. Carbon Fiber Microelectrodes

Carbon fibers, which are a new breed of high-strength materials, are mainly used as reinforcements in composite materials such as carbon fiber reinforced plastics, carbon-carbon composite, carbon fiber reinforced materials, and carbon fiber reinforced cement. Carbon fibers offer the highest specific modulus and highest specific strength of all reinforcing fibers. Typical values of tensile properties of different carbon fibers are given in Table 2.2 [53]. The fibers do not suffer from stress corrosion or stress rupture failures at room temperatures, as glass and organic polymer fibers do. Especially at high temperatures, the strength and modulus are outstanding compared to other materials [53]. Carbon fiber composites are ideally suited to applications where strength, stiffness, lower weight, and outstanding fatigue characteristics are critical requirements. They are also finding applications where high temperature, chemical inertness, and high damping are important. Carbon fibers also have good electrical conductivity, thermal conductivity, and low linear coefficient of thermal expansion [54].

The two main sectors of carbon fiber applications are high technology sector, which includes aerospace and nuclear engineering, and the general engineering and transportation sector, which includes engineering components such as bearings, gears, cams, fan blades, etc., and automobile bodies. However, the requirements of two sectors are fundamentally different. The large scale use of carbon fibers in aircraft and aerospace is driven by maximum performance and fuel efficiency, while the cost factor and the production requirements are not critical.

Table 2.2. Axial tensile properties of carbon fibers [53]

Precursor	Tensile strength (GPa)	Tensile modulus (GPa)	Elongation at break (%)
Polyacrylonitrile	2.5–7.0	250–400	0.6–2.5
Mesophase pitch	1.5–3.5	200–800	0.3–0.9
Rayon	~1.0	~50	~2.5

The use of carbon fibers in general engineering and surface transportation is dominated by cost constraints, high production rate requirements, and generally less critical performance needs. This necessitates two different approaches in the areas of production as well as research for two sectors. A number of achievements have been made in the past in the area of cost reduction as well as fiber quality improvement.

After all the developments, we have been able to achieve 90–95% of the modulus of perfect graphite (~1025 GPa), a material with highest absolute and specific modulus of all the materials known [53]. However, carbon fiber in its current strength level range is 15–20 times below the theoretical strength limit. A common rule of thumb is that the strength of a fiber should be about 10% of the modulus of a single crystal. Thus, possible strength for carbon fiber is estimated to be about 100 Gpa. Though the theoretical tensile strength of single crystal of graphite is 150 Gpa [53], highest of all the materials known.

Carbon fibers when used without surface treatment produce composites with low interlaminar shear strength (ILSS). This has been attributed to weak adhesion and poor bonding between the fiber and matrix. All the carbon fibers are thus given a surface treatment, the exact nature of which is a trade secret. These treatments increase the surface area and surface acidic functional groups and thus improve bonding between the fiber and the resin matrix [55-57]. This tends to increase the wettability of the carbon fiber and enhances the ILSS. Surface treatments may be classified into oxidative and non-oxidative treatments. Oxidation treatments involve gas-phase oxidation, liquid-phase oxidation carried out chemically [58] or electrochemically [59], and catalytic oxidation. The non-oxidative treatments involve deposition of more active forms of carbon, such as the highly effective whiskerization, the deposition of pyrolytic carbon, or the grafting of the polymers on the carbon fiber surface. Carbon fibers can also be plasma treated to improve bonding between the fiber and matrix. Liquid phase oxidation treatments are milder, very effective and are preferred.

Although whiskerization treatment gives excellent results, it is not commercially used because it is expensive and difficult to carry out precisely. It also needs to be understood that many times a weak interface is desired between fiber and a brittle matrix to improve toughness of the composite. A weak and elastic interface provides better crack resistance. Though, a strong interface between fiber and a ductile matrix results in improvement in tensile strength, compressive strength, and yield strength of the composite [58]. Zhu *et al*. [60-62] overcame this limitation of interface by using bone-shaped fibers with enlarged ends in conjunction with weak interface, in short fiber composites.

2.6. Electrochemical Composite Systems

The electrocopolymerization of carbazole and acrylamide on highly oriented pyrolytic graphite (HOPG) from ACN solutions via cyclovoltammetry (CV) was studied in order to evaluate the possibility to deposit uniform and thin but pinhole-free and still reactive coatings onto graphite-like substrates. The morphology of the coatings was investigated using atomic force microscopy and the coating thicknesses and optical parameters were measured using ellipsometry. It was found that under the chosen conditions thin (coating thickness h(f) > 180 nm) and relatively smooth (root mean square surface roughness RMS < 150 nm) P(Cz-co-AAm)-coatings exhibiting a uniform globuoidal morphology can be deposited onto graphite. From a certain coating thickness (h(f) > 50 nm) no pinholes could be detected. It was found that the thickness of the deposited coatings increases almost linearly with increasing number of CV-cycles while keeping all other experimental parameters (scan rate and comonomer concentration ratio) constant. No influence of the comonomer concentration ratio on the film thickness and coating appearance could be observed, however, at quite low initial concentrations. However, the CV-scanning rate has quite a significant influence on the thickness of the deposited coatings. Higher scan rates (100 mV/s) result in thin (h(f) approximate to 22 nm) coatings whereas at lower scan rates (< 50 mV/s) coatings with thicknesses of approximately 50 nm were obtained.[63]

A simple method of creating defined PMMA and poly (MMA-co-Cz) electrocoatings on carbon fibres is described. The electrodeposition of poly methylmethacrylate (PMMA) onto unsized, unmodified carbon fibres was performed by simple constant current electrolyses of methylmethacrylate (MMA) monomer in dimethylformamide (DMF) solutions and the 'pure' liquid monomer using sodium nitrate and lithium perchlorate as supporting electrolytes. Performing the electrolysis in dilute MMA in DMF solutions ((MMA) < 5 M) results in the deposition of powder-like polymer on the carbon fibre electrodes. Increasing the MMA concentration in the DMF solution results in a homogeneous PMMA coating of the carbon fibres. The degree of grafting or coating increases with increasing MMA concentration, except when pure MMA is used without solvent. The adhesive strength between the electrocoated carbon fibres and a PMMA matrix was determined using the single fibre pullout test. It was found

that the interfacial fracture behaviour of all carbon fibre/PMMA model composites is rather brittle.

The adhesion strength between the unmodified carbon fibres and the PMMA matrix was equal to the cohesive strength of the polymer matrix itself. Nevertheless, the electrodeposition of thin and homogeneous PMMA coatings resulted in much improved adhesion strengths. [52]

Ion beam-secondary ion mass spectroscopy (FIB-SIMS) analysis in the study of micro-sized carbon fiber electrocoated by conjugated-nonconjugated polymers such as poly(N-vinylcarbazole-comethylthiophene), poly(N-vinylcarbazole-co-vinylbenzene sulfonic acid) and polycarbazole were studied by Sarac et. el. [51] The aim of the study was to investigate by FIB-SIMS analysis the presence and concentration gradient of certain elements via depth profiling of the coating on selected carbon fibers. The presence of dopant ions together with their gradient of concentration in the coating layer was elucidated as well as the thickness of the copolymer layer electrocoated onto the carbon surface.

Polypyrrole, poly(3,4- ethylenedioxythiophene) and the copolymer of pyrrole and 3,4- ethylenedioxythiophene films [64] and 3,6 bis(3,4-ethylenedioxythiophenyl)-9-Ethylcarbazole (EDOT-ECZ-EDOT or EEE) films [65] were synthesized electrochemically on carbon fibre microelectrodes (CFME). Deposition conditions on the carbon fibre and the influence of monomer concentrations on the copolymerization, as well as the electrochemistry of the resulting polymers and copolymers, were studied. Structural studies of the polymers were conducted using different techniques such as cyclic voltammetry, in situ spectroelectrochemistry, FTIR and scanning electron microscopy. The effect of the monomer ratio on the formation of copolymer is reported.

Polycarbazole, carbazole and indole containing copolymers were electrochemically coated onto carbon fiber. Characterization of the thin polymer films were performed on the polymer-coated surface of the carbon fiber. Therefore, the results obtained could elucidate the relationship between the initial feed monomer ratio, the resulting polymer/copolymer film morphology and the surface structure formed. The thickness increase (in diameter) was 0.3 and 0.9 mu m, for two different composition of

carbazole / indole on the carbon fiber. The carbon fibers coated with copolymer thin films were from 6.5 to 8.2 in diameter (from AFM measurement). [66]

The surface properties of original high strength and preoxidized high modulus carbon fibers were altered by electrocopolymerizing acryl amide and carbazole and therefore depositing a copolymer coating onto the fibers. Scanning electron microscopy and zeta-potential measurements confirmed the presence of a rough but dense and continuous electrocoating with a basic surface character. Therefore, 'good' adhesion behavior between the electrocoated carbon fibers and an epoxy resin matrix should be expected. The interfacial adhesion was measured using the single fiber pull-out and single fiber indentation test. It was shown that only 'intermediate' adhesion was present between the carbon fibers and the electrocoating, but superior adhesion between the coating and epoxy resin exists. The single fiber model composites always failed at the fiber/electrocoating interface. However, as shown by using the indentation test, the interfacial adhesion between fibers and electrocoating can be significantly improved if preoxidized fibers are used as substrate for electropolymerization. A very high tensile strength for the electrocoating can be expected as derived from the single fiber pull-out tests.[67]

A different, more macroscopic, approach for the preparation of transparent conducting intrinsically conducting polymer (ICP) films is to minimize the absorbance of visible light by minimizing the amount of ICP in the film. In order to achieve this, blends of ICPs with other, non-conducting but processable and transparent, polymers and composite materials of ICPs and other polymers have been developed. Preparation methods include mechanical mixing, casting of a solution containing the components of the blend or polymerization of one polymer into or onto the other. The latter method can be achieved either chemically or electrochemically, producing blends or interpenetrating networks. A very important property of composite systems is the percolation threshold. In order to transfer charges, a continuous connection of the ICP has to be present in the material. If the fraction of ICP is beneath a certain value, the connecting path is interrupted and the conducting properties are lost. The minimum amount of ICP necessary to maintain conductivity in the composite system is usually called the percolation threshold. One of the first attempts to obtain composite systems of ICPs and other polymers was by Galvin and Wnek [68]. They impregnated low density polyethylene (LDPE) films

with a Ziegler-Natta catalyst and subsequently exposed this film to acetylene gas at 100–110 °C. Conductivities of ca.10 S/cm were measured after doping the flexible film with iodine. This method has the advantage that the host polymer matrix is hardly changed during the preparation of the conducting composite and therefore preserves its desired mechanical properties. A further advantage was that the decay of the conductivity of the composite film was much less than that of pure polyacetylene, indicating that a further effect of the LDPE is to protect the overoxidation of the ICP. The method was soon improved, allowing the preparation of more stable conducting composites like PPy/polystyrene using chemical polymerization. Composite films with about 10 wt% PPy were prepared having a conductivity of about 50 S/cm and mechanical properties similar to pure polystyrene. Since strong dilution of the ICP was possible without losing much of the conductivity, this method was very promising for the production of transparent, conducting ICP films. Such transparent films were reported to be formed when a poly(vinyl alcohol) film containing ferric chloride with PET as a substrate was exposed to pyrrole vapor [69]. By sorbing the pyrrole monomer in a PET film, followed by chemical polymerization using $FeCl_3$, films possessing high transmittance (70–85%) and conductivity (0.1 S/cm) could be produced [70]. Using a similar procedure, it is possible to produce transparent, conducting polymer films with other ICPs like PANI [71]. In a slightly different procedure, various non-conducting substrates have been made conducting by placing them in a chemical polymerization of pyrrole or aniline [72]. Because the ICP chains are not soluble in water, they are deposited on the non-conducting substrate, thus forming a thin conducting coating. About 85% transparent films of PPy/acrylic with a resistance of about 500 kOhm were produced. The major disadvantage of this method is that the ICP is formed in its final form and that no further processing is possible. Therefore efforts have been made to develop composite systems from which the conducting film can be formed subsequently. Cooper et al. [73] have prepared mixtures of a poly(methyl methacrylate)/poly(butyl acrylate) (PMMA/PBA) latex with preformed PANI and PPy particles. From these water-based systems, films could be prepared with a conductivity of about 10^{-2} S/cm with only about 5 wt% PANI or about 20 wt% PPy. These percolation thresholds have been confirmed in later studies with other solid matrix polymers [74,75]. The difference in the percolation threshold is attributed to the difference in shape of the ICP particles; the PANI particles are

needle shaped and the PPy particles have a more globular appearance. Cooper et al. reported that the films essentially retain the mechanically properties of PMMA/PBA films up to ICP particle concentrations of ~20 wt%. At higher concentrations the films become brittle and easily torn [73]. Very low percolation thresholds have been obtained using preformed ICP particles and solutions of matrix polymers [76]. Using very small-sized PANI particles (± 20 nm), composite films with poly(vinyl chloride) (PVC) and poly(vinyl alcohol) (PVA) have been prepared with a calculated percolation threshold of $4x10^{-4}$ volume fraction of PANI [76]. From these systems, 50% transparent freestanding films with a conductivity of about 10^{-2} S/cm have been prepared with only 2½ wt% PANI [77]. A different approach in obtaining conducting composite systems with low percolation threshold involves mixing solutions of an ICP and of a matrix polymer. Upon film formation of such a mixed solution, phase separation should take place leading to a conducting ICP path through an insulating matrix. Soon after the development of the soluble PANI with the camphorsulfonic acid (CSA) counter anion by Cao et al. [78,79], such solution processable blends of PANI with different host polymers have been reported. Solution cast PANI/CSA/PMMA films from meta-cresol having a surface resistance of about 400 Ω/□ and a transparency over 80% in the visible range have been prepared [79]. Electrical conductivities of the order of 10 S/cm were obtained in blends containing only about 5 wt% PANI. Similar results could be obtained with blends of PANI in a variety of other amorphous polymers; for example polystyrene, polyvinylacetate, amorphous nylon etc [79]. Such transparent, conducting blends can be used for instance as electrodes in polymer light emitting diodes [80] or in polymer transistors [81]. It was found that PANI forms fibrillar networks in the polymeric matrix, resulting in the low percolation threshold in these materials [82]. Comparable results have been obtained with other counter anions and in different solvents, like xylene and hexafluoro-2- propanol [83]. A disadvantage of these solution-processable blends is the use of organic solvents. Because of safety and environmental reasons, there is a demand for water-based systems. The aqueous solution of PEDOT/PSS has the disadvantage that it is an extremely diluted solution (0.5 wt% ICP). Evaporation of the water is energy consuming and it limits the practical applicability for other applications than antistatic foils. As stated above, water-based systems of dispersions have been developed, but the percolation threshold was rather high [73]. A decrease of the percolation threshold might be obtained if core–shell latex particles with a

conductive shell are used instead of pure ICP particles. Such core–shell particles may be formed if the polymerization of pyrrole is carried out in the presence of conventional latex particles, as was shown by Yassar et al [84].

Conducting electroactive polymers (CEPs) based on polypyrrole (PPy) have been the subject of extensive investigations owing primarily to their usefulness in fuel cells, electrochromic displays, sensors, actuator components in microsurgical tools, corrective implantable aids, nerve repair conduits, lifelike prosthetic limbs and artificial muscles. These seemingly ubiquitous applications of PPy in electronics, industry and medicine are due to its good electrical conductivity, good environmental stability, relative ease of synthesis and the potential for copolymerization without compromise of electroactivity. However, the major problems associated with the use of PPy and other CEPs include their very fragile structure and insolubility, which give rise to processing difficulties. Thus, attempts to overcome these have centered on incorporating PPy within the matrix of other stabilizing materials.

There are three general techniques to the preparation of conducting polymer composites. One technique involves mechanically blending a conducting polymer with an insulating material; another method involves the electrochemical or chemical oxidative polymerization of the conducting polymer onto or within another polymer matrix that has been deposited onto same substrate; while the third technique involves the creation of a composite by co-deposition of the conducting polymer and the insulating polymer.

3. EXPERIMENTAL WORK

3.1. Materials

Acetonitrile was used as received from Riedel-de Haen Chemical without further purification. Electrolytes , TEATFB was used from Fluka Chemicals without a purification with a ratio of %99 purity, $NaClO_4$ was used from Riedel-de Haen Chemicals as pure, $LiClO_4$ was used from Aldrich Chemical with a purity of %99.99.Monomers, thiophene and n-methyl pyrrole, were used from Lancester and Aldrich Chemicals with a purity of higher than %99. A high strength (HS) carbon fibers C 320.000A (CA) (Sigri Carbon, Meitingen, Germany) containing 320000 single filaments in a roving were used as working electrodes. All of the electrodes were prepared by using CF (diameter = 7 μm) attached to a copper wire with a Teflon tape. The electrode area keeps up constant (~ 3.3 cm^2) by adjusting the dipping length and covering the rest of the fibers with the Teflon tape. A platinium wire was used as a counter electrode and Ag/AgCl (was stocked in 3M NaCl) was used as a reference electrode.

3.2. Characterizations

Polymerization reactions were performed electrochemically in acetonitrile (ACN) solution with different electrolyte systems such as containing 0.1M $LiClO_4$, 0.1M $NaCLO_4$, 0.2M $NaClO_4$, 0.1M TEATFB for various electrodes with different monomer concentrations and scan rates. Cyclic voltammogram (CV), of the polymers was performed on an Princeton Applied Research (PAR) branded, Parstat 2263 model potentiostat, which is a self-contained unit that combines potentiostatic circuitry with phase-sensitive detection (Faraday cage that BAS Cell Stand C3). A three-electrode system employing CFME as working electrode, Platinum wire as counter electrode, and a Ag/AgCl (reference electrodes were stocked in 3.5M KCl). EIS measurements were also performed with Parstat 2263 Potentiostat with PowerSine software package. Both polymers, composites and copolymers electrocoated onto carbon fiber surface were analyzed by FT-IR reflectance

spectrophotometer. (Perkin Elmer, Spectrum One; with a Universal ATR attachment with a diamond and ZnSe crystal C70951). The morphological studies were analyzed using a SEM, AFM. A JEOL-SEM (JEOL Ltd., Japan) scanning electron microscope (SEM) was used to observe the morphological features of the coated carbon fiber electrodes. The fibers were attached on copper plate by use of a double sided carbon tape. The AFM images reported in this study were obtained using an Explorer Scanning Probe Microscope (TopoMetrix-ThermoMicroscope-VEECO). Non-contact mode was used throughout. The tips used were high resonance frequency silicon tips (frequency range 354–409 kHz), with a 120-micron-long cantilever and tip of 3–6 micron base, 10–20 micron long, 20 nm tip radius. The raw data collected were processed by the TopoMetrix SPMLab NT Version 5.0, using left shadowing. In order to perform AFM analysis, the carbon fibers were attached to a piece of silicon wafer using a thin layer of adhesive.

The glass transition temperatures of the copolymers were measured by differential scanning calorimetry (TA DSC Q10) in a flowing nitrogen atmosphere at heating rate 10^0C / min.

Thermal gravimetrical analysis was performed on a TA TGA Q50 instrument.

3.3. Preparation of Carbon Fiber Microelectrodes CFMEs

The electrodes were prepared by using 3 cm. of the CFME with a diameter of about 7 μm attached to a copper wire with a Teflon tape. Generally number of carbon fibers was about 500-1000. Between 1 and 2 cm of the CFME was dipped into the solution in order to keep up the electrode area around 3 cm^2. The CFMEs were firstly cleaned with methanol and then dried up in a stove for 15 min. before electrochemical coatings were done.

3.4. Electropolymerization and Characterization of Polymers on CFME

3.4.1. Electrochemical polymerization procedure of CFME/PTh base electrode

The electrochemical polymerization was carried out in a three-electrode system employing CFME as a working electrode at room temperature. 0.5M was chosen as a standard monomer concentration for Th during this study. Electropolymerization process was performed in 0.2M $NaClO_4$ (except in investigating electrolytic effect

with TEATFB, $LiClO_4$) in ACN with a scan rate of 50mV/sec for four cycles by CV. The oxidation potential was between 0-1.7V.

3.4.2. Electrografting of NMPy on CFME/Pth base electrode as an electrochemical composite

After polymerization of PTh on CFME, second step of the process, NMPy electrodeposition, has been performed in order to obtain a composite coating. The same base electrode was used in all of the NMPy electrodeposition experiments. Since PNMPy has a lower oxidation potential, the potential value was varied from 0 to 1.1V. The schematic representation of electrochemical composite formation can be seen in Scheme 3.1. In order to investigate effect of the monomer concentration to the polymer structure and the morphology, NMPy between 0.008M and 0.5M were electrografted on CFME/PTh base electrode. In addition the effect of cycle number was investigated between 2 to 8 cycles.

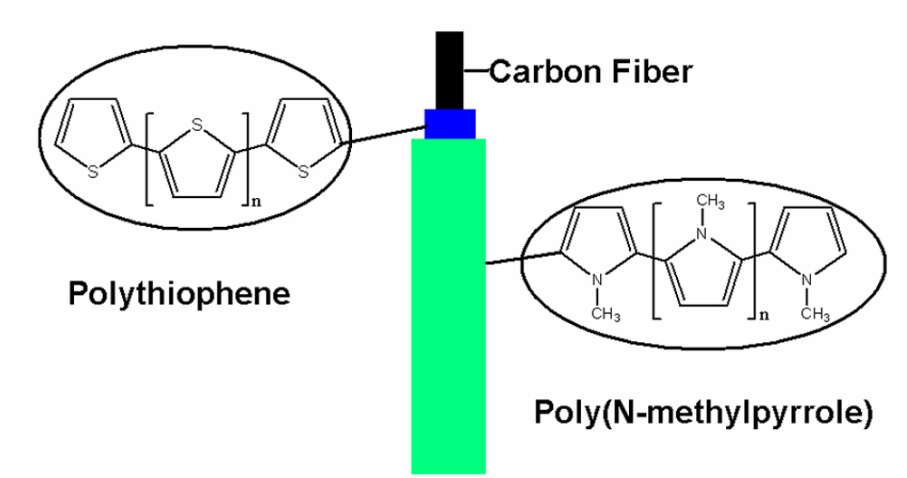

Scheme 3.1: Schematic representation of electrochemical composite preparation on CFME.

In scheme 3.1 as it can be seen Th is coated on CFME as a first layer than NMPy is deposited on CFME/PTh base electrode.

Electrochemical polymerization conditions employed during this work were summarized in Scheme 3.2. Electrolyte type was changed for both monomers when the electrolyte effect was studied.

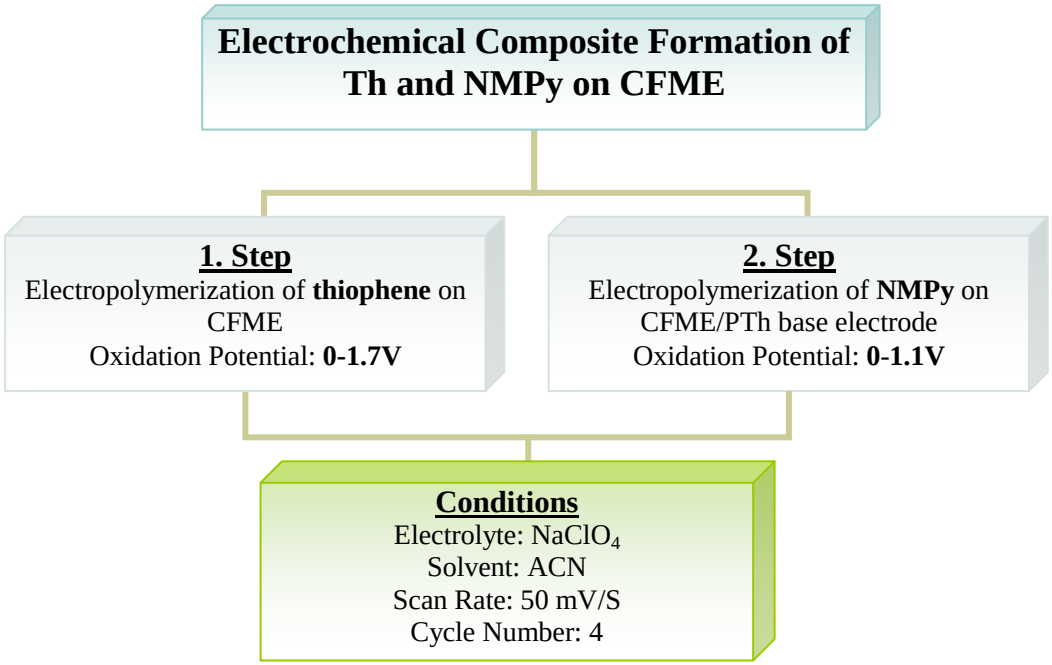

Scheme 3.2: Electrochemical polymerization conditions.

4. RESULTS AND DISCUSSION

4.1. Thiophene Polymer Characterization

0.5M thiophene was electropolymerized on CFME and formed a homopolymer base electrode which was used to analyze the effect of NMPy's concentration and cycle number during electrochemical formation of composite coatings. Electrogrowth of thiophene monomer onto CFME had broad peaks which can be seen in Figure 4.1.

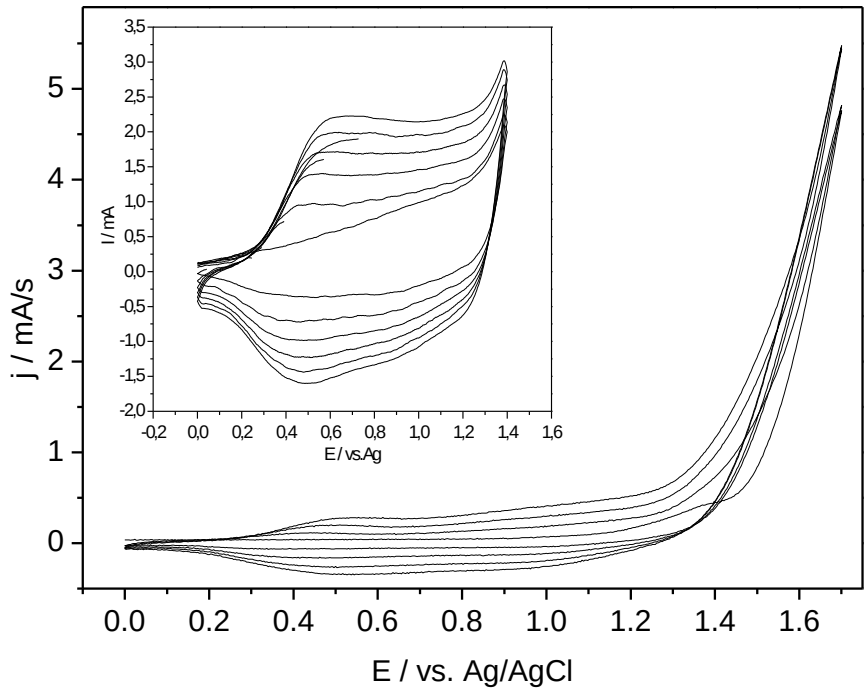

Figure 4.1: Electrogrowth of thiophene in 0.2M $NaClO_4$ in ACN with 50 mV/s for 4 cycles on CFME. Inset: Scan Rate dependence of 0.5M Th coated CFME in monomer free electrolyte between 50-300 mV/s.

During oxidation and reduction, anodic and cathodic peak potentials were determined by taking the average values of five points on peaks. The values were taken from the forth cycles of oxidation and reduction of electrogrowth process. Anodic and cathodic peak potentials, in electrogrowth of Th homopolymer, were determined as 0.52 V and 0.48 V. Oxidation potential was found to be 1.43V. Current densities corresponding to anodic and cathodic peaks were 0.58mA/cm^2 and

0.54mA/cm^2. Current ratios of anodic and cathodic peak values were calculated as 0.93 which indicates to reversibility (See Table 4.1).

In order to compare CFMEs and button platinum electrodes, 0.5M Thiophene was electropolymerized in 0.2M $NaClO_4$ in ACN with 50mV/s for 4 cycles. The fourth cycles of electrogrowth processes were shown in Figure 4.2.

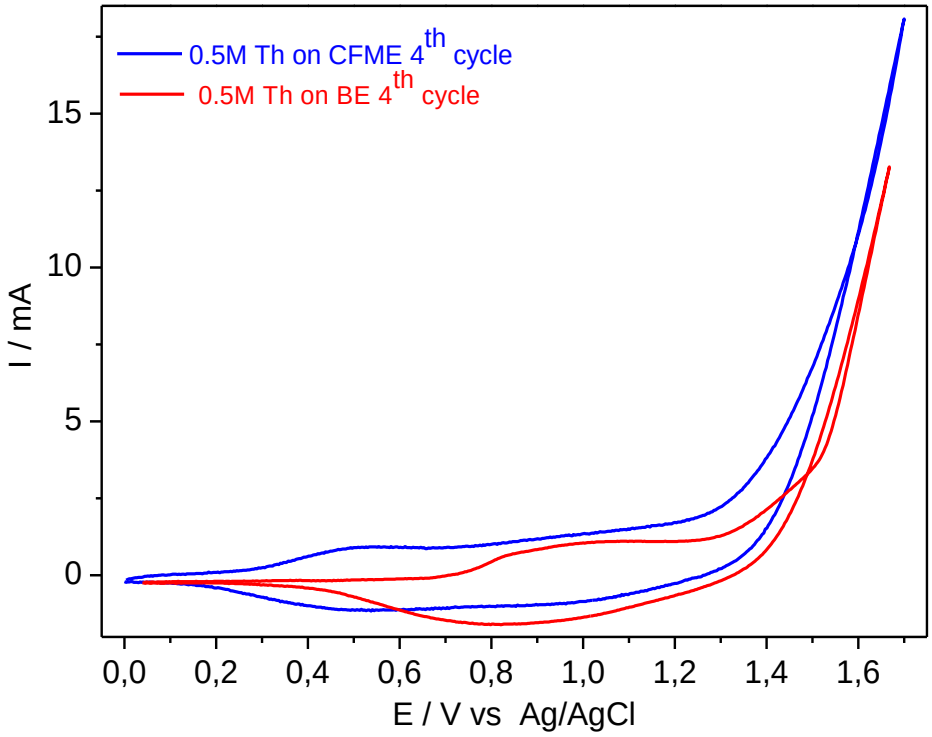

Figure 4.2: Electrogrowth of PTh in 0.2M $NaClO_4$ in ACN at 50 mV/s on Platinum Button electrode and CFME.

For platinum button electrodes and CFMEs onset potentials were 1.55V and 1.43V, respectively. From these results it can be seen that using CFMEs rather than button platinum electrodes decreases the oxidation potential. Decreasing oxidation potential is an advantage for better and easier electron transfer for electropolymerization.

Table 4.1. Corresponding potential and current ratio values of Th on CF and PE obtained from CV.

[Th]	E_c (V)	E_a(V)	E_{onset}(V)	I_a / I_c
0.1M on CFME	0.60	0.58	1.45	0.53
0.5M on CFME	**0.52**	**0.48**	**1.43**	**0.93**
0.5M on PE	1.1	0.80	1.55	0.88

The polymer electrodeposited in 0.5M Th on CFME has a higher current density value than homopolymers electrografted at 0.5M Th on Pt button electrode.

Th concentration was decreased to 0.1M in order to compare the concentration effect on CFME (Figure 4.3). Increasing Th monomer concentration causes an increase in current density.

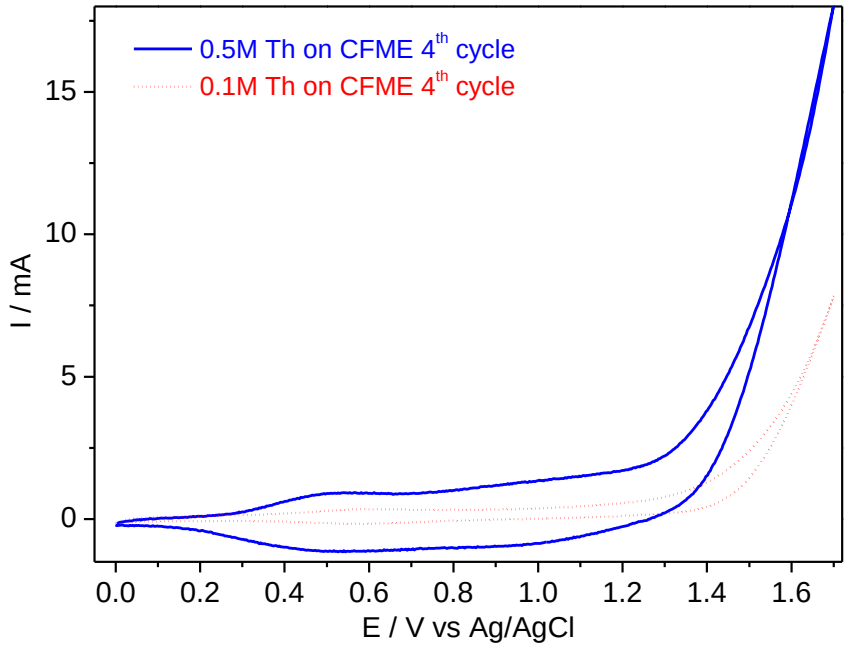

Figure 4.3: Electrogrowth of PTh 0.1M and 0.5M Th concentration and in 0.2M $NaClO_4$ in ACN at 50 mV/s on CFME.

4.2. Characterization of Electrochemical Composite Formation of N-Methylpyrrole on CFME/PTh base electrode

In order to investigate the NMPy interaction and resulting product on the CFME/PTh base electrode surface, current-potential curves with different concentrations, cycle numbers of NMPy composites in acetonitrile were taken.

4.2.1. Cyclovoltammetric investigations

4.2.1.1. Effect of NMPy concentration

Some of the cyclic voltammograms (CV) obtained for electropolymerization of NMPy's at a potential sweep rate of 50mVs^{-1} on CFME/PTh base electrode can be seen in figures 4.4- 4.6. To determine the effect of the monomer concentration on the growth of the films, the films were grown on CFME (Area:3.3cm^2 for approximately 1000 single fibers) in solutions of varying monomer concentrations from 0.008M to 0.5M of NMPy cycling the potential between 0.00 and 1.1 V (Ag/AgCl, scan rate, 50 mVs^{-1}) for four cycles.

For the electrogrowth processes the current densities, anodic potentials and cathodic potentials were measured from the fourth cycles. From these measurements redox parameters were determined and summarized in Table 4.2. The oxidation potentials of the monomers were 0.86V, 0.76V and 0.73V for forth cycles with increasing NMPy concentrations. An increase in the concentration of NMPy resulted in a decrease in onset potential of the electrochemical composites.

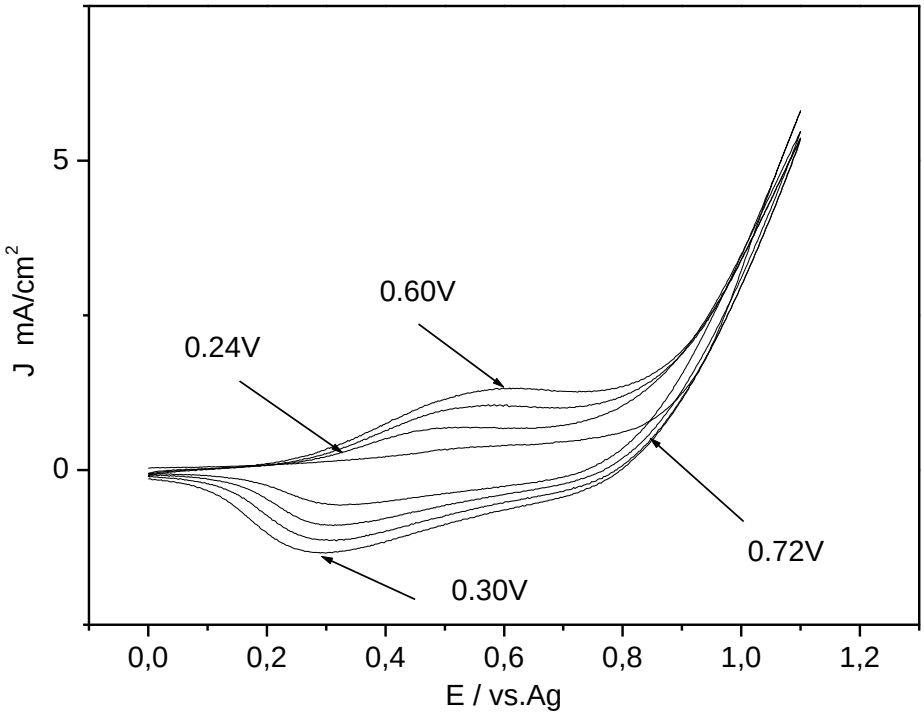

Figure 4.4: Multisweep experiment for the electropolymerization of NMPy ([NMPy]= 0.008M) on CFME/PTh base electrode in 0.2M $NaClO_4$ in ACN.

Table 4.2. Redox parameters in effect of NMPy's concentration for electrogrowth and monomer free conditions

		Polymer Growth			
Concentration NMPy	**E_{a*} (V)**	**E_{c*} (V)**	**E_{onset}**	**ΔE**	**I_a/I_c**
0.008M	0.60	0.30	0.86	0.30	0.96
0.02M	0.60	0.21	0.82	0.39	0.95
0.04M	0.63	0.19	0.77	0.44	0.89
0.08M	0.67	0.28	0.76	0.39	0.98
0.5M	0.68	0.17	0.73	0.51	0.88

*Average values for five points were taken as anodic and cathodic peaks were broad

The irreversible oxidation of the monomer appears clearly on the first cycle followed by a nucleation loop for five different NMPy concentrations. A regular and reversible growth was observed for all composites with a deposition rate that appeared to be faster with an increase in NMPy concentration. The results showed no significant

differences between Ea, but for Ec values there has been a drastic decrease with increasing the monomer concentration, however, reversibility of electrogrowth of composites were better in case of 0.08M NMPy concentration with a value of 0.98.

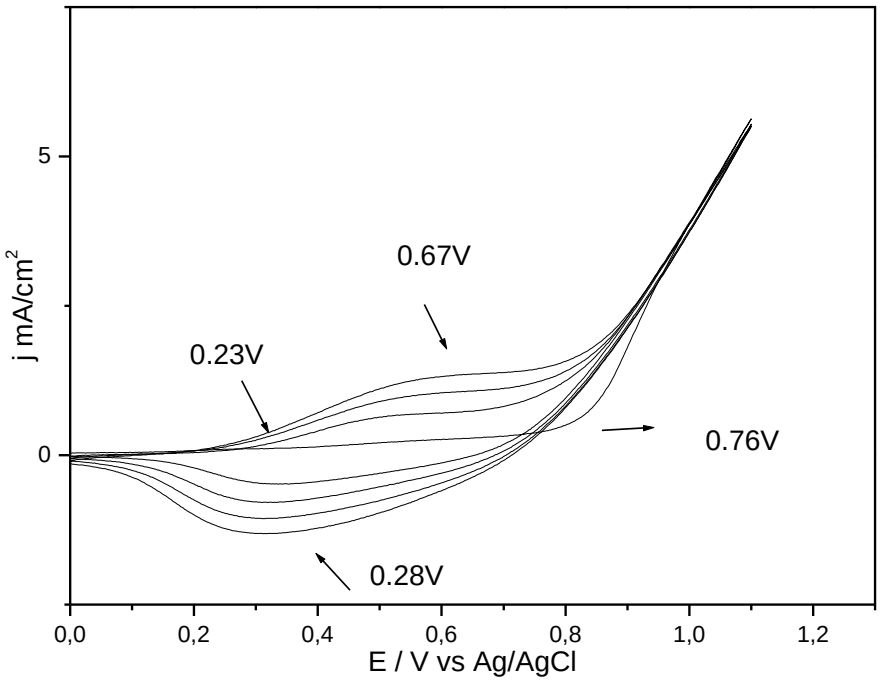

Figure 4.5: Multisweep experiment for the electropolymerization of NMPy ([NMPy]= 0.08M) on CFME/PTh base electrode in 0.2M $NaClO_4$ in ACN.

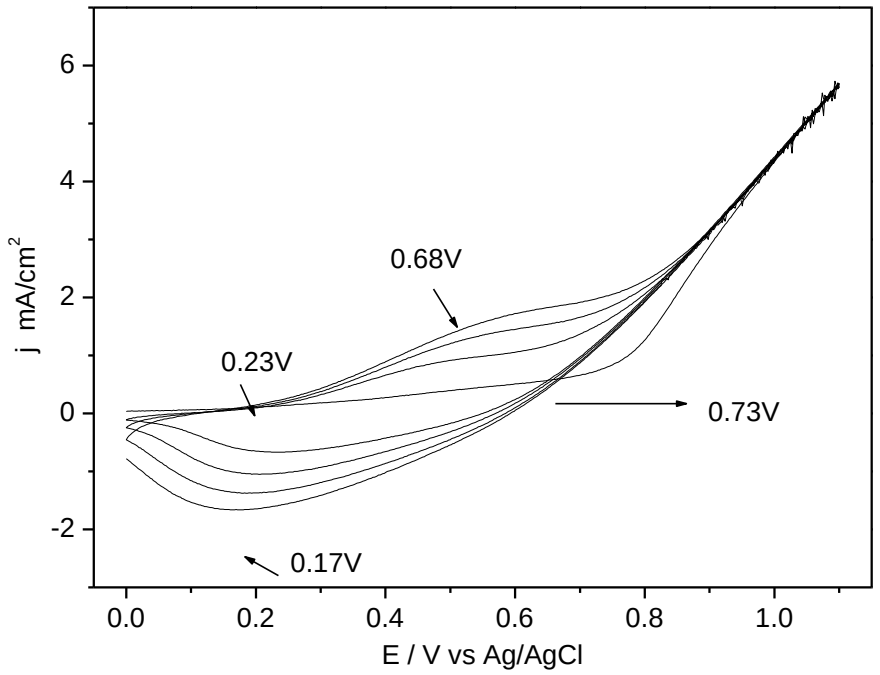

Figure 4.6: Multisweep experiment for the electropolymerization of NMPy ([NMPy]= 0.5M) on CFME/PTh base electrode in 0.2M $NaClO_4$ in ACN.

The amount of the film deposited can be assumed to be proportional to the charge passed during the fourth oxidative cycle [2,85-87]. As it can be seen from the monomer free solution results, increasing NMPy's concentration also causes a rise in the current and current density values. 0.08M NMPy's monomer free graph can be seen in figure 4.7.

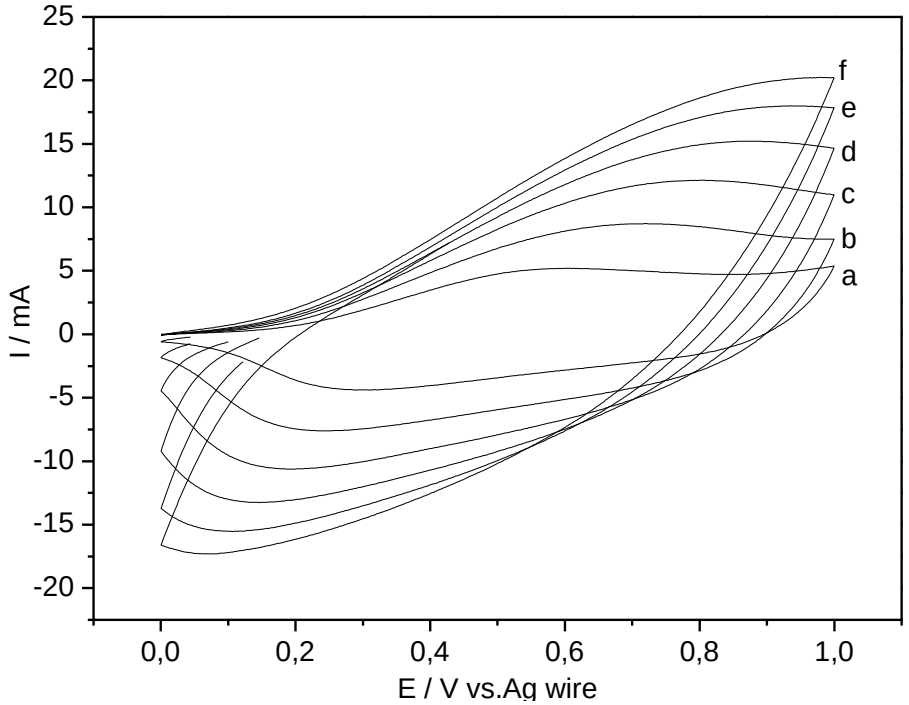

Figure 4.7: Cyclic Voltammogram of 0.08M PNMPy on CFME/Th base electrode in monomer free solution of 0.2M $NaClO_4$ in ACN at a scan rate of a)50 b)100 c)150 d)200 e)250 f)300 mV/s

The comparison of different concentrations of NMPy's current-scan rate relationship can also be seen in figure 4.8. It is clear that to a limit value of 0.5M NMPy, current increases but in 0.5M NMPy there is a significant decrease in current values. This can be explained when the monomer concentration of NMPy increases to a higher value, transportation of ions in the solvent, which is acetonitrile, becomes harder, this causes a decrease in current values.

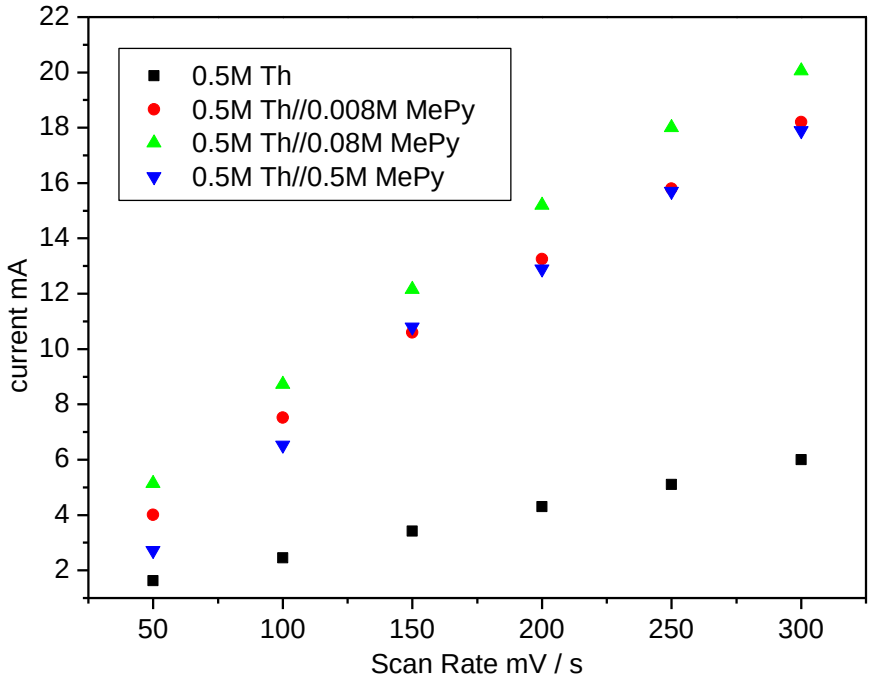

Figure 4.8: Comparison of composites current values in monomer free electrolyte

In figure 4.8 the electrogrowth data of fourth cycles of NMPy's for the concentrations of 0.008M, 0.02M, 0.04M, 0.08M and 0.5M dataset were collected. Fourth cycle of electrodeposition of 0.5M Th was also drawn and it is investigated that electrografting NMPy as composite coating increased the current values. Correlation coefficient of 0.5M Th homopolymer was calculated as 0.9997 from the figure 4.8. For the composites correlation values were estimated for 0.008, 0.08 and 0.5M NMPy as 0.9974, 0.9961, and 0.9913 respectively on CFME/PTh base electrode.

4.2.1.2. Effect of NMPy's cycle number on CFME/PTh base electrode

Increasing cycle number of NMPy's on CFME/PTh base electrode caused an increase in current values for anodic peaks from 3.1 mA to 32.3 mA for same sample and for cathodic peaks current was changed 2.76 mA to 27.3mA for 2 to 8 cycles

The scan rate dependence of the anodic and cathodic peak currents shows a linear dependence on scan rate as illustrated in figure 4.9 and 4.10 for all composites. This demonstrates that the electrochemical process is not diffusion limited and is extremely reversible even at high scan rates. The ability to be switched reversibly in

a non diffusion limited process at scan rates as high as 800mV/s is unusual for conducting polymers may stem from thickness of polymer films.

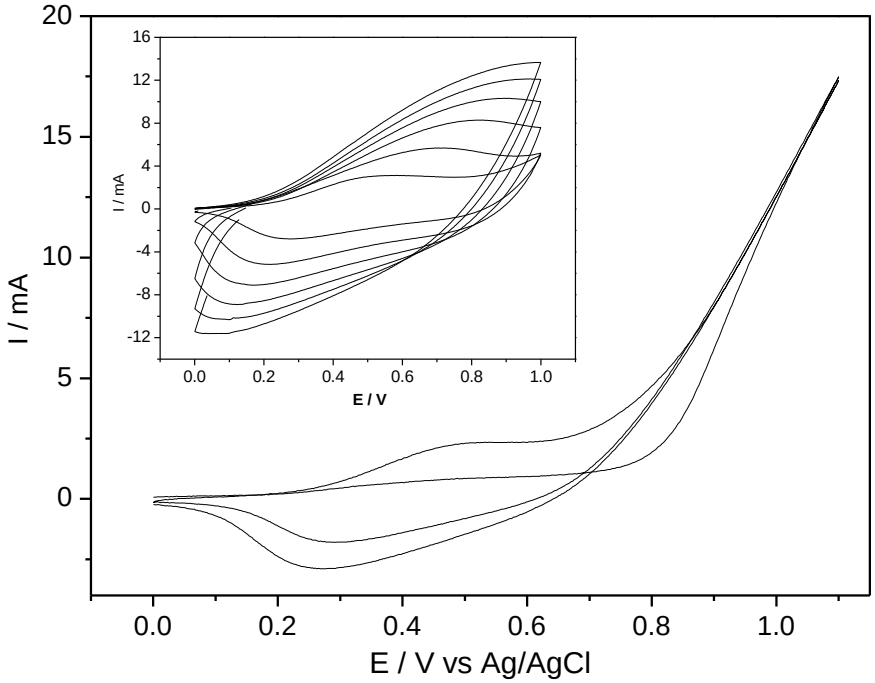

Figure 4.9: Multisweep experiment for oxidation 0.08M NMPy on CFME/PTh base electrode for 2 cycles in 0.2M $NaClO_4$ in ACN in 50mV/sec.Inset: Scan rate dependence of 0.08M NMPy on CFME/PTh base electrode in 0.2M $NaClO_4$ in ACN from 50-300 mV/sec.

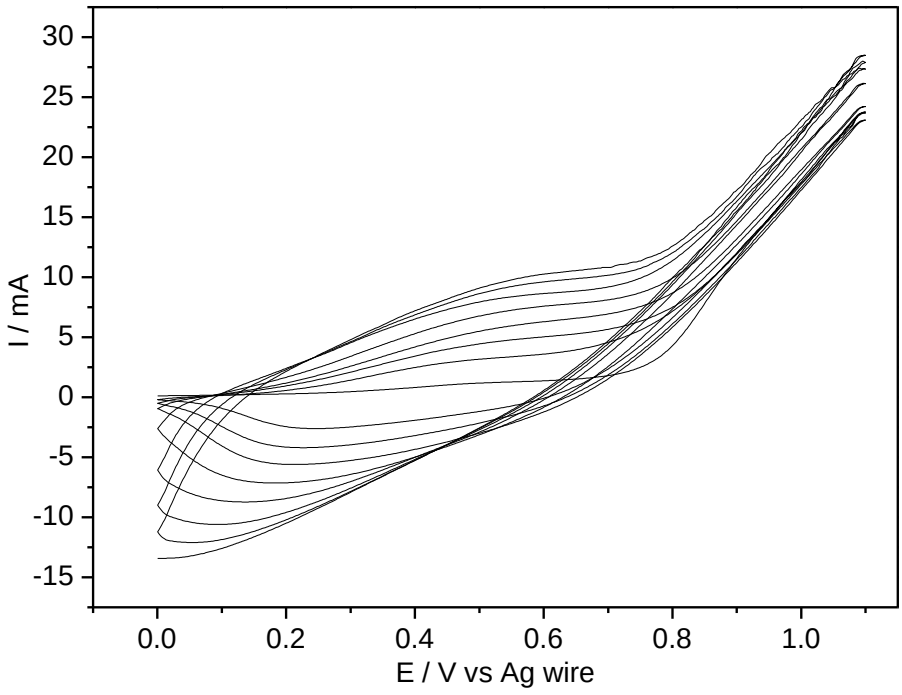

Figure 4.10: Multisweep experiment for oxidation 0.08M NMPy on CFME/PTh base electrode for 8 cycles in 0.2M $NaClO_4$ in ACN in 50mV/sec.

4.2.1.3. Effect of electrolyte

All of these electrolytes were investigated in the same solvent, ACN 0.08M NMPy concentration was chosen as a standard during investigation of electrolyte effect on CFME/PTh. The cyclic voltammograms of composites in 0.1M TEATFB, 0.1M $NaClO_4$ and 0.1M $LiClO_4$ in ACN can be seen in figures 4.11, 4.12 and 4.13.

Changing the electrolyte type from $NaClO_4$ to TEATFB and $LiClO_4$ has affected the oxidation potentials Increasing the electrolyte concentration of $NaClO_4$ from 0.1M to 0.2M caused an decrease in oxidation potential from 0.84V to 0.76V, I_a/I_c was increased from 0.94 to 0.96 reflecting the reversibility of the system. The lowest oxidation potential with a value of 0.82V was obtained for 0.2M $NaClO_4$ which is lower than 0.1M $NaClO_4$. In table 4.3. all results were summarized.

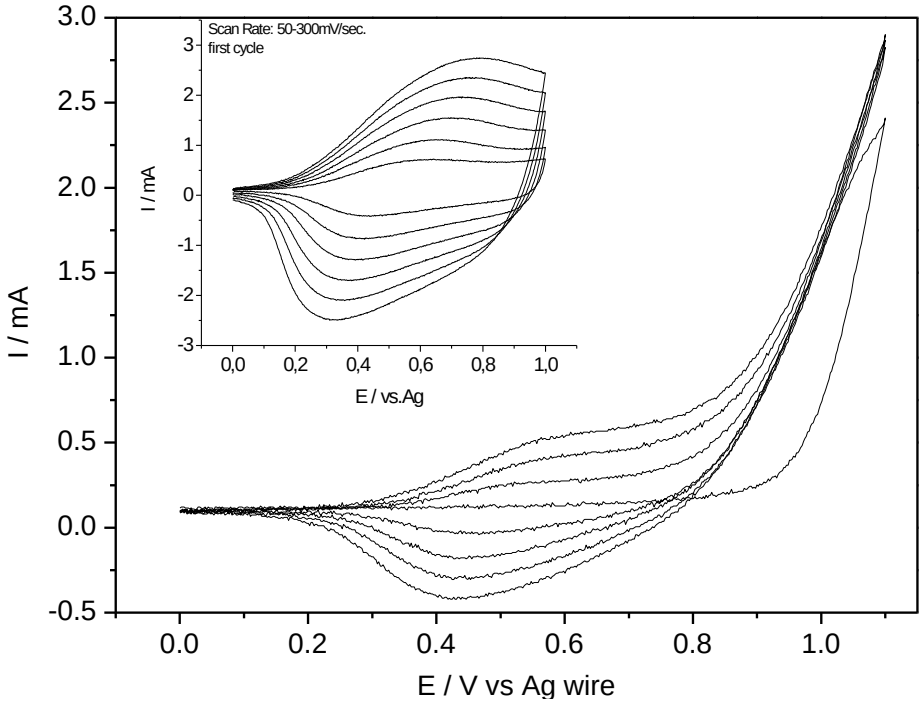

Figure 4.11: Electrogrowth of 0.08M NMPy on CFME/PTh base electrode in 0.1M TEATFB in ACN with a scan rate of 50mVs^{-1}. Inset : Monomer free solution results in 0.1M TEATFB

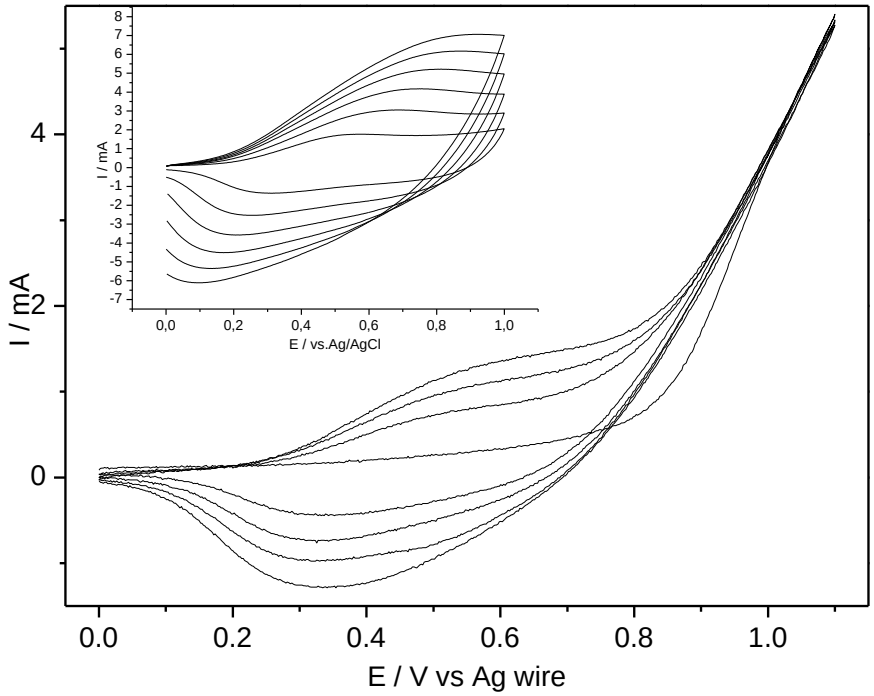

Figure 4.12: Electrogrowth of 0.08M NMPy on CFME/PTh base electrode in 0.1M $LiClO_4$ in ACN with a scan rate of 50mVs^{-1}. Inset: Monomer free solution results in 0.1M $LiClO_4$ scan rate between 50-300mVs^{-1}.

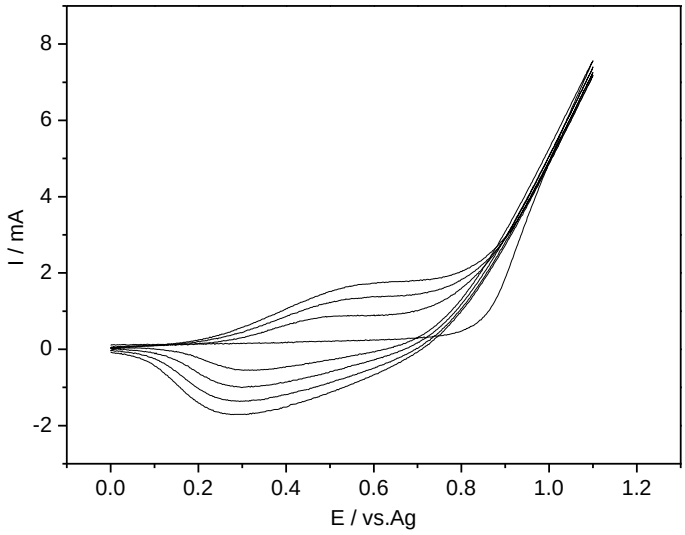

Figure 4.13: Electrogrowth of 0.08M NMPy on CFME/PTh base electrode in 0.1M $NaClO_4$ in ACN with a scan rate of 50 mVs^{-1}.

Table 4.3. Electrogrowth redox parameters in effect of electrolyte.

Electrolyte	E_a (V)	E_c (V)	I_a (mA)	I_c (mA)	I_a/I_c	E_{onset} (V)
0.1M TEATFB	0.67	0.58	0.58	0.42	0.72	0.97
0.1M $LiClO_4$	0.66	0.35	1.45	1.30	0.90	0.82
0.1M $NaClO_4$	0.65	0.30	1.81	1.70	0.94	0.84
0.2M $NaClO_4$	0.67	0.28	3.65	3.5	0.96	0.76

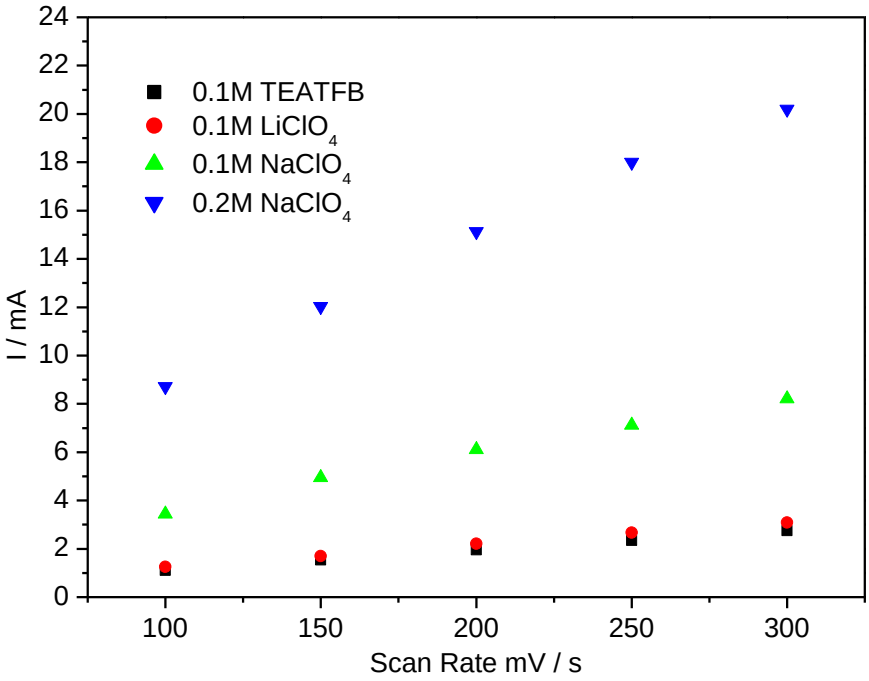

Figure 4.14: Effect of electrolyte on current vs. scan rate.

4.2.1.4. Stability of electrochemical composites in different electrolytes

Stability is a primordial feature, and although PPy is known to be highly sensitive to over-oxidation [88]. The presence of a substituent such as alkylenedioxy groups avoids this type of degradation, as in N-methylpyrrole. It is important to investigate the stability of the polymer on CFME for the practical applications.

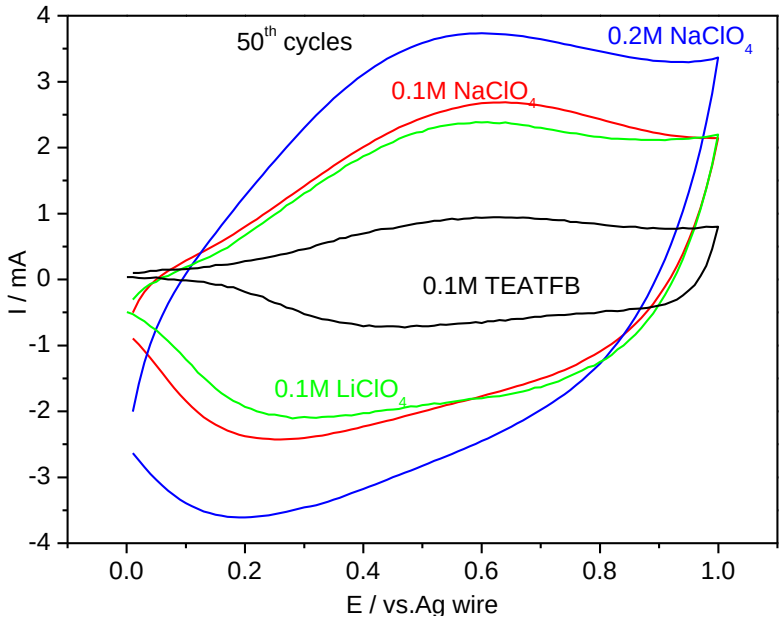

Figure 4.15: Current relations between stability effect of 0.08M NMPy on CFME/PTh base electrode in different electrolytes.

In figure 4.15 the stability effect was investigated according to different electrolyte types. As before 0.08M NMPy was chosen as a standard monomer concentration for formation of electrochemical composites. In monomer free solution 50th cycles were recorded for all types of electrolytes. When increasing the electrolyte concentration from 0.1M to 0.2M current densities were raised up, too. 0.1M TEATFB has the lowest current density values.

Percentage degree of decrease in electroactivity calculated with equation 4.1 and decrease of electroactivity by cycle number was given in Figure 4.16. 0.1M TEATFB was found as the most stable electrolyte during investigations.

$$\text{Decrease in Electroactivity} = \frac{Q_{FRESH} - Q_{FINAL}}{Q_{FRESH}} \times 100 \qquad (4.1)$$

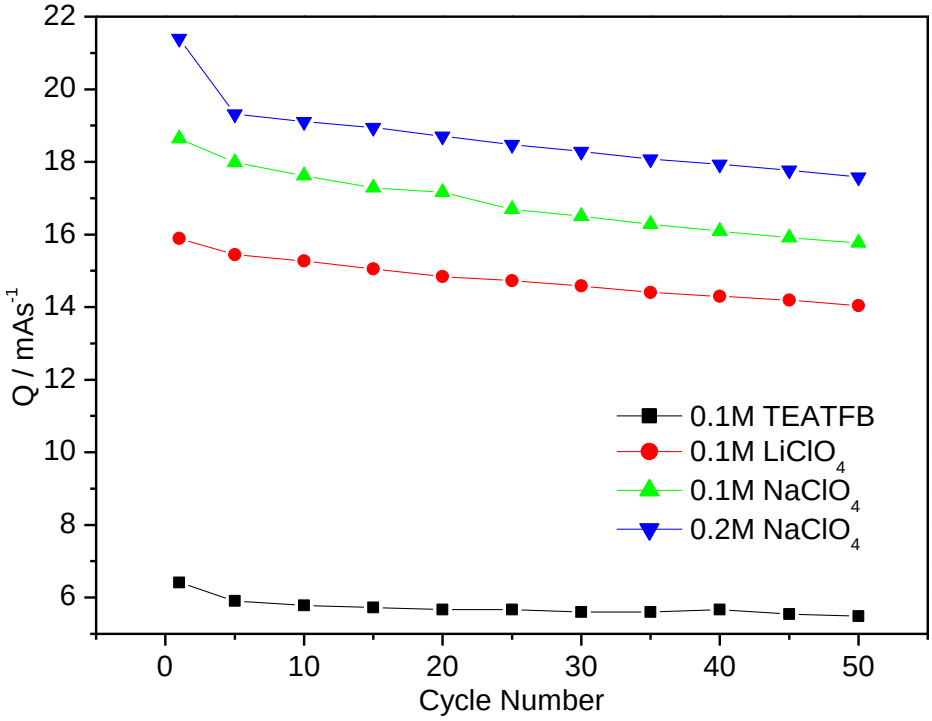

Figure 4.16: Effect of different electrolytes on the stability for 50 cycles in monomer free solutions with a sweep rate of 100mVs^{-1}.

4.3 ATR-FTIR Characterization of Electrocoated Polymer Surfaces

4.3.1. Effect of NMPy's concentration on CFME/PTh

FTIR-ATR was used to characterize the electrografted composite structure. Doping of the respective anion of the supporting electrolyte into the composite structure was also observed by FTIR-ATR from these spectra. This technique seems to be a precise

and practical method, and is a good tool for characterization of the structure of copolymers having a thickness of nano- to micron size.

The electropolymerization of NMPy was achieved on CFME/PTh in 0.2M $NaClO_4$/ACN. The composites that were obtained at different NMPy concentrations were analyzed with FTIR-ATR spectroscopy. Figure 4.17 shows the corresponding spectra between 650 and 4000cm^{-1}. FTIR-ATR of PTh can be seen in Figure 4.17, the bands at 1418cm^{-1} (aromatic stretching of C=C bonds), a broad peak at 1332-1200cm^{-1} (deformation in plane of C-H bond at β position) are known to be characteristic vibrational peaks of polythiophene. When NMPy concentration increased, there is appearance of characteristic peaks of PPy, was seen ie. asymmetric ring stretching mode at 1515cm^{-1} and the symmetric mode at 1420 cm^{-1}. And also a peak at about 1300 cm^{-1} shows N-C stretching of NMPy. The peak intensities increased with NMPy concentration, which confirms the inclusion of NMPy into the composite structure see Figure 4.17. Since ClO_4^- absorbs at 1075cm^{-1}, and the presence of a strong absorption band at this wave number in all composite electrodes clearly indicates the doping of these composites with this anion. The characteristics peaks can be seen in Table 4.4.

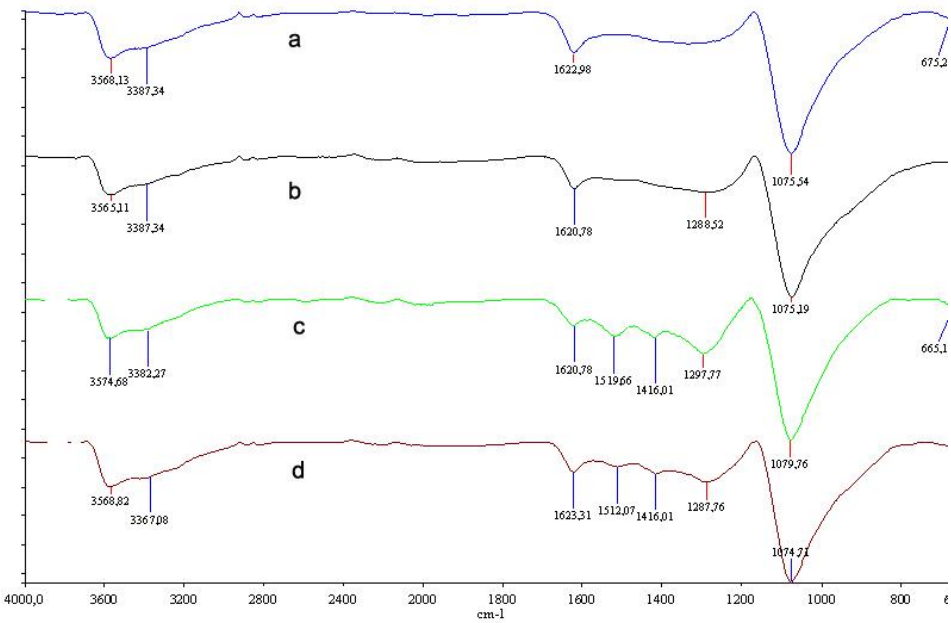

Figure 4.17: Initial concentration effect of increasing NMPy concentration in the ATR-FTIR anaylsis. Thiophene concentration was held constant at 0.5M Th and NMPy concentration varies as a) [NMPy]=0.008M b) thiophene homopolymer c) [NMPy]=0.08M d) [NMPy]=0.5M

Table 4.4. Assignment of the bands in the ATR-FTIR spectra of NMPy.

Bands (ν / cm^{-1})	**Assignment**
1610	ν (C=C), ν (C-C) in the ring and ring bending
1520	C-N asymmetric ring stretching
1440	C=C aromatic stretching
1420	C-N symmetric mode
1330-1200	ν(C-H) bond deformation at β position
1300	N-C stretching
1075	ClO^-_4
675	γ(C-H) r(CH_3)

Stretching (ν), out of plane bending (γ), rocking (r)

4.3.2. Effect of NMPy's cycle number on CFME/PTh

FTIR-ATR spectra of electrochemical composites with different cycle numbers shown in Figure 4.18 Characteristic peaks of NMPy were between 1200 and 1600 cm^{-1} for 2 cycles of NMPy indistinct peaks can be seen. Intensity of characteristic peaks were increased linearly with the cycle numbers. Larraz et al.[89] attributed the bands of 1460cm^{-1} for NMPy refers to the characteristic peaks of C-N, C=C, C=C-N which we also observed peaks at 1416cm^{-1} for 4 cycles of NMPy and 1433 cm^{-1} for 8 cycle. No significant characteristic peaks of NMPy were observed for the electrografting of NMPy for 2 cycles.

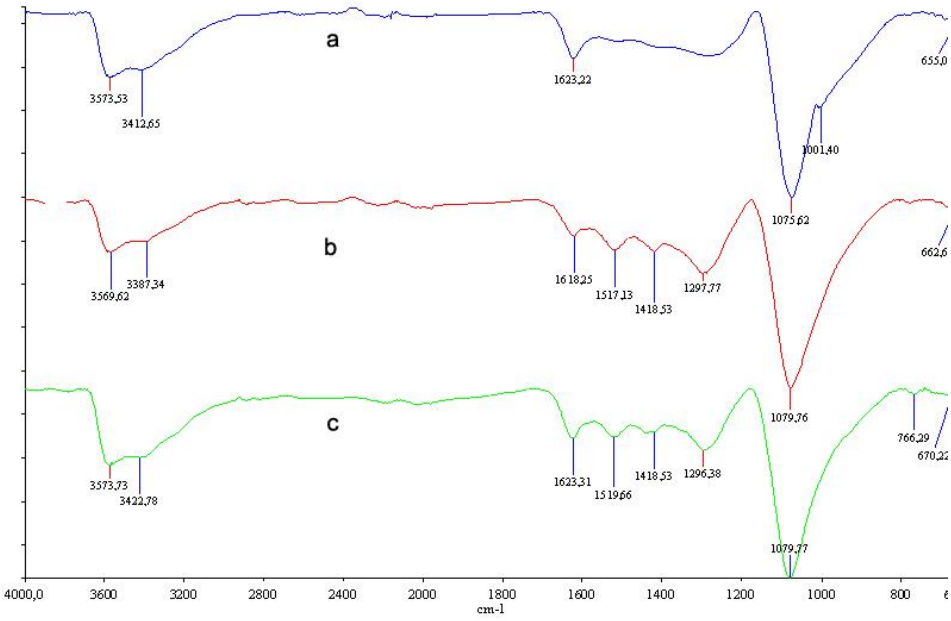

Figure 4.18: IR analysis of cycle effect.Thiophene cycle number was held constant at 4 cycle,NMPy cycle number was changed for 0.5M Th // 0.08M NMPy composite. a) 2 cycle of NMPy b) 4 cycle of NMPy c) 8 cycle of NMPy

4.3.3. Effect of electrolyte

Monomer concentrations were held constant for the electrocomposite prepared at 0.5M Th and 0.08M NMPy. For electrochemical composites only electrolytes were changed as 0.1M $NaClO_4$, 0.2M $NaClO_4$, 0.1M $LiClO_4$ and 0.1M TEATFB in ACN. In figure 4.19 it can be seen that increasing the electrolyte concentration from 0.1M to 0.2M causes a raise in the inclusion of ClO_4^- as dopant.

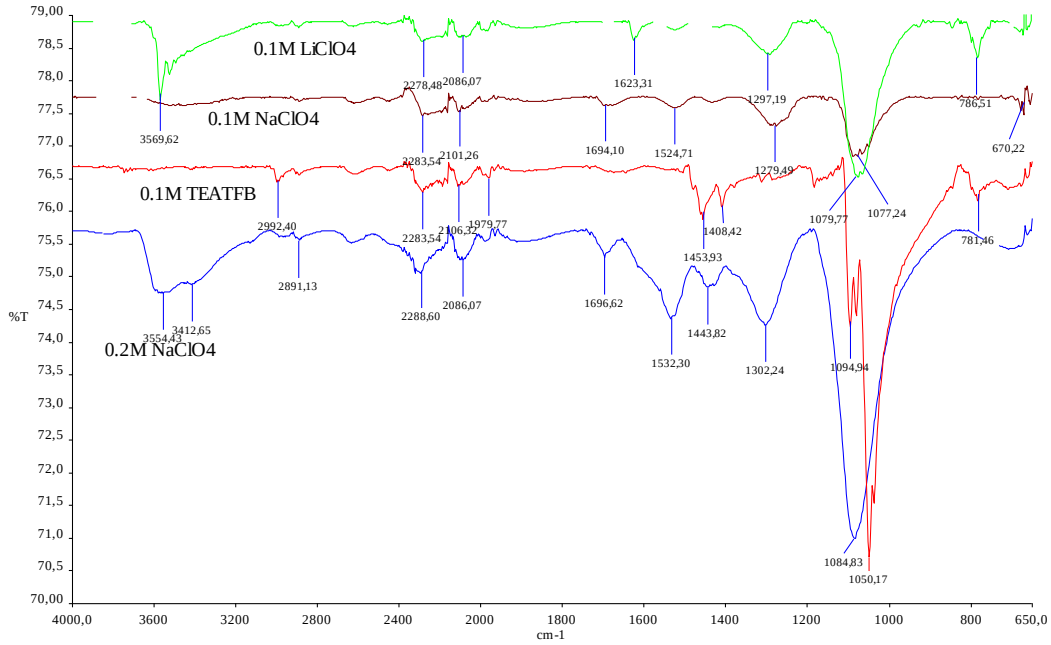

Figure 4.19: FTIR-ATR analyses of different electrolytes in ACN for 0.08M NMPy on CFME/PTh. a) 0.1M $LiClO_4$ b) 0.1M $NaClO_4$ c) 0.1M TEATFB d) 0.2M $NaClO_4$.

4.4. Morphological Analysis

The morphology of NMPy electrochemical composites were investigated by scanning electron microscopy (SEM) and compared with the effect of monomer concentration, cycle number and NMPy's copolymer (see in Figure A. 7) in order to understand the surface structure. Figure 4.20 shows electrochemically deposited sample with scan rate of 50mV/s by CV. NMPy concentration was found to have an effect on the film morphology. PTh has shown very smooth and homogenous structure (see in Figure A.8), however, small grains formed with the inclusion of NMPy. The thickness of 0.04M NMPy and 0.08M NMPy composite on CFME/PTh were 0.6 and 0.7µm please note that thickness of carbon fiber excluded.

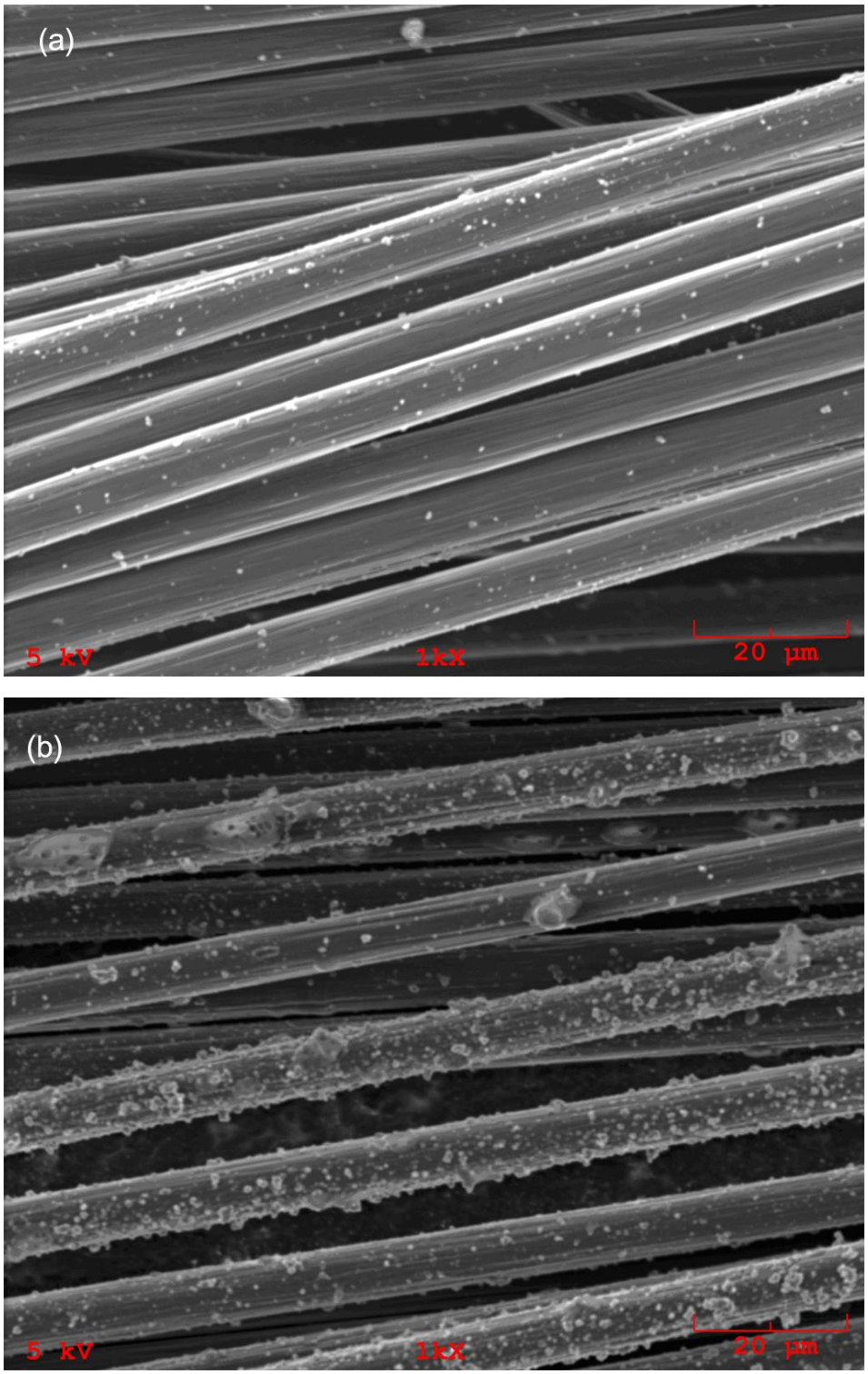

Figure 4.20: a) SEM image of NMPY on CFME/PTh 0.04M NMPy on CFME/PTh with a thickness of 0.6µm **b)** SEM image of NMPY on CFME/PTh 0.08M NMPy on CFME/PTh with a thickness of 0.7µm

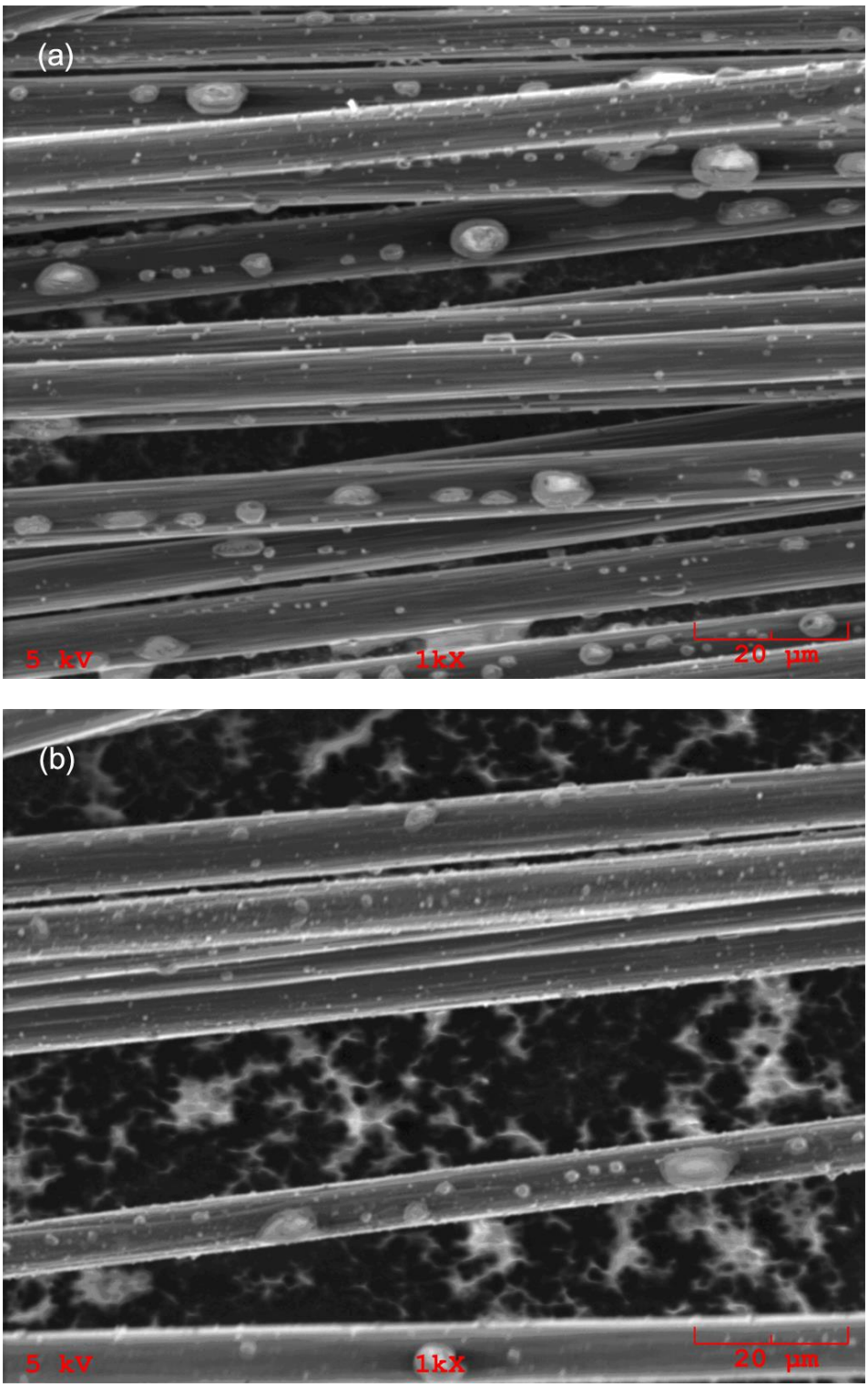

Figure 4.21: a) SEM images of NMPY on CFME/PTh 0.08M NMPy on CFME/PTh with 2 cycles. **b)** SEM images of NMPY on CFME/PTh 0.08M NMPy on CFME/PTh with 8 cycles

As the monomer concentration of NMPy increases from 0.04M to 0.08M, the grains that are formed on the surface of CFME/PTh also showed a raise (Figure 4.20b) .The structure of NMPy is more cauliflower like on higher concentrations.

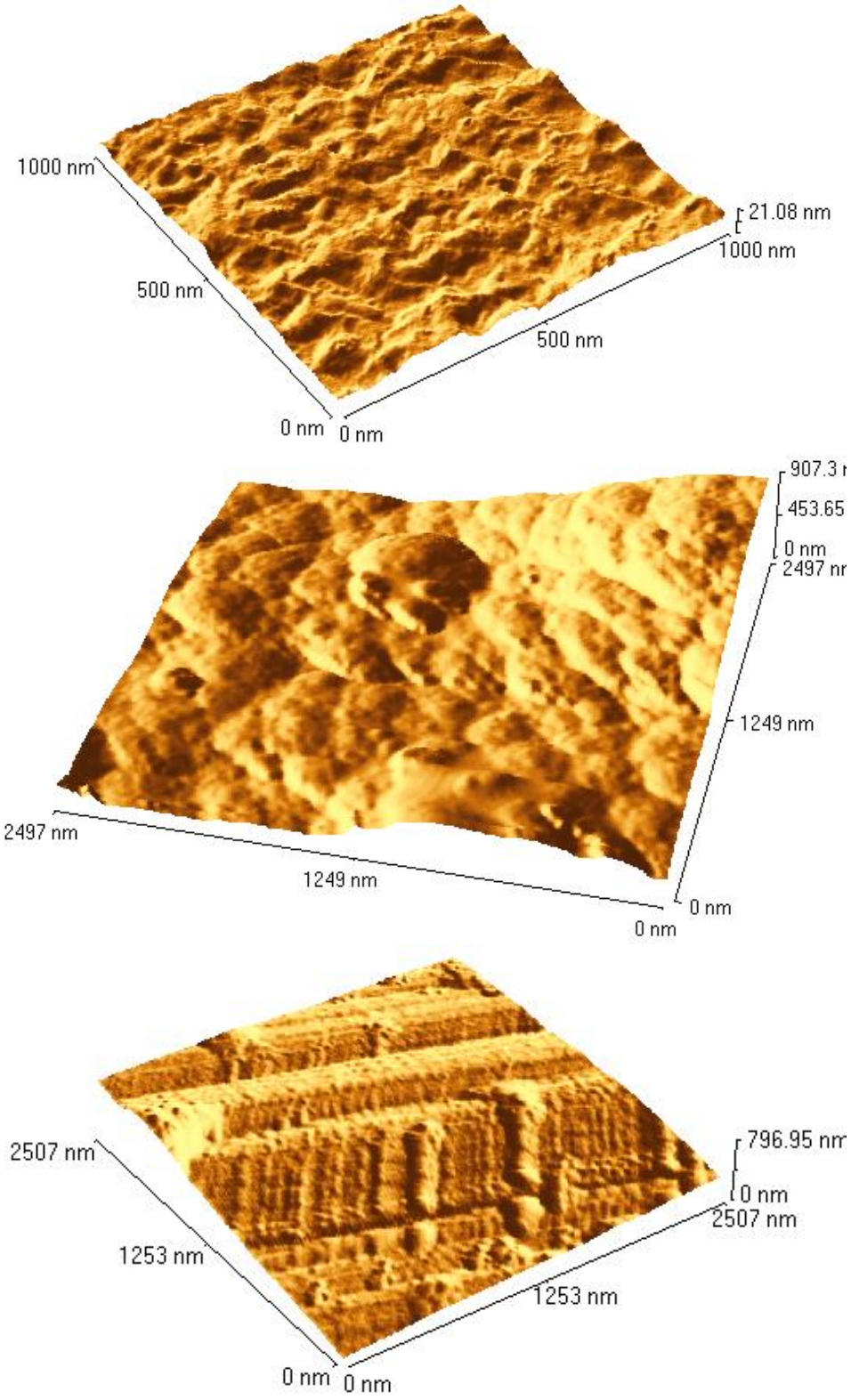

Figure 4.22: AFM images electrografting NMPy on CFME/PTh **a)** 0.008M NMPy **b)** 0.8M NMPy **c)** 0.5M NMPy

Effect of cycle number was also investigated with respect to 0.08M NMPy concentration on CFME/PTh base electrode in 0.2M $NaClO_4$ in ACN by cyclic voltammetry with a scan rate of $50mVs^{-1}$. Monomer concentrations and thiophene's cycle number was held constant. The only parameter which was changed is NMPy's

cycle number from 2 to 8 for 3 steps. Morphological structures can be seen in figure 4.21. Increasing cycle number of NMPy also increases the grains of NMPy which were on the surface of CFME/PTh electrode.

The preparation of the composites onto CFMEs was followed by atomic force microscopy (AFM). During electropolymerization, we studied the effect of monomer concentration in the cyclic voltammetric experiments on the growth of the conducting polymer films. Figure 4.22 shows the AFM images of composite grown on the carbon fiber thiophene base electrodes.

As shown in the AFM images obtained at the lowest concentration of NMPy (0.008M) surface roughness is extremely low. This indicates that deposition of NMPy extremely limited <10 nm and surface was very smooth (Figure 4.22a).

Due to the addition of NMPy (0.08) in the same amount than thiophene (0.5M) the surface of the polymer coating is not structured and the grains are larger than in samples containing a lower amount of NMPy. The grain has an oval shape of ~240 x 180 nm. At the optimum conditions (0.08M) surface looks very rough and the gap between highest and lowest point of the coated film is approximately 600 nm (Figure 4.22b)

The thickness of the PNMPy layers after four cycles increased with increasing monomer concentration i.e. 0.5M NMPy, showing highly oriented grains. The thickness of the coating is relatively high it is roughly 0.7 micrometer which can be compared to the thickness of the carbon fiber electrode. The organized structure of thiophene is not always present, grain size: 90 x 30 nm. (Figure 4.22c).

4.5. Thermal Analysis

The thermal properties of the homopolymers of PTh on CFME and PNMPy on PTh/CMFE base electrode were thermogravimetric analysis (TGA). The results of the measurements are summarized in Table 4.5.

All the compounds exhibited a glass transition in the first heating, and no crystallization exotherms and except for 0.1M TEATFB and 0.1M $LiClO_4$ cases no melting endotherms were noticed.

Table 4.5. Summary of the results obtained from TGA .

	Weight loss at 550 ºC[*1], TGA
0.5M Th Homopolymer	6%
0.008M NMPy on CFME/PTh	7%
0.1M TEATFB, 0.08M NMPy	< 1%
0.1M $LiClO_4$, 0.08M NMPy	2%
0.1M $NaClO_4$, 0.08M NMPy	4%

[*1] Weight loss of bare carbon fiber is 8% at 550 **ºC**

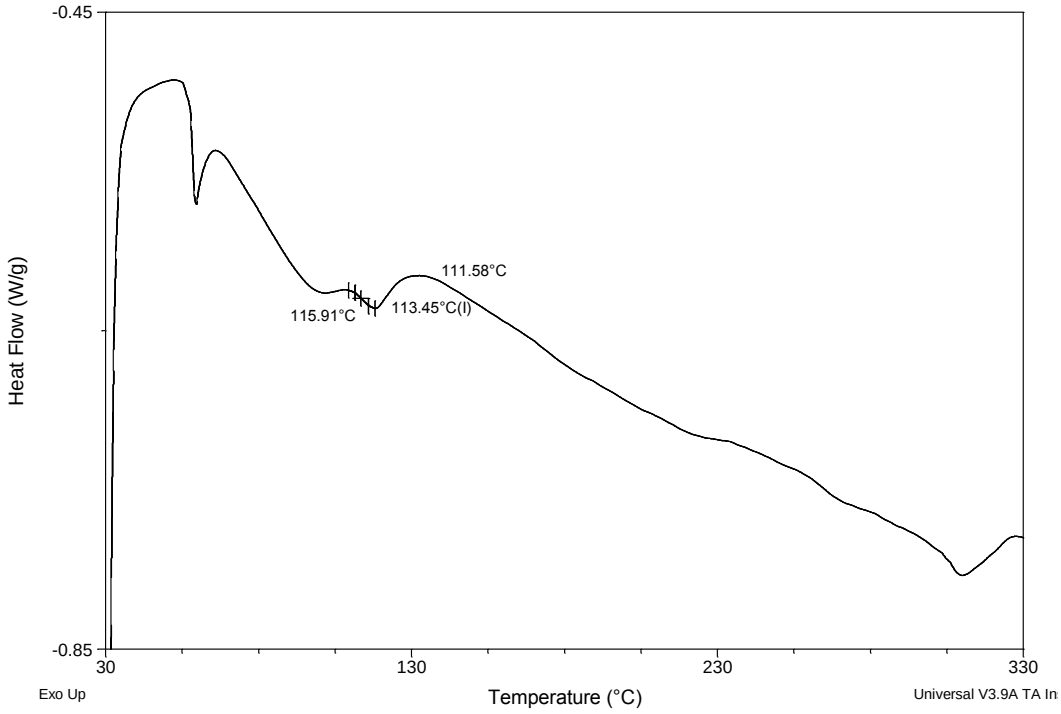

Figure 4.23: DSC thermogram of PTh was prepared in 0.5M Th and 0.1M $NaClO_4$ on CFME.

DSC thermogram of the pure PTh showed two endothermic transitions. The first peak stats at 85 and gives Tg at 115°C for the removal of solvent, and the second broad endohtermic peak centered at 310°C for the loss of dopant ion. (ACN bp for ACN is 81-82°C)

For PTh, the DSC thermogram shows a transition centered at 50°C, which can be attributed to a relaxation of conformons. This transition temperature seem too low to be taken as *Tg* for a linear PT with α, α'-coupling, which would be higher than 50°C. Such low *Tg's* must be due to structure defects such as cross-linking and α,β

couplings for thiophene rings, which usudly appear in PTh with a thickness greater than 1 μm prepared using the electrochemical method. [4,90]

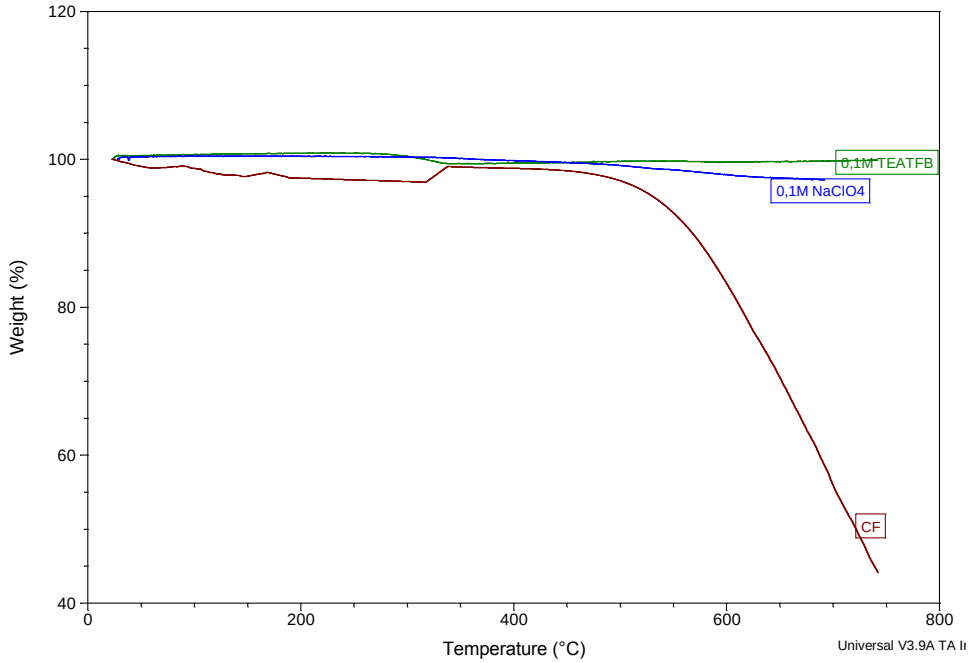

Figure 4.24: TGA of **a)** 0.1M TEATFB **b)** 0.1M $NaClO_4$ **c)** bare CF

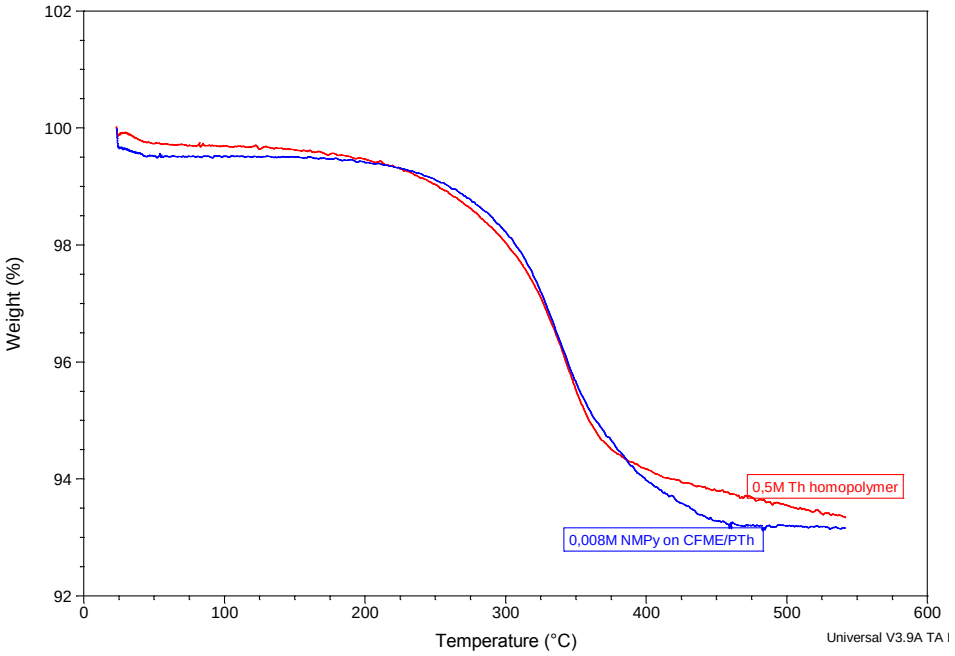

Figure 4.25: TGA of **a)** 0.5M Th on CFME Homopolymers **b)** 0.008M NMPy on CFME/PTh base electrode Composite.

TGA results indicate that composite material on CF increases the thermal stability of CF. Weight loss of bare CF is around 8% at 550ºC while 0.5M Th coated CF is 6% and 0.08M NMPy coated CFME/PTh is 4%. Bare CF was stable up to 550ºC and

sharply decomposes starting from this value at 750ºC, 55% of the CF decomposes, whereas at same temperature decomposition percentage of the CF which is coated in 0.1M $NaClO_4$, 0.08M NMPy is around 5% and in 0.1M 0.1M TEATFB, 0.08M NMPy is less than 2%. (Figure 4.25 and 4.26). Thermal stability of the obtained composite materials appears to be influenced by the type of dopant; small molecules e.g. $LiClO_4$ and $NaClO_4$, can be easily removed by heating, whereas large molecules e.g. TEATFB, are more strongly bound.

4.6. Electrical Conductivity

In order to perform solid state conductivity measurements, polymerization reactions were performed electrochemically at a constant current in ACN solution containing 0.2M $NaClO_4$ and the monomers.

Table 4.6. Electrical conductivities of the polymers measured with four point probe solid conductivity.

Initial Concentrations of Monomers, [M]	Conductivity [S cm^{-1}]	Deposition Time [min]
Homopolymers		
0.5M Th	423.7	30
0.008M MPy	133.7	30
Composites		
0.5M Th//0.008M MPy	120.4	30
0.5M Th//0.08M MPy	126.1	30
Copolymers		
Th-co-NMPy(0.5M-0.08M)	381.5	30

Polymer films were electrografted by galvanostatically way onto platinum plate electrodes. Obtained polymers were removed from electrode from surface and prepared as pellet and used for solid state conductivity measurements. An electrometer connected to a four probe head. Electrical conductivity has been calculated from conductivity equation (Eq 2.7). Measurements indicated that conductivities of the polymers as high as 400 S cm^{-1} for homopolymer of Th and copolymer of Th-co-NMPy. Solid state conductivity of NMPy homopolymer is three times lower than that of thiophene and copolymer prepared with Th and NMPy, conductivities of all composite coatings remained very close to homopolymer of NMPy (Table 4.6). Due to the outermost layer is NMPy coating and the measured conductivity may be only conductivity of NMPy and it is lower than expected value.

4.7. Electrochemical Impedance Spectroscopy (EIS)

Electrochemical impedance spectroscopy was employed to monitor the electrochemical behavior of the composite electrodes. All composites show a slight deviation from capacitive line, indicating fast charge transfer at the carbon fiber | polymer and polymer | solution interfaces, as well as fast charge transport in the polymer bulk. If the slope of the Nyquist plot is higher than 45° composite shows capacitive behavior also if the plot closer to Zim axis this indicates that higher capacitive behavior. Obtaining composite electrode with PNMPy on CFME/PTh base electrode increased capacitive behavior as can be seen in figure 4.7. Increase in NMPy concentration from 0.02M to 0.08M the charge storage ability decrease because of lower capacitive behavior of NMPy.

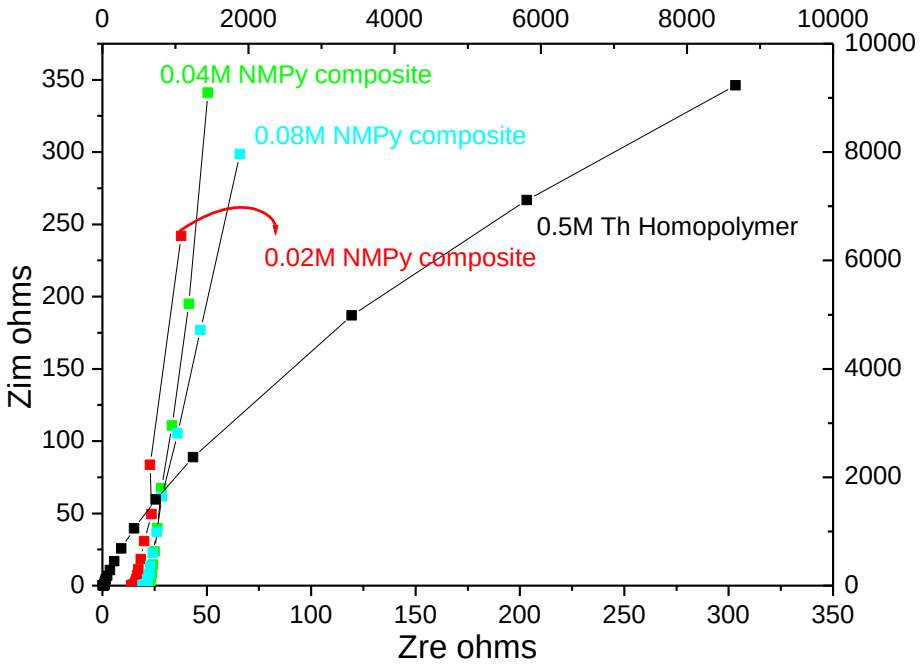

Figure 4.26: Nyquist plots of 0.02, 0.04 and 0.08M NMPy on CFME/PTh base electrode and 0.5M Th homopolymer on CFME in in 0.2M $NaClO_4$ in ACN at 50 mV/s.

In the Bodephase graphics 0.5M Th homopolymer showed a capacitive behavior as 68° and after obtaining composite coating over PTh with NMPy increased the Bodephase angle to 80° which related to higher capacitive behavior see figure 4.28.

The slope of the impedance magnitude and frequency plot indicated that the magnitude of total resistance does not change with the frequency, especially 0.008M and 0.08M NMPy composites that means the composites obtained would be more

homogenous film. The resistance of these composites smaller than other composites and also PTh that may indicate that conductivities of former composites higher than PTh and 0.5M NMPy composite see 4.29.

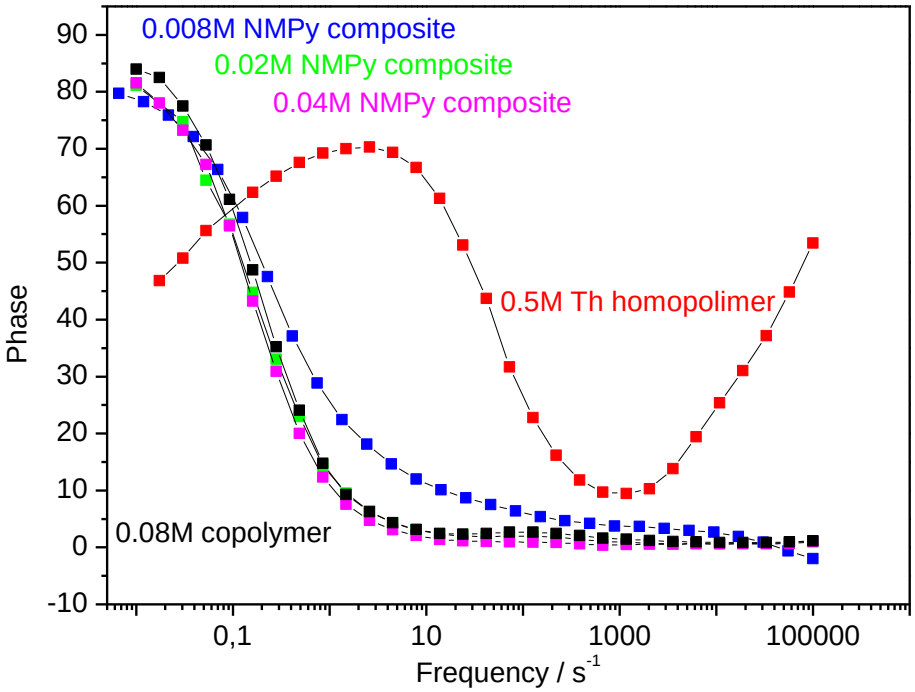

Figure 4.27: Bodephase graphics of 0.008M, 0.02M, 0.04M, 0.08M and 0.5M NMPy on CFME/PTh base electrode in 0.2M $NaClO_4$ in ACN at 50mV /s.

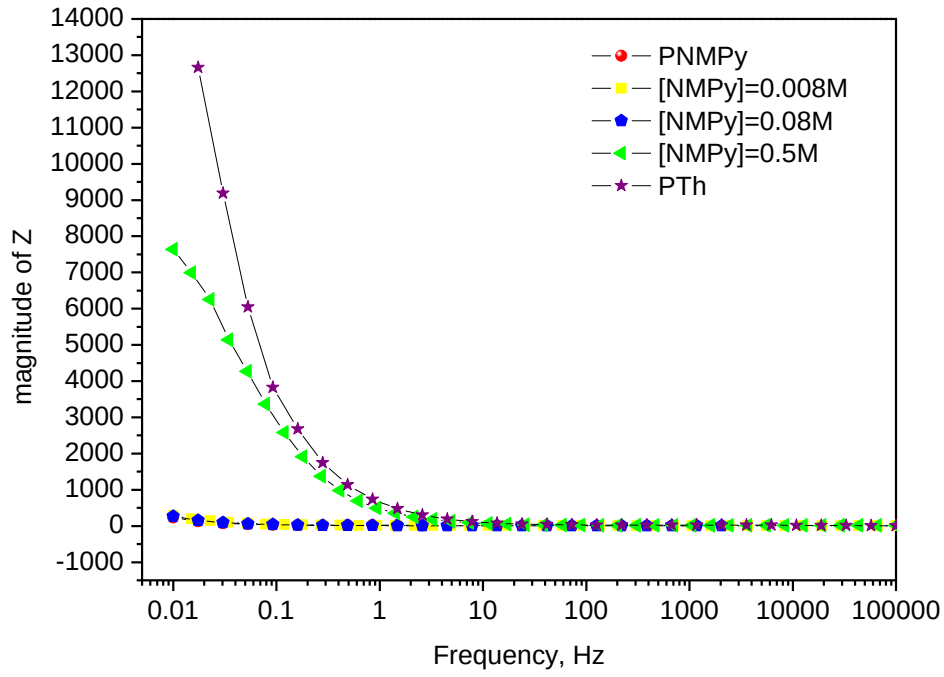

Figure 4.28: Bode magnitude of Z vs frequency plot of the composites obtained with different NMPy concentrations on CFME/PTh in 0.2M $NaClO_4$/ACN.

The EIS results presented in the Bode plots in Figure 4.30 constitute the different capacitor behavior of PTh from the composites and copolymer. The Bode plot of the composite and copolymer shows with a maximum phase angle at 10 mHz of near 90° as expected for an ideal capacitor. The plot for PTh presents phase angle of about 70° (0.5Hz-7.5Hz), that is also capacitive, however smaller than the composites and copolymer.

Figure 4.31 indicated that the thicker film for composite brings about more vertical line to the imaginary impedance axis that means more capacitive behavior of composite film. That result supported with the Bode plot (Figure 4.32) since the thicker composite film presents phase angle of 80° (near ideal capacitor) and the thin film shows a phase angle of 70°(smaller).

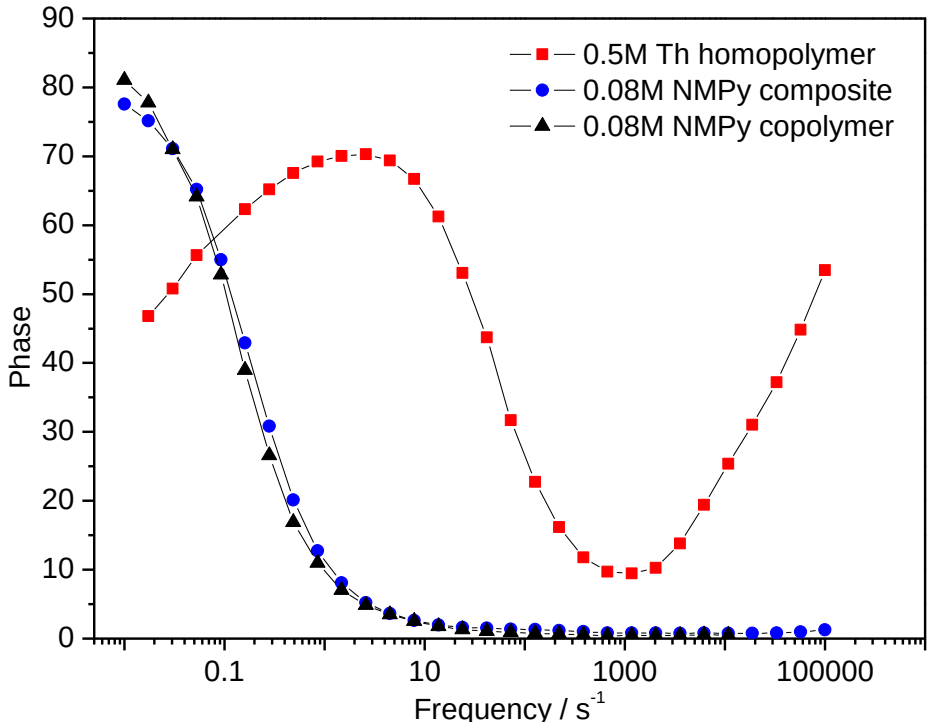

Figure 4.29: Bodephase graphics of 0.5M Th homopolymers, 0.08M NMPy on CFME/PTh base electrode and copolymer of 0.08M NMPy and 0.5M Th in 0.2M $NaClO_4$ in ACN at 50mV/s.

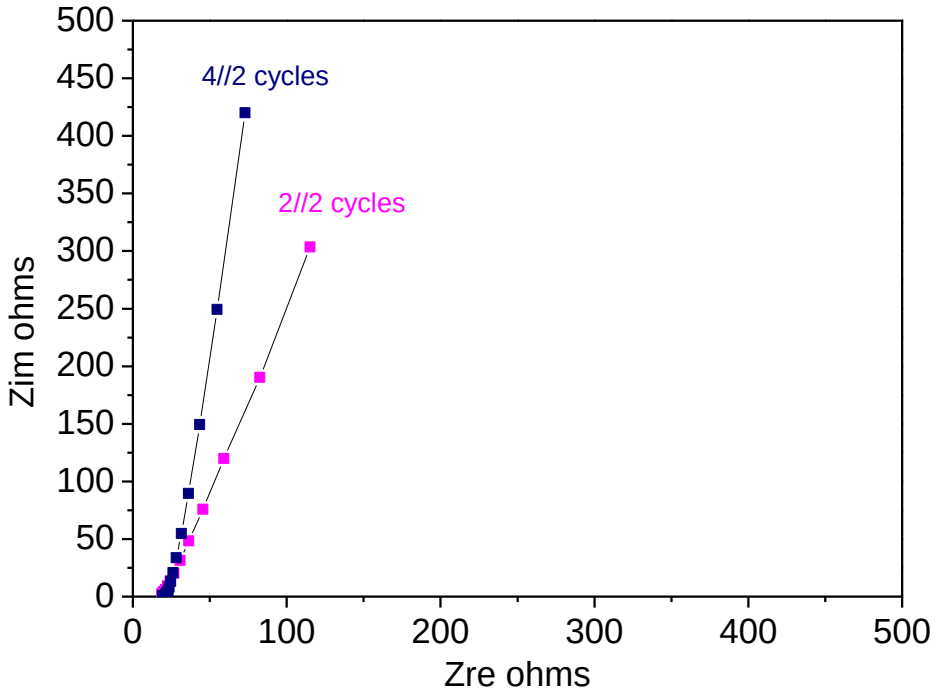

Figure 4.30: Nyquist plot of 0.08M NMPy on CFME/PTh base electrode repeated by 4 and 2 cycles of Th in 0.2M $NaClO_4$ in ACN at 50 mV/s.

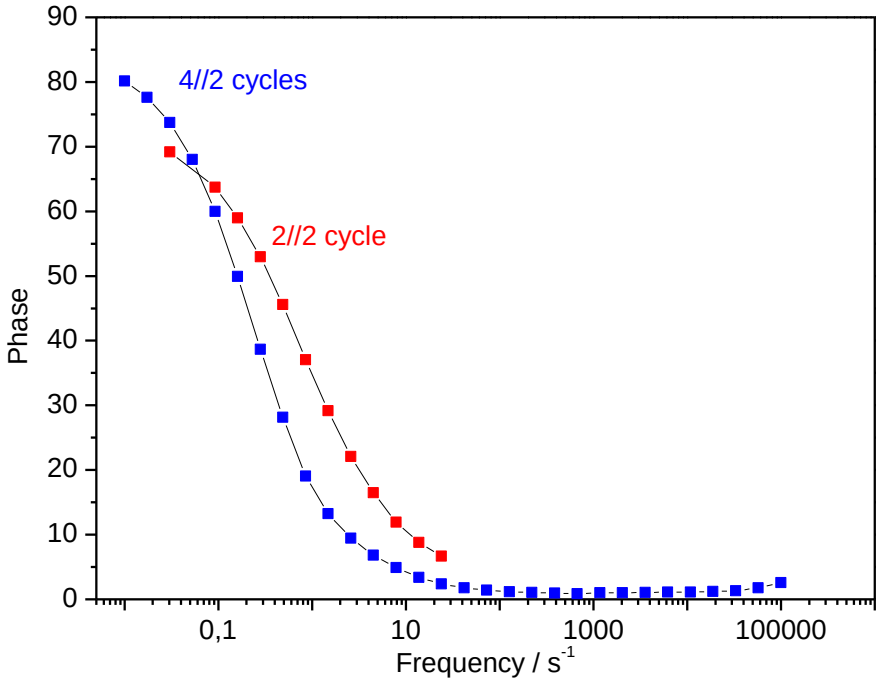

Figure 4.31: Bodephase graphics of 0.08M NMPy on CFME/PTh base electrode for 2 and 4 cycles of 0.5M Th in 0.2M $NaClO_4$ in ACN at 50 mV/s.

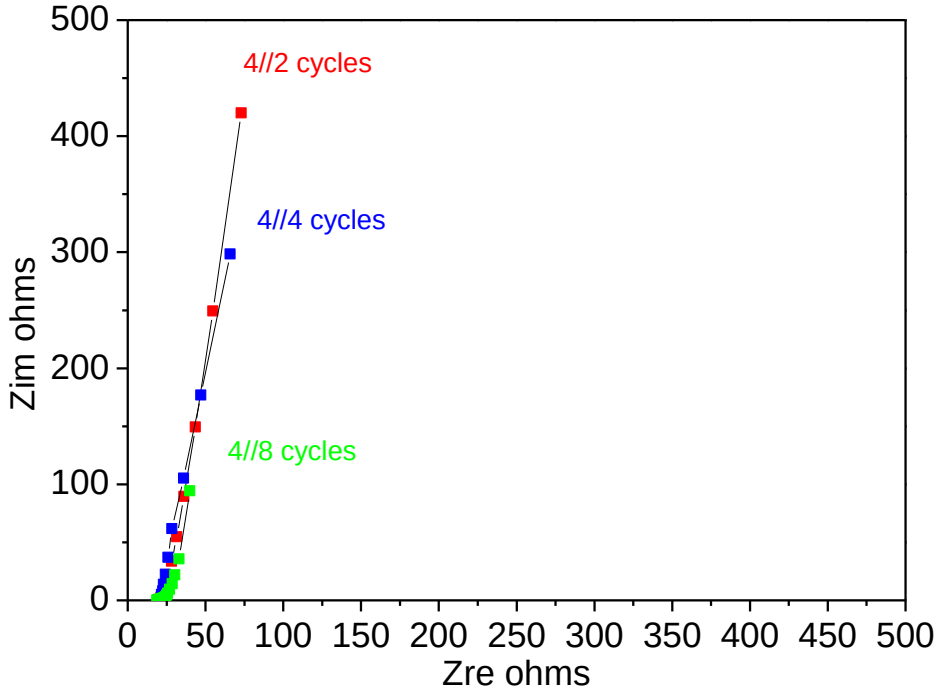

Figure 4.32: Nyquist plots of 0.08M NMPy with 2 , 4 and 8 cycles on CFME/Pth base electrode in 0.2M $NaClO_4$ in ACN at 50 mV/s.

When it is increased PNMPy cycles to obtain composite film, the Nyquist plot indicated that increasing PNMPy cycles does not raised up capacitive responses, see figure 4.33., however, decreased polymer resistance values that indicates the conductivity values of the composites which should be increased, figure 4.34.

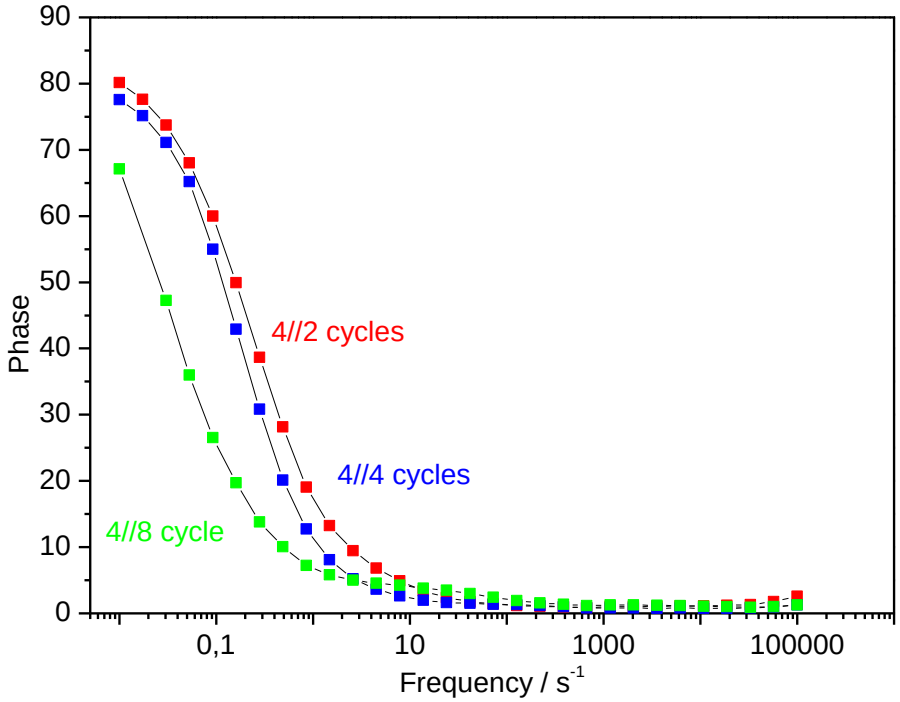

Figure 4.33: Bodephase graphics of 0.08M NMPy on CFME/PTh base electrode for 2, 4 and 8 cycles in 0.2M $NaClO_4$ in ACN at 50 mV/s.

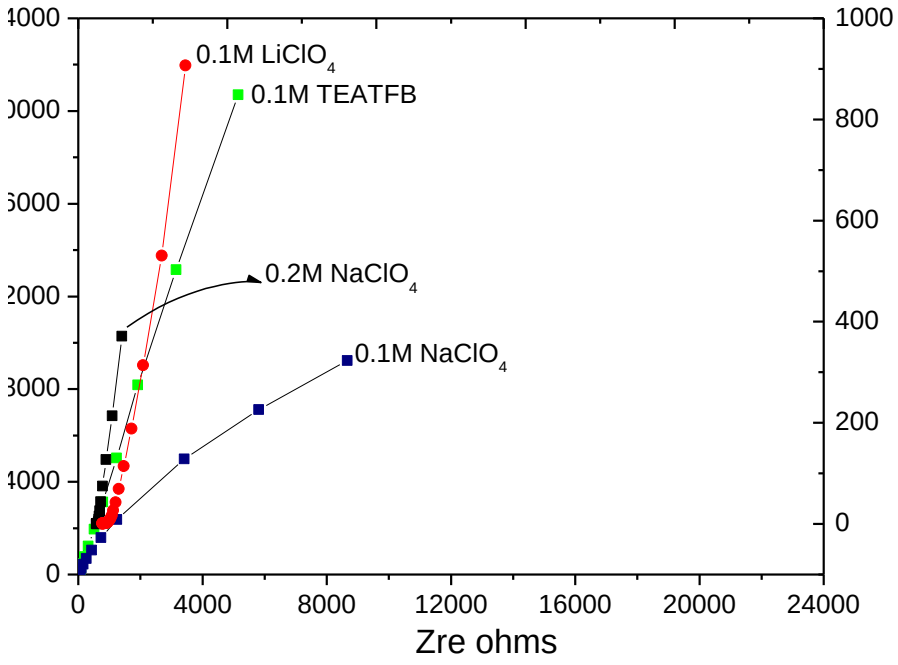

Figure 4.34: Nyquist plot data of 0.08M NMPy on CFME/PTh base electrode in different electrolytes

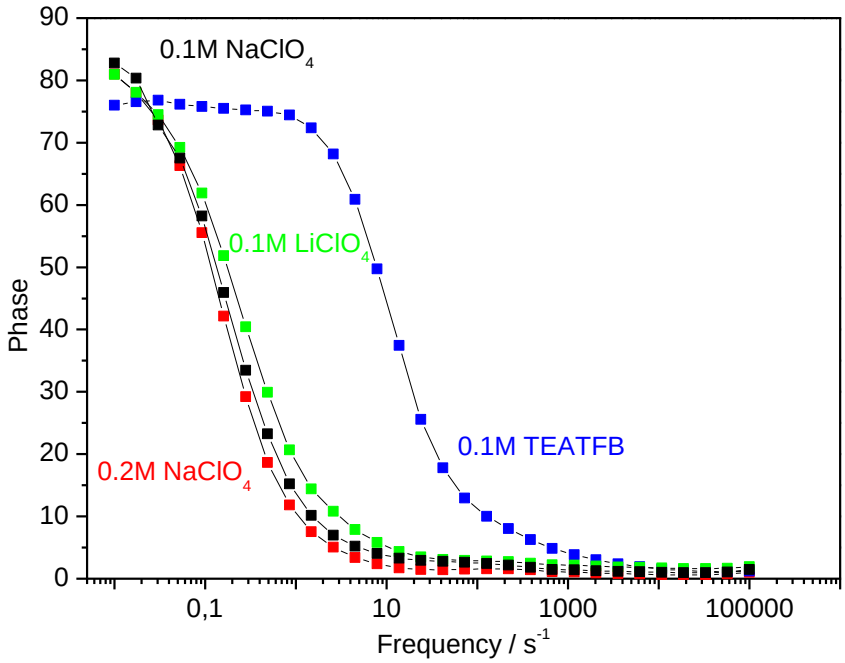

Figure 4.35: Bode phase graphics of 0.08M NMPy on CFME/PTh base electrode with different electrolytes as 0.1M TEATFB, 0.1M $LiClO_4$, 0.1M $NaClO_4$ and 0.2M $NaClO_4$ in 0.2M $NaClO_4$ in ACN at 50 mV/s.

The effect of electrolyte on the composites was also investigated by EIS. The Nyquist plots of the composite obtained in $LiClO_4$, TEATFB and $NaClO_4$ are presented in Figure 4.35. The spectra for $LiClO_4$ indicated more capacitive behavior

since a line vertical to imaginary axis, and the spectra for 0.1M and 0.2M $NaClO_4$ showed a linear line with a slope of 45° this behavior indicates Wardburg diffusion region attributable to the semi-infinite diffusion at polymer-electrolyte interfaces. As increased electrolyte concentration from 0.1M to 0.2M in $NaClO_4$, increased capacitive behavior of the composite film, which is would be helpful to ease electron transfer at the carbon fiber | polymer and polymer | solution interfaces (Figure 4.36).

5. CONCLUSIONS

In conclusion using CFMEs rather than platinum electrode were investigated as an advantage in electrochemical polymerization techniques due to obtained high current values in carbon fibers.

During cyclic Voltammetry characterizations effect of NMPy concentrations on CFME/PTh as an electrochemical composite showed a strong influence on oxidation potential. Increasing NMPy concentration showed decrease in onset potentials. Also cycle number effect of NMPy examined increasing NMPy cycle number also increase current values linearly.

Between the electrolytes 0.2M $NaClO_4$ has the highest value of anodic current vs cathodic current as 0.96 which corresponds better reversibility than the other electrolytes. It has the lowest oxidation potential as 0.76 as compared to the others.

From ATR-FTIR results increase in NMPy concentrations shows an increase in intensity of NMPy's characteristics peaks. Increasing cycle number of NMPy also makes the same effect.

Solid state conductivity of NMPy homopolymer is three times lower than that of thiophene and copolymer prepared with Th and NMPy, conductivities of all composite coatings remained very close to homopolymer of NMPy. Measurements indicated that conductivities of the polymers as high as 400 S cm^{-1} for homopolymer of Th and copolymer of Th-co-NMPy.

Morphological results indicate the inclusion of NMPy in composite structure of CFME/PTh base electrode. Increasing NMPy concentrations obviously showed more grain formation on electrode surface also cycle effect support this idea.

Thermal analysis showed that electrocoating the bare carbon fiber with Th and NMPy composite system increases the thermal stability.

Inclusion of NMPy into the structures increases the capacitive behavior compared to the homopolymer. Changing PTh's cycle number causes an increase in Bode Phase angles and the values get closer to supercapacitor behavior. Contrary to that

increasing NMPy cycle number shows a decrease in capacitive behavior. Examination of electrolyte effect suggested that 0.2M $NaClO_4$ in ACN shows the highest capacitive behavior for the composite system.

Finally, from CV and ATR-FTIR results it is concluded that plausible electrochemical composite reaction mechanism of NMPy on CFME/Th base electrode might be suggested as in Scheme 5.1.

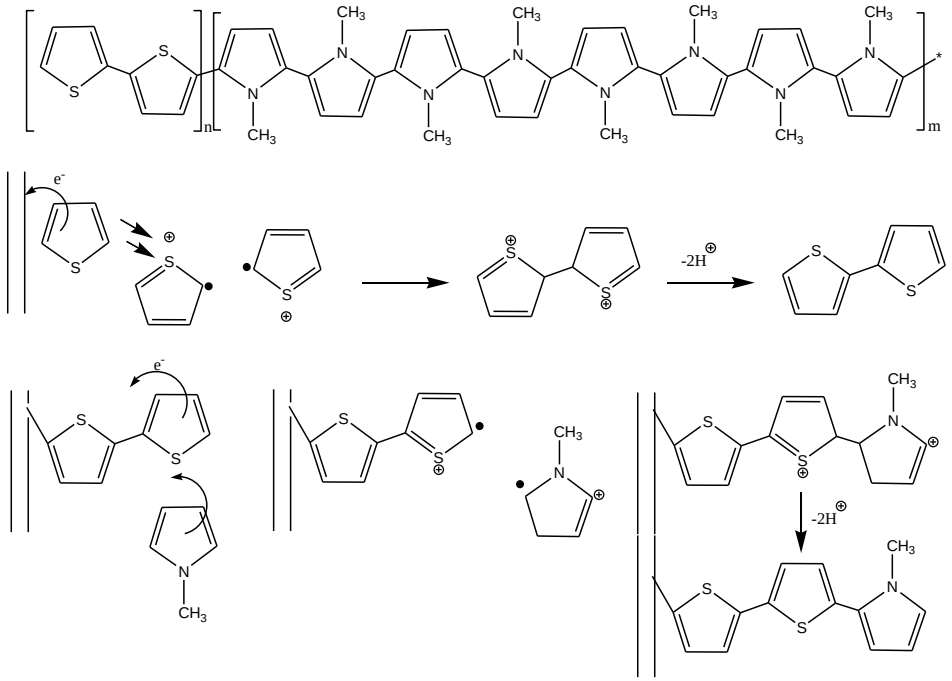

Scheme 5.1: Electrochemical composite reaction mechanism of NMPy on CFME/Th base electrode.

REFERENCES

[1] **H. Shirakawa, E. J. Louis, A. G. Macdiarmid, C. K. Chiang , A. J. Heeger.** in Journal of the Chemical Society-Chemical Communications, 1977, p 578-580.

[2] **H. S. Nalwa**, 1997, Handbook of organic conductive molecules and polymers, Wiley, Chichester ; New York.

[3] **J. L. Reddinger , J. R. Reynolds,** 1999, Molecular engineering of pi-conjugated polymers, *Radical Polymerisation Polyeletrolytes*, **145**, 57-122.

[4] **T. A. Skotheim, R. L. Elsenbaumer , J. R. Reynolds**, 1998, Handbook of conducting polymers, M. Dekker, New York.

[5] **R. H. Friend, R. W. Gymer, A. B. Holmes, J. H. Burroughes, R. N. Marks, C. Taliani, D. D. C. Bradley, D. A. Dos Santos, J. L. Bredas, M. Logdlund , W. R. Salaneck,** 1999, Electroluminescence in conjugated polymers, *Nature*, **397**, 121-128.

[6] **I. D. Brotherston, D. S. K. Mudigonda, J. M. Osborn, J. Belk, J. Chen, D. C. Loveday, J. L. Boehme, J. P. Ferraris , D. L. Meeker,** 1999, Tailoring the electrochromic properties of devices via polymer blends, copolymers, laminates and patterns, *Electrochimica Acta*, **44**, 2993-3004.

[7] **B. L. Groenendaal, F. Jonas, D. Freitag, H. Pielartzik , J. R. Reynolds,** 2000, Poly(3,4-ethylenedioxythiophene) and its derivatives: Past, present, and future, *Advanced Materials*, **12**, 481-494.

[8] **R. Peierls**, 1955, In quantum theory of solids, Oxford Universtiy Press, Oxford.

[9] **K. Shimamura, F. E. Karasz, J. A. Hirsch , J. C. W. Chien,** 1981, Crystal-Structure of Trans-Polyacetylene, *Makromolekulare Chemie-Rapid Communications*, **2**, 473-480.

[10] **P. Bauerle, U. Segelbacher, A. Maier , M. Mehring,** 1993, Electronic-Structure of Monomeric and Dimeric Cation Radicals in End-Capped Oligothiophenes, *Journal of the American Chemical Society*, **115**, 10217-10223.

[11] **M. G. Hill, J. F. Penneau, B. Zinger, K. R. Mann , L. L. Miller,** 1992, Oligothiophene Cation Radicals - Pi-Dimers as Alternatives to Bipolarons in Oxidized Polythiophenes, *Chemistry of Materials*, **4**, 1106-1113.

[12] **A. Dall'Olio, Y. Dascola, V. Varacco , C. R. Bocchi,** 1968, CRC Seances Acad. Sci. Ser. C, 466.

[13] **K. K. Kanazawa, A. F. Diaz, R. H. Geiss, W. D. Gill, J. F. Kwak, J. A. Logan, J. F. Rabolt , G. B. Street,** 1979, Organic Metals - Polypyrrole, a Stable Synthetic Metallic Polymer, *Journal of the Chemical Society-Chemical Communications*, 854-855.

[14] **M. Schnoller, W. Wersing , H. Naarman,** 1987, Intrinsically Conductive Organic Polymers as Electrode Material for Functional Ceramics in Electronics, *Makromolekulare Chemie-Macromolecular Symposia*, **8**, 83-95.

[15] **A. O. Patil, Y. Ikenoue, F. Wudl , A. J. Heeger,** 1987, Water-Soluble Conducting Polymers, *Journal of the American Chemical Society*, **109**, 1858-1859.

[16] **R. Bittihn, G. Ely , F. Woeffler,** 1987, Polypyrrole as an Electrode Material for Secondary Lithium Cells, *Makromolekulare Chemie-Macromolecular Symposia,* **8**, 51-59.
[17] **J. H. Burroughes, D. D. C. Bradley, A. R. Brown, R. N. Marks, K. Mackay, R. H. Friend, P. L. Burns , A. B. Holmes,** 1990, Light-Emitting-Diodes Based on Conjugated Polymers, *Nature,* **347**, 539-541.
[18] **S. Roth**, 1995, One-Dimensional Metals, Weinheim VCH,
[19] **W. R. Salaneck, I. Lundstrom , B. Randby**, 1993, Nobel Symposium in Chemistry: Conjugated Polymers and Related Materials, Oxford Sci, Oxford.
[20] **M. Berggren, O. Inganas, G. Gustafsson, J. Rasmusson, M. R. Andersson, T. Hjertberg , O. Wennerstrom,** 1994, Light-Emitting-Diodes with Variable Colors from Polymer Blends, *Nature,* **372**, 444-446.
[21] **A. J. Bard, L. R. Faulkner**, 2001, Electrochemical methods : fundamentals and applications, John Wiley, New York.
[22] **M. E. G. Lyons**, 1997, Advances in Chemical Physics, Polymeric Systems, John Wiley & Sons, New York.
[23] **M. D. Levi, C. Lopez, E. Vieil , M. A. Vorotyntsev,** 1997, Influence of ionic size on the mechanism of electrochemical doping of polypyrrole films studied by cyclic voltammetry, *Electrochimica Acta,* **42**, 757-769.
[24] **C. P. Andrieux, P. Audebert, P. Hapiot , J. M. Saveant,** 1991, Observation of Some Reactive Pyrrolic Radical-Cations by Use of Fast Voltammetry at Ultramicroelectrodes, *Synthetic Metals,* **43**, 2877-2880.
[25] **E. Beelen, J. Riga , J. J. Verbist,** 1991, Electrochemical Doping of Polypyrrole - Xps Study, *Synthetic Metals,* **41**, 449-454.
[26] **A. Kassim, F. J. Davis , G. R. Mitchell,** 1994, The Role of the Counterion during Electropolymerization of Polypyrrole Camphor Sulfonate Films, *Synthetic Metals,* **62**, 41-47.
[27] **L. F. Warren , D. P. Anderson,** 1987, Polypyrrole Films from Aqueous-Electrolytes - the Effect of Anions Upon Order, *Journal of the Electrochemical Society,* **134**, 101-105.
[28] **S. Kuwabata, J. Nakamura , H. Yoneyama,** 1988, The Effect of Basicity of Dopant Anions on the Conductivity of Polypyrrole Films, *Journal of the Chemical Society-Chemical Communications*, 779-780.
[29] **K. Imanishi, M. Satoh, Y. Yasuda, R. Tsushima , S. Aoki,** 1988, Solvent Effect on Electrochemical Polymerization of Aromatic-Compounds, *Journal of Electroanalytical Chemistry,* **242**, 203-208.
[30] **R. J. Waltman, A. F. Diaz , J. Bargon,** 1984, Electroactive Properties of Polyaromatic Molecules, *Journal of the Electrochemical Society,* **131**, 1452-1456.
[31] **M. G. Cross, D. Walton, N. J. Morse, R. J. Mortimer, D. R. Rosseinsky , D. J. Simmonds,** 1985, A Voltammetric Survey of Steric and Beta-Linkage Effects in the Electropolymerization of Some Substituted Pyrroles, *Journal of Electroanalytical Chemistry,* **189**, 389-396.
[32] **A. F. Diaz, J. I. Castillo, J. A. Logan , W. Y. Lee,** 1981, Electrochemistry of Conducting Polypyrrole Films, *Journal of Electroanalytical Chemistry,* **129**, 115-132.
[33] **A. Merz, R. Schwarz , R. Schropp,** 1992, 3,4-Dimethoxpyrrole - Monomer Synthesis and Conducting Polymer Formation, *Advanced Materials,* **4**, 409-411.

[34] **C. L. Gaupp, K. W. Zong, P. Schottland, B. C. Thompson, C. A. Thomas , J. R. Reynolds,** 2000, Poly(3,4-ethylenedioxypyrrole): Organic electrochemistry of a highly stable electrochromic polymer, *Macromolecules*, **33**, 1132-1133.

[35] **C. A. Thomas, K. Zong, P. Schottland , J. R. Reynolds,** 2000, Poly(3,4-alkylenedioxypyrrole)s as highly stable aqueous-compatible conducting polymers,vith biomedical implications, *Advanced Materials*, **12**, 222-+.

[36] **P. Audebert , G. Bidan,** 1985, Polyhalopyrroles - Electrochemical Synthesis and Some Characteristics, *Journal of Electroanalytical Chemistry*, **190**, 129-139.

[37] **R. J. Waltman , J. Bargon,** 1985, The Electropolymerization of Polycyclic-Hydrocarbons - Substituent Effects and Reactivity Structure Correlations, *Journal of Electroanalytical Chemistry*, **194**, 49-62.

[38] **M. E. G. Lyons**, 1994, Electroactive polymer electrochemistry, Plenum Press, New York.

[39] **R. A. Bull, F. R. F. Fan , A. J. Bard,** 1982, Polymer-Films on Electrodes .7. Electrochemical-Behavior at Polypyrrole-Coated Platinum and Tantalum Electrodes, *Journal of the Electrochemical Society*, **129**, 1009-1015.

[40] **P. G. Pickup,** 1990, Alternating-Current Impedance Study of a Polypyrrole-Based Anion-Exchange Polymer, *Journal of the Chemical Society-Faraday Transactions*, **86**, 3631-3636.

[41] **X. M. Ren , P. G. Pickup,** 1994, The Origin of the Discrepancy between the Low-Frequency Ac Capacitances and Voltammetric Capacitances of Conducting Polymers, *Journal of Electroanalytical Chemistry*, **372**, 289-291.

[42] **W. J. Albery, C. Elliot , A. R. Mount,** 1990, *Journal of Electroanalytical Chemistry*, **288**,

[43] **M. F. Mathias , O. Haas,** 1992, An Alternating-Current Impedance Model Including Migration and Redox-Site Interactions at Polymer-Modified Electrodes, *Journal of Physical Chemistry*, **96**, 3174-3182.

[44] **M. E. Kumru, J. Springer, A. S. Sarac , A. Bismarck,** 2001, Electrografting of thiophene, carbazole, pyrrole and their copolymers onto carbon fibers: electrokinetic measurements, surface composition and morphology, *Synthetic Metals*, **123**, 391-402.

[45] **A. S. Sarac, A. Bismarck, M. E. Kumru , J. Springer,** 2001, Electrografting of poly(carbazole-co-acrylamide) onto several carbon fibers - Electrokinetic and surface properties, *Synthetic Metals*, **123**, 411-423.

[46] **N. J. Harrick**, 1979, Internal Reflection Spectroscopy, New York.

[47] **A. S. Sarac, M. Serantoni, S. A. M. Tofail , V. J. Cunnane,** 2004, Morphological and spectroscopic analyses of poly [N-vinylcarbazole-co-vinylbenzenesulfonic acid] copolymer electrografted on carbon fiber: the effect of current density, *Applied Surface Science*, **229**, 13-18.

[48] **A. S. Sarac, M. Serantoni, S. A. M. Tofail, J. Henry, V. Cunnane , J. B. McMonagle,** 2005, Characterisation of nanosize thin films of electrografted N-vinylcarbazole copolymers (P[NVCz-co-VBSA] and P[NVCz-co-3-MeTh]) onto carbon fibre AFM, XPS, and Raman spectroscopy, *Applied Surface Science*, **243**, 183-198.

[49] **G. Sonmez , A. S. Sarac,** 2003, Structural study of pyrrole-EDOT copolymers on carbon fiber micro-electrodes, *Synthetic Metals*, **135**, 459-460.

[50] **M. Jamal, A. S. Sarac , E. Magner,** 2004, Conductive copolymer-modified carbon fibre microelectrodes: electrode characterisation and electrochemical detection of p-aminophenol, *Sensors and Actuators B-Chemical,* **97**, 59-66.

[51] **M. Serantoni, A. S. Sarac , D. Sutton,** 2005, FIB-SIMS investigation of carbazole-based polymer and copolymers electrocoated onto carbon fibers, and an AFM morphological study, *Surface & Coatings Technology*, **194**, 36-41.

[52] **A. Bismarck, A. F. Lee, A. S. Sarac, E. Schulz , K. Wilson,** 2005, Electrocoating of carbon fibres: A route for interface control in carbon fibre reinforced poly methylmethacrylate?, *Composites Science and Technology,* **65**, 1564-1573.

[53] **W. S. Smith**, 1987, Engineered Materials Handbook, ASM International, Ohio.

[54] **J.-B. Donnet**, 1998, Carbon fibers, Marcel Dekker, New York.

[55] **C. L. Weitzsacker, M. Bellamy , P. M. A. Sherwood,** 1994, Studies of the Effect of Size on Carbon-Fiber Surfaces, *Journal of Vacuum Science & Technology a-Vacuum Surfaces and Films,* **12**, 2392-2397.

[56] **C. L. Weitzsacker , P. M. A. Sherwood,** 1995, X-Ray Photoelectron Spectroscopic Studies of Carbon-Fiber Surfaces .19. Surface Chemical-Changes during Electrochemical Oxidation in Base, *Surface and Interface Analysis*, **23**, 551-558.

[57] **C. L. Weitzsacker, M. Xie , L. T. Drzal,** 1997, Using XPS to investigate fiber matrix chemical interactions in carbon-fiber-reinforced composites, *Surface and Interface Analysis,* **25**, 53-63.

[58] **L. Ibarra, A. Macias , E. Palma,** 1996, Stress-strain and stress relaxation in oxidated short carbon fiber-thermoplastic elastomer composites, *Journal of Applied Polymer Science,* **61**, 2447-2454.

[59] **M. Delamar, G. Desarmot, O. Fagebaume, R. Hitmi, J. Pinson , J. M. Saveant,** 1997, Modification of carbon fiber surfaces by electrochemical reduction of aryl diazonium salts: Application to carbon epoxy composites, *Carbon,* **35**, 801-807.

[60] **Y. T. Zhu, J. A. Valdez, I. J. Beyerlein, S. J. Zhou, C. Liu, M. G. Stout, D. P. Butt , T. C. Lowe,** 1999, Mechanical properties of bone-shaped-short-fiber reinforced composites, *Acta Materialia,* **47**, 1767-1781.

[61] **Y. T. Zhu, W. R. Blumenthal, S. T. Taylor, T. C. Lowe , B. L. Zhou,** 1997, Analysis of size dependence of ceramic fiber and whisker strength, *Journal of the American Ceramic Society*, **80**, 1447-1452.

[62] **Y. T. Zhu, J. A. Valdez, N. Shi, M. L. Lovato, M. G. Stout, S. J. Zhou, D. P. Butt, W. R. Blumenthal , T. C. Lowe,** 1998, A composite reinforced with bone-shaped short fibers, *Scripta Materialia*, **38**, 1321-1325.

[63] **A. Bismarck, A. Menner, J. Barner, A. F. Lee, K. Wilson, J. Springer, J. P. Rabe , A. S. Sarac,** 2001, Electrografting of poly (carbazole-co-acrylamide) onto highly oriented pyrolytic graphite. A cyclovoltammetric, atomic force microscopic and ellipsometric study, *Surface & Coatings Technology,* **145**, 164-175.

[64] **A. S. Sarac, G. Sonmez , F. C. Cebeci,** 2003, Electrochemical synthesis and structural studies of polypyrroles, poly(3,4-ethylenedioxythiophene)s and copolymers of pyrrole and 3,4-ethylenedioxythiophene on carbon fibre microelectrodes, *Journal of Applied Electrochemistry,* **33**, 295-301.

[65] **E. Sezer, A. H. S. Sarac , E. A. Parlak,** 2003, Electrochemical synthesis of EDOT-ECZ-EDOT copolymer on carbon fiber micro-electrodes, *Journal of Applied Electrochemistry*, **33**, 1233-1237.

[66] **A. S. Sarac, M. Serantoni, S. A. M. Tofail , V. J. Cunnane,** 2005, Nanoscale characterization of carbazole-indole copolymers modified carbon fiber surfaces, *Journal of Nanoscience and Nanotechnology*, **5**, 1677-1682.

[67] **A. Bismarck, A. Menner, M. E. Kumru, A. S. Sarac, M. Bistritz , E. Schulz,** 2002, Poly(carbazole-co-acrylamide) electrocoated carbon fibers and their adhesion behavior to an epoxy resin matrix, *Journal of Materials Science*, **37**, 461-471.

[68] **M. E. Galvin , G. E. Wnek,** 1982, Electrically Conductive Polymer Composites - Polymerization of Acetylene in Polyethylene, *Polymer*, **23**, 795-797.

[69] **T. Ojio , S. Miyata,** 1986, Highly Transparent and Conducting Polypyrrole Polyvinyl-Alcohol) Composite Films Prepared by Gas State Polymerization, *Polymer Journal*, **18**, 95-98.

[70] **C. J. Li , Z. G. Song,** 1991, Electronic-Properties of Junctions between Polypyrrole Poly(Ethylene-Terephthalate) Composites and Metals, *Synthetic Metals*, **44**, 159-163.

[71] **M. X. Wan , J. Yang,** 1993, Growth-Mechanism of Transparent and Conducting Composite Films of Polyaniline, *Journal of Applied Polymer Science*, **49**, 1639-1645.

[72] **K. F. Schoch, W. A. Byers , L. J. Buckley,** 1995, Deposition and Characterization of Conducting Polymer Thin-Films on Insulating Substrates, *Synthetic Metals*, **72**, 13-23.

[73] **E. C. Cooper , B. Vincent,** 1989, Electrically Conducting Organic Films and Beads Based on Conducting Latex-Particles, *Journal of Physics D-Applied Physics*, **22**, 1580-1585.

[74] **F. M. Huijs, F. F. Vercauteren, B. de Ruiter, D. Kalicharan , G. Hadziioannou,** 1999, Shell morphology of core-shell latexes based on conductive polymers, *Synthetic Metals*, **102**, 1151-1152.

[75] **S. F. Lascelles , S. P. Armes,** 1997, Synthesis and characterization of micrometre-sized, polypyrrole-coated polystyrene latexes, *Journal of Materials Chemistry*, **7**, 1339-1347.

[76] **P. Banerjee , B. M. Mandal,** 1995, Conducting Polyaniline Nanoparticle Blends with Extremely Low Percolation Thresholds, *Macromolecules*, **28**, 3940-3943.

[77] **N. Gospodinova, P. Mokreva, T. Tsanov , L. Terlemezyan,** 1997, A new route to polyaniline composites, *Polymer*, **38**, 743-746.

[78] **Y. Cao, P. Smith , A. J. Heeger,** 1992, Counterion Induced Processibility of Conducting Polyaniline and of Conducting Polyblends of Polyaniline in Bulk Polymers, *Synthetic Metals*, **48**, 91-97.

[79] **Y. Cao, G. M. Treacy, P. Smith , A. J. Heeger,** 1992, Solution-Cast Films of Polyaniline - Optical-Quality Transparent Electrodes, *Applied Physics Letters*, **60**, 2711-2713.

[80] **Y. Yang , A. J. Heeger,** 1994, Polyaniline as a Transparent Electrode for Polymer Light-Emitting-Diodes - Lower Operating Voltage and Higher Efficiency, *Applied Physics Letters*, **64**, 1245-1247.

[81] **Y. Yang , A. J. Heeger,** 1994, A New Architecture for Polymer Transistors, *Nature*, **372**, 344-346.

[82] **C. Y. Yang, Y. Cao, P. Smith , A. J. Heeger,** 1993, Morphology of Conductive, Solution-Processed Blends of Polyaniline and Poly(Methyl Methacrylate), *Synthetic Metals*, **53**, 293-301.
[83] **J. Fraysse, T. Olinga, J. Planes, A. Pron , M. Nechtshein,** 1999, Polyaniline blends cast from hexafluoro-2-propanol, *Synthetic Metals*, **101**, 722-723.
[84] **A. Yassar, J. Roncali , F. Garnier,** 1987, Aqueous Suspension of Conducting Material from Polypyrrole-Coated Submicronic Latex-Particles, *Polymer Communications*, **28**, 103-104.
[85] **G. Tourrillan.** in Handbook of Conducting Polymers; T. A. Skotheim, Ed.; Marcel Dekker, New York, 1986, p 293.
[86] **A. Kossmehl.** in Handbook of conducting polymers; T. A. Skotheim, Ed.; Marcel Dekker, New York, 1986, p 351.
[87] **G. Schopf , G. Kossmehl**, 1997, Polythiophenes-Electrically Conducting Polymers, Springer Verlag,
[88] **X. B. Chen, J. P. Issi, J. Devaux , B. D.J.,** 1997, *Mater. Sci.*, **32**, 1515.
[89] **E. Larraz, M. I. Redondo, M. J. Gonzalez-Tejera, M. A. Raso, J. Tortajada, E. S. de la Blanca , M. V. Garcia,** 2001, Influence of pH on poly-(N-methylpyrrole) electrochemically synthesized in aqueous solution: an infrared study, *Synthetic Metals*, **122**, 413-423.
[90] **A. Yassar, J. Roncali , F. Garnier,** 1989, Conductivity and Conjugation Length in Poly(3-Methylthiophene) Thin-Films, *Macromolecules*, **22**, 804-809.

APPENDICES

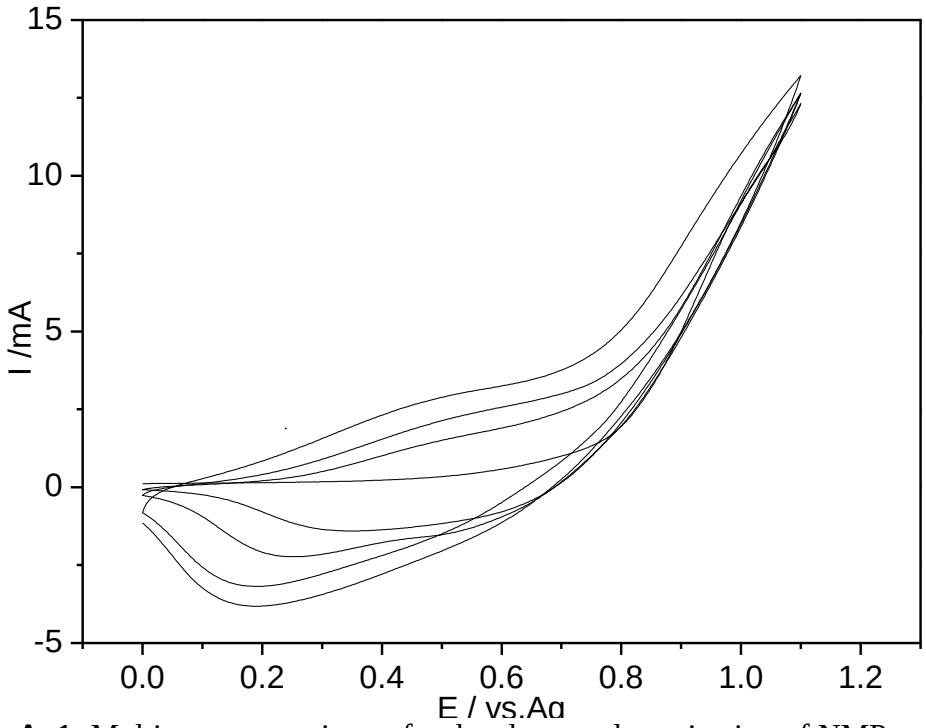

Figure A. 1: Multisweep experiment for the electropolymerization of NMPy ([NMPy]= 0.02M) on CFME/PTh base electrode in 0.2M $NaClO_4$ in ACN. 0.04M NMPy.

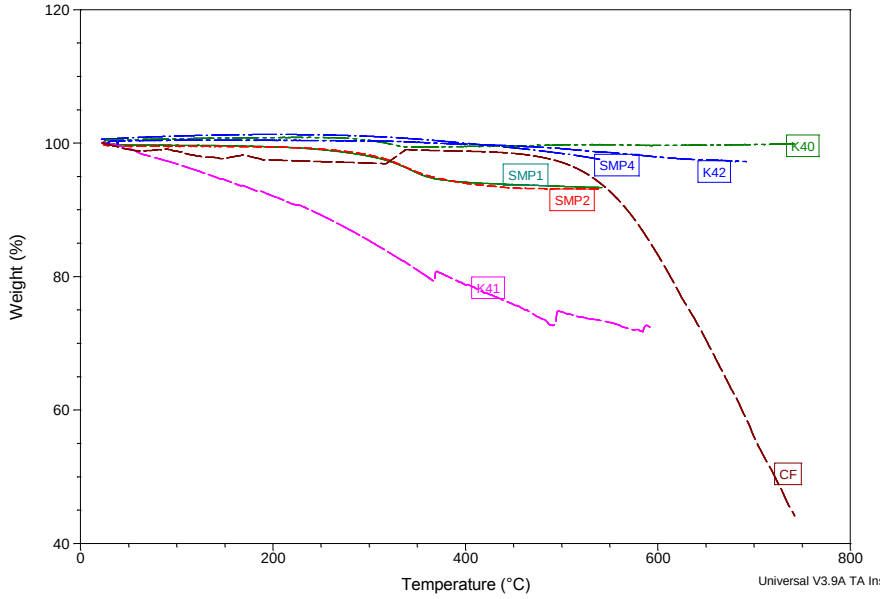

Figure A. 2: TGA of a) bare CF b)K40: 0.08M NMPy in 0.1M TEATFB in ACN c)K41: 0.08M NMPy in 0.1M $LiClO_4$ in ACN d)K42 SMP4 0.08M NMPy in 0.1M $NaClO_4$ in ACN e) SMP1: 0.5M Th on CFME in 0.2M $NaClO_4$ in ACN f) SMP2: 0.008M NMPy on CFME/PTh base electrode in 0.2M $NaClO_4$ in ACN.

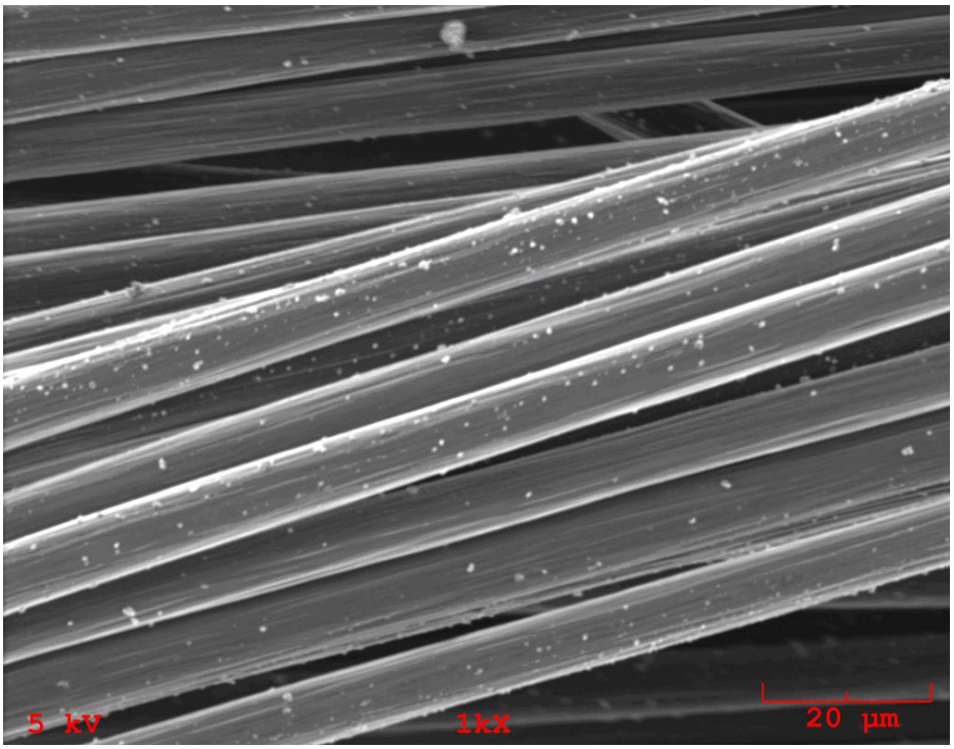

Figure A. 3: SEM images of 0.04M NMPy on CFME/PTh base electrode

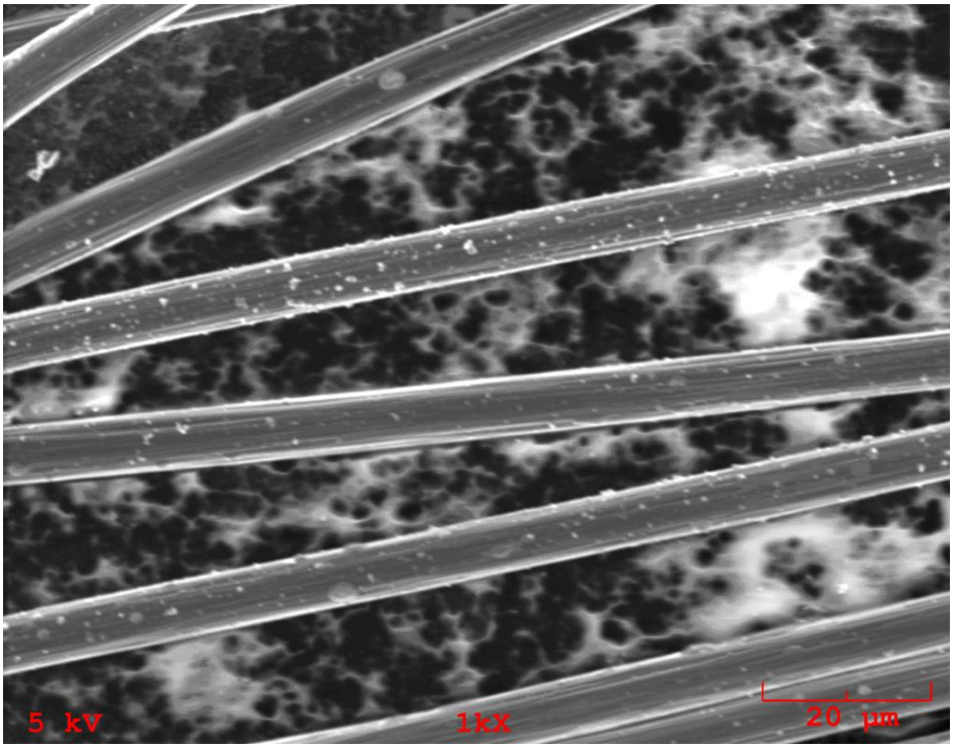

Figure A. 4: SEM image of 0.02M NMPy on CFME/PTh base electrode

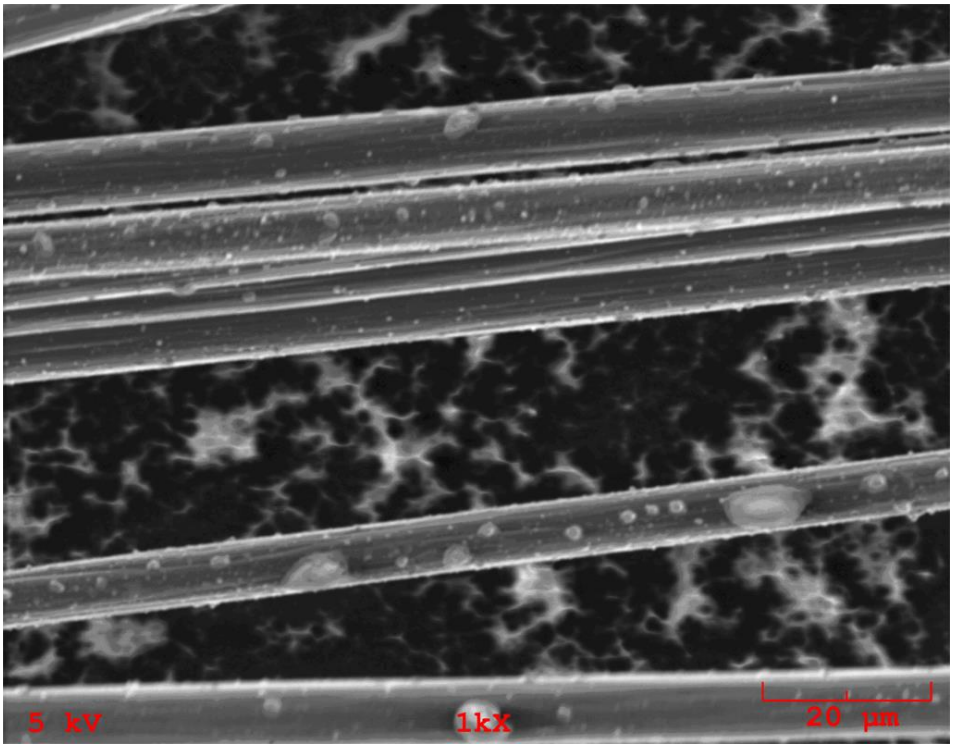

Figure A. 5: SEM image of 8 cycles of 0.08M NMPy on CFME/PTh base electrode

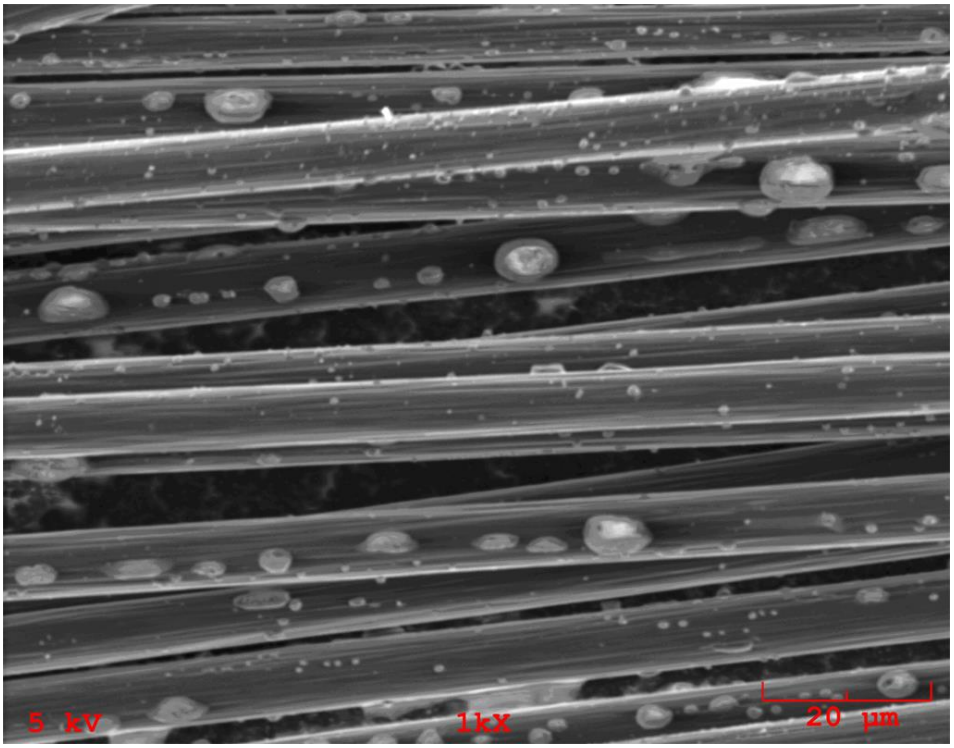

Figure A. 6: SEM image of 2 cycles of 0.08M NMPy on CFME/PTh base electrode

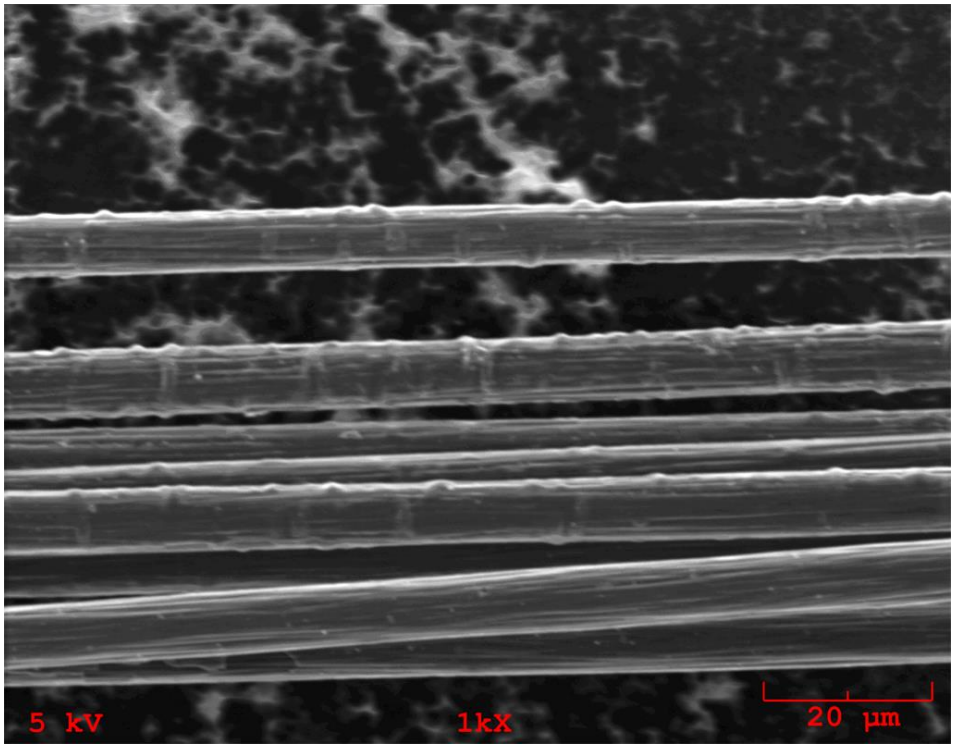

Figure A. 7: SEM image of copolymer. [Th]= 0.5M and [NMPy]= 0.08M

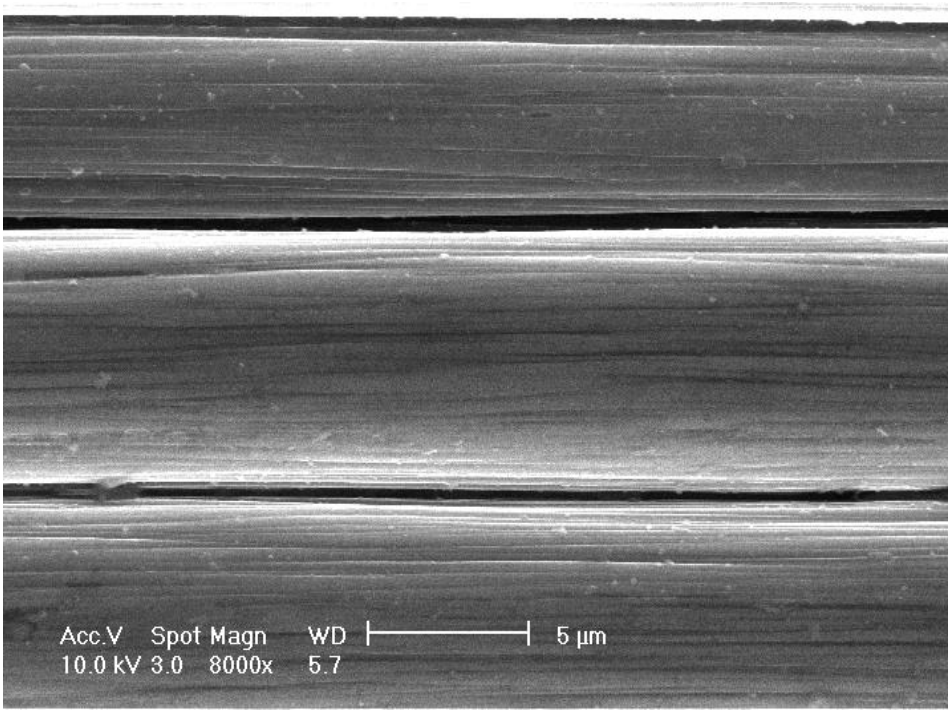

Figure A. 8: SEM image of 0.5M Thiophene on CFME in 0.2M $NaClO_4$ in ACN.

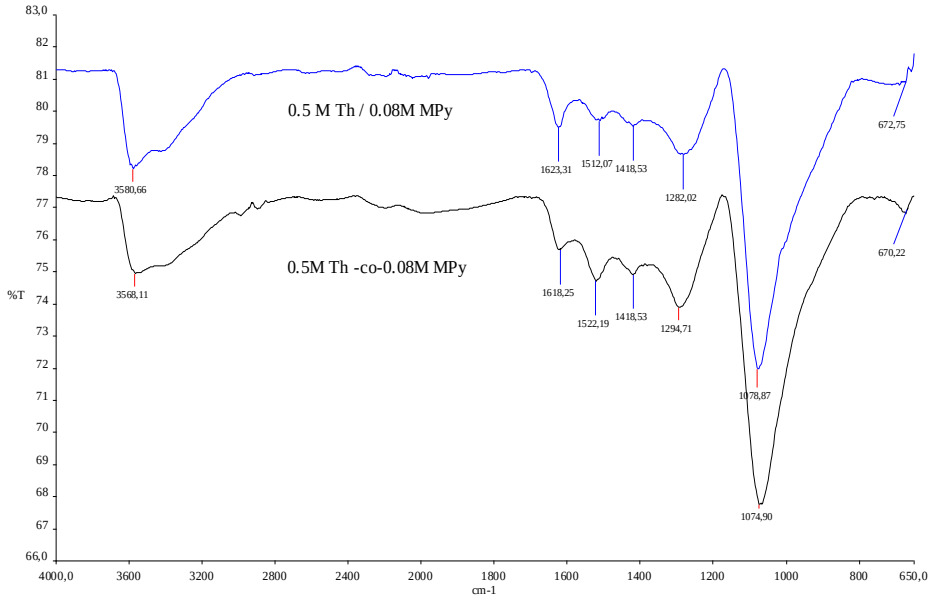

Figure A. 9: IR analysis of copolymer of P(Th-co-NMPy) and composite of 0.08M NMPy on CFME/PTh base electrode.

BIOGRAPHY

Hülya GEYİK was born in Ankara in 1979. She was graduated from Ugur College in 1994 and Macka Akif Tuncel Anatolian Technical High School in 1998. She admitted to Istanbul Technical University, Astronautical Engineering Department in 1998 and graduated as a Astronautical Engineer in 2003

She was accepted as a M.Sc. student to the Polymer Science and Technology Programme of the Institute of Science and Technology of Istanbul Technical University in 2003 in which she is about to graduate.